EFFECT OF BRIDGE CONSTRICTION ON SCOUR AND BACKWATER

by

H. K. Liu,

F. M. Chang,

and

M. M. Skinner

Prepared for

BUREAU OF PUBLIC ROADS

under Contract CPR11-5480

Civil Engineering Section
Colorado State University
Fort Collins, Colorado

February 1961

CER60HKL22

EFFECT OF BRIDGE CONSTRICTION ON SCOUR AND BACKWATER

by

H. K. Liu,

F. M. Chang,

and

M. M. Skinner

Prepared for

BUREAU OF PUBLIC ROADS

under Contract CPR11-5480

Civil Engineering Section
Colorado State University
Fort Collins, Colorado

February 1961

CER60HKL22

TABLE OF CONTENTS

TABLE OF CONTENTS - Cont'd

LIST OF FIGURES

LIST OF FIGURES - cont'd.

NOTATIONS AND SYMBOLS

A_o	A coefficient in Equation 31
a	Length of the obstruction perpendicular to the flow
B	Channel width
b	Opening width
C	Chezy coefficient
c	$c = e^{A_o (1-y)^{1/2}}$
C_a	Discharge coefficient
D	Pier width
D_L	Lacey's regime depth for a straight channel
D_S	Depth of scour measured from water surface
d	Representative size of the bed material
d_s	Depth of scour at time t
d_{SE}	Equilibrium depth of scour measured from the normal bed surface
d_{SL}	Limiting depth of scour measured from the normal bed surface
d_{SM}	Maximum depth of scour measured from the normal bed surface
Δd_s	Increase of scour depth within a time interval Δt
F_n	Froude Number of the normal flow
f	Lacey's silt factor
G	Geometry of the obstruction

NOTATIONS AND SYMBOLS - cont'd.

g	Gravitational acceleration
h_n	Normal depth of flow
h_1^*	Maximum backwater
Δh_s	Maximum difference of water surface elevation across an embankment
K	A coefficient in Equation 27
K_{max}	A coefficient in Equation 12
k	A coefficient in Equation 9
M	Opening ratio $= \frac{b}{B}$
m	An exponent in Equation 3
N	An exponent in Equation 3
n	Manning's coefficient
P_w	Regime width, see Equation 6
Q	Total discharge
Q_s	Total sediment discharge
Q_{s1}	Total sediment supply at Section 1
Q_{s2}	Total sediment transport at Section 2
q	Discharge intensity
q_b	Average discharge intensity in the contracted section

NOTATIONS AND SYMBOLS - cont'd.

q_s	Sediment discharge per foot of width
R_b	Hydraulic radius pertaining to the bed
S	Energy gradient
t	Time
t_m	Time required for d_s to reach d_{SM}
t_o	Time factor
V	Mean velocity of the flow
V_*	Shear velocity $= \sqrt{\tau_b / \rho}$
V_o	Mean velocity of approach flow
$\forall_s$	Volume of scour
x	An exponent in Equation 4 for velocity formula
y	$y = \frac{ds}{d_{SM}}$ or $\frac{d_s}{d_{SL}}$ and also used as an exponent in Equation 4
γ	Specific weight of water
γ_s	Specific weight of sediment
$\Delta\gamma_s$	Difference in specific weight between sediment and fluid
θ	Skew angle of abutment with respect to the flow direction and also angle between upstream edge of scour hole and bed
λ	An exponent in Equation 3 for Liu and Hwang's Formula

NOTATIONS AND SYMBOLS - Cont'd.

μ	Dynamic viscosity of the fluid
ν	Kinematic viscosity of the fluid
ξ	Distance perpendicular to the bank
ρ	Density of the fluid
σ	A measure of the gradation of the bed material
T	Tractive force
T_b	Tractive force pertaining to the bed level
T_c	Critical tractive force of the bed material
Ω	An exponent in Equation 3
ω	Representative fall velocity of the bed material

EFFECT OF BRIDGE CONSTRICTION ON SCOUR AND BACKWATER

I. INTRODUCTION

In an earlier study (1) sponsored by the U. S. Bureau of Public Roads, backwater effects caused by bridge abutments and piers in a rigid channel were investigated. The method developed in that study for estimating backwater may not be applicable to the case of an alluvial channel. Once scour has been developed, the backwater will be reduced. Furthermore, scouring and undermining of bridge foundations have been a major cause of bridge failures. In view of the expanding highway system, such a study of the effect of bridge constriction on scour and backwater is very timely. This report is a result of a laboratory investigation on scour and backwater in alluvial channels conducted in the hydraulic laboratory of Colorado State University under the sponsorship of the U. S. Bureau of Public Roads.

Scope of this Study

Scour at bridge abutments is the main subject of this report. Since this study stresses the applied side of the problem, detailed investigation on the mechanics of scour has not been made. Several parameters of scour such as, depth, cross-section, location of the maximum scour, and rate of scour, will be related to factors, such as, geometry of the constriction, sediment properties, and flow properties.

In addition, the maximum backwater and the water-surface drop across the embankment will be studied.

II. ALLUVIAL HYDRAULICS

The effect of an obstruction in a channel is to alter the condition of flow which had been established prior to the installation of the obstruction to a new equilibrium state in the vicinity of the obstruction. In order to study such an effect, it is necessary to know the normal flow which exists before the installation of the obstruction. Such a normal flow is used throughout this report as a reference for the study of channel constriction; for example, the depth of scour is measured downward from the normal bed surface, and the change of water surface is measured with respect to the normal water surface.

Numerous studies have been made on normal flow conditions of alluvial channels - commonly known as regime flow. It is beyond the scope of this report to discuss in detail all aspects of regime flow. In general, there are two important principles of regime flow; namely, (a) continuity of the fluid flow, and (b) continuity of the sediment flow. These two principles are inevitably related to: (a) alluvial roughness and (b) sediment transport. The significance of these two can be explained as follows:

For a constant discharge through a wide, prismatic channel composed of homogeneous sediment, the depth of flow and the rate of sediment transport per foot width can be expressed respectively as:

$$h_n = h_n\,(q,\ S,\ \rho,\ \mu,\ g,\ d,\ \sigma,\ \Delta\gamma,\ \omega) \qquad (1)$$

and

$$q_s = q_s\,(q,\ S,\ \rho,\ \mu,\ g,\ d,\ \sigma,\ \Delta\gamma_s,\ \omega) \qquad (2)$$

in which

h_n = Normal depth of flow

q_s = Sediment discharge per foot of width

q = Flow discharge per foot of width

S = Energy gradient

ρ = Density of the fluid

μ = Dynamic viscosity of the fluid

g = Gravitational acceleration

d = Representative size of the bed material

σ = A measure of the gradation of the bed material

$\Delta\gamma_s$ = Difference in specific weight between the bed material and fluid

ω = Representative fall velocity of the bed material depending upon d, σ, $\Delta\gamma_s$, and particle shape.

Since $q = Vh_n$, Eq (1) is a function relating V and h_n for given properties of fluid and sediment. Eq (1) can be considered as a function approximating alluvial roughness. Eq (2) can be considered as a function approximating sediment transport.

Progress of finding a law of alluvial roughness, hence a corresponding discharge equation, has been rather slow because of the complexity of the problem. The problem of alluvial roughness is related to turbulent flow near a movable, wavy boundary composed of moving particles. In addition, history of the flow, presence of a free surface, and presence of lateral boundaries make a theoretical analysis of the problem impossible at present.

Although the Chezy and Manning formulas have been widely used in engineering practice, accuracy of these formulas depends upon a proper choice of the Chezy C or the Manning n. There are various criteria available for selecting Chezy's C or Manning's n. These criteria are largely based upon engineering experience. In a sense, such a practice is more of an art than a science.

In case the bed material is composed of coarse sand or larger sizes, and the bed is essentially plane, Strickler's formula (2) may be used to estimate the Manning n.

A more scientific approach to the problem has been proposed by Einstein and Barbarossa (3). Their method is based upon an assumption that alluvial roughness, hence the bed shear, is composed of two elements; one pertaining to the grain roughness, the other pertaining to the sand waves, which in turn depends upon the shear pertaining to the grain roughness. The computation procedure is rather cumbersome. Accuracy of the method is still uncertain.

Recently Liu and Hwang (4) have found that variables pertaining to normal flow in alluvial channels can be grouped into two dimensionless parameters:

$$\frac{V_* d}{\nu} \quad \text{and} \quad \frac{\dfrac{V}{V_*} \quad \dfrac{T_b}{\Delta \gamma_s d} S^{\lambda}}{\left(\dfrac{R_b}{d}\right)^m F_n^N}$$

in which

T_b = Shear at the bed level

V_* = Shear velocity = $\sqrt{\frac{T_b}{\rho}}$

ρ = Fluid density

d = Mean size of the bed material

V = Mean velocity of flow

$\Delta\gamma_s$ = Difference in specific weight between the sediment and the fluid

ν = Kinematic viscosity of the fluid

S = Energy gradient

R_b = Hydraulic radius pertaining to the bed

F_n = Froude number of the normal flow

λ, m, N = Exponents depending upon the bed configuration and the size of the bed material

Normal flow data grouped according to these two parameters generally follow a set of two straight lines on log-log paper. A general equation can be written for such a set of straight lines as:

$$\frac{V_* d}{\nu} = A \left[\frac{\frac{V}{V_*} \quad \frac{T_b}{\Delta\gamma_s d} S^{\lambda}}{\left(\frac{R_b}{d}\right)^m \quad F_n^N} \right]^{\Omega} \tag{3}$$

in which

A depends upon $\frac{\omega d}{\nu}$ of the mean size of the bed material

ω is the fall velocity of the mean size

Ω depends upon the bed configuration

Solving for V from Eq (3) results

$$V = C_a R_b^x S^y \qquad (4)$$

in which C_a = a discharge coefficient, and

x,y = dimensionless numbers

Values of C_a, x, and y depend upon the bed configuration and the mean size of the bed material.

According to Liu and Hwang, Eq (4) has been verified satisfactorily by laboratory data and canal data of known bed configuration.

In case the bed configuration is not known, accuracy of the formula depends largely on the accuracy of estimating the bed configuration. At the present, criteria for various bed configurations: plane, ripples, dune, bars, flat, and anti-dunes are largely unknown except for Liu's criterion for ripple formation (5).

According to Liu, at the stage of ripple formation, two conditions are necessary:

(a) Bed shear is large enough to move the bed particles

and,

(b) The zone of high velocity gradient near the bed has to be unstable.

Based upon these two conditions, a pair of parameters $\frac{V*}{\omega}$ and $\frac{V*d}{\nu}$, can be used to correlate data pertaining to ripple formation. Liu's criterion for ripple formation is shown in Fig. 1.

Extensive studies of an empirical nature on rate of sediment transport have been made by engineers and scientists. However, to the writer's knowledge, no formula of sediment transport is suitable over the entire range of application. Results obtained from bed load formulas by various authors, such as Einstein, Kalinski, Meyer-Peter, and Straub differ appreciably. Additional research on sediment transport is needed.

III. HYDRAULICS OF OPEN CHANNEL CONSTRICTION

Backwater caused by a contraction in a rigid channel has been discussed in detail in a previous publication entitled "Backwater Effects at Bridge Piers and Abutments", by Liu, Bradley, and Plate (1). The backwater h_1^* is therein classified as, (a) contraction backwater and, (b) resistance backwater. For the case of a rigid channel when the flow is critical at the contracted section, the maximum backwater is called the contraction backwater; when the flow is tranquil in the contracted section, the backwater is called resistance backwater. At a given Froude number for the normal flow, the tranquil depth of flow at the contraction decreases as the opening ratio decreases until the depth reaches critical depth. The corresponding resistance backwater upstream from the contraction increases as the opening ratio decreases until the flow becomes critical at the contraction; the resistance backwater then becomes the contraction backwater. Further reduction of the opening ratio will cause an increase of the contraction backwater.

For the case of an alluvial channel--assuming (a) the bed material to be such that when the flow in the contracted section approaches critical, the bed material will be eroded and a scour hole will develop, and (b) the flow at the contracted section does not reach critical stage--the backwater h_1^* upstream from the constriction can be considered as resistance backwater. Furthermore, for a given opening ratio, as the scour hole increases with time, the contraction of flow decreases and, therefore, the backwater decreases.

The portion of the backwater accounted for by the energy loss due to convergence of flow in a rigid channel is usually considered to be insignificant. Such is not the case if a scour hole is developed as a result of the contracted section. Additional energy loss may occur as a result of flow separation at the upstream edge of the scour hole, see Fig. 2., which produces a spiral motion, commonly associated with flow around a bend. Since the size of the scour hole may change appreciably with time, the energy loss and, therefore, the backwater may also change with time. The phenomenon is further complicated by the movement of sediment waves associated with alluvial flow. The flow pattern, or the energy loss downstream of the constriction, is also influenced by sediment deposition immediately downstream of the embankment. Hence, the backwater found in a rigid channel may not be directly usable as an indication of the energy loss in an alluvial stream.

It should be noted also, that the backwater h_1* in a rigid channel depends upon the contraction ratio, whereas scour at bridges may be a local phenomena independent of the contraction ratio. Although high backwater may cause excessive local scour, the degree of scouring is not necessarily associated with high backwater h_1*.

In practice, the water-surface drop across the embankment is a primary concern. Such a drop of water surface can be measured very easily in the field during various flow conditions at a given bridge site. Measurements on water surface change contained in this report will be mainly the water-surface drop across the model embankment.

IV. MECHANICS OF SCOUR AT BRIDGE CONSTRICTION

It may be stated that there are two kinds of scour caused by a constriction:

(1) General scour--caused by a long contraction of flow which is of sufficient length that a new regime of flow can be established. A change of flow regime requires changes of such flow characteristics as: depth, width, channel roughness, velocity distribution, channel slope, and sediment discharge. In general, the bed in the contracted section is degraded to an elevation lower than that of the uncontracted section. Such general decrease of bed elevation in the contracted section is defined as general scour.

(2) Local scour--caused by a local constriction of flow due to an abutment, a pier, or any other hydraulic structure placed in the channel. The present study is limited to local scour caused by abutments. Should the spacing of the structures be so close together that the local scour holes interfere with one another to produce a general decrease of bed elevation in the constricted section, the phenomenon will still be considered as local scour in this report.

A. General Scour Due To A Long Contraction

Strictly speaking, the mechanics of local scour are different from general scour and discussions of one can be made without reference to the other. However, because very little is known up to the present about the mechanics of local scour, attempts have been made by several engineers to correlate local scour with general scour under the same degree of contraction.

Laursen (6) has made comparisons between local scour and general scour resulting from the same degree of contraction, and concluded:

(a) In the case of an embankment extending over the flood plain and ending at the edge of the channel (with no sediment transported by the approaching over-bank flow, and where the scour holes around the neighboring obstructions overlap) the maximum depth of local scour below normal bed surface may be about four times the depth of scour due to a long constriction.

(b) In the case of no overlap of the scour holes and the scour is caused by a constriction of part of the main channel, such a ratio is 12 to 1.

In comparing local scour with general scour, it is important to realize that:

(a) In order to estimate general scour, it is necessary to calculate the regime depth of flow in both the uncontracted and the contracted reach.

(b) Present methods of determining the regime depth of an alluvial channel are very inadequate.

(c) It is difficult to determine the true maximum depth of local scour.

In case an alluvial channel of a constant gradient is contracted, the regime depth is related to the total discharge and total sediment transport rate. In other words, the computation of general scour requires the use of discharge and sediment transport equations. For given bed material and channel slope, the flow depth and other characteristics of flow must vary as a result of the general contraction in order to satisfy these two equations of continuity.

Various ways of writing equations (1) and (2) have been made. Straub (7) used the Manning equation for flow discharge and the DuBoys' equation for sediment transport. Laursen (6) used the Manning equation, and his equation for sediment transport (8). An experienced investigator probably can choose suitable equations to estimate general scour which agrees with laboratory results. In the case of the prototype, however, such an agreement is difficult to achieve for lack of suitable formulas to use.

B. Local Scour At A Bridge Constriction

Review of Literature

Laboratory measurements indicate that the velocity of the flow in the area away from the vicinity of the abutment is not influenced by the presence of the abutment. Hence, scour at abutments can be considered as a local phenomenon, and not being significantly related to the overall geometry of the flow.

Most of the studies on local scour are empirical in nature. The following is a brief review of studies on local scour:

Lacey (9) gave approximate values of maximum scour at a constricted section by equating the scour depth to the regime depth of flow, D_L , computed according to the following formula:

$$D_L = 0.47 \left(\frac{Q}{f}\right)^{1/3} \tag{5}$$

in which

D_L is Lacey's regime depth for a straight channel

Q is total discharge

f is Lacey's silt factor.

Khosla (10) has shown that with the aid of Lacey's equation for regime width, P_w , of a prismatic channel,

$$P_w = 2.67 \sqrt{Q} \tag{6}$$

and that therefore,

$$q = Q/P_w = \frac{\sqrt{Q}}{2.67} \tag{7}$$

Equation (5) can be changed to

$$D_L = 0.9 \left(\frac{q^2}{f}\right)^{1/3} \tag{8}$$

Assuming that local scour is proportional to the regime depth, Khosla has proposed accordingly:

$$D_s = kD_L \tag{9}$$

or

$$D_s = k0.9 \left(\frac{q^2}{f}\right)^{1/3} \tag{10}$$

in which

D_s is maximum scour measured from the water surface

q is the flow intensity, i.e., discharge per foot of width,

and k depends upon the type of obstruction.

Inglis (11) reasoned that the effect of bridge piers is to deflect the current like a bend, and therefore proposed that the maximum depth of scour, D_s, at a bridge pier is proportional to Lacey's regime depth, D_L.

According to Inglis:

(a) The maximum scour downstream of bridges is of the order $D_s = 4D_L$

(b) Scour at straight spurs facing upstream, with steeply sloping heads (1-1/2: 1) is of the order $D_s = 3.8D_L$; and with long sloping heads (1: 20) $D_s = 2.25\ D_L$

(c) Scour at noses of large-radius guide banks, $D_s = 2.75\ D_L$

(d) The maximum scour around bridge piers, $D_s = 2\ D_L$.

(e) Scour at spurs along river banks, $D_s = 1.7\ D_L$ to $3.8\ D_L$ depending on severity of attack, which varies according to conditions such as length of projection, sharpness of curvature, and angle and position relative to embankment.

Inglis found empirically that the maximum scour can be expressed in terms of the unit discharge and pier width as follows:

$$\frac{D_s}{D} = 1.7 \left(\frac{q^{2/3}}{D}\right)^{0.78} \tag{11}$$

in which D is pier width.

A similar approach has been used by Blench (12) to correlate the maximum scour at an obstruction with the regime depth based upon his regime formulas.

By dimensional analysis and limited laboratory study, Ahmad (13) has proposed

$$D_s = K_{max} \, q_b^{2/3} \qquad (12)$$

in which

q_b is local discharge intensity in the contracted channel and,

K_{max} is a constant.

Ahmad recommended further experiments on the following factors:

(a) Effect of protrusion ratio

(b) Effect of major variation in bed material

(c) Effect of curvature of flow

According to Blench (12), the scour depth is expected to vary with either $Q^{1/3}$ or $q^{2/3}$, although, his data show that the exponent of q is not exactly $2/3$. According to both Inglis and Blench, scour depth depends upon the size of the bed material. According to Ahmad the rate of scour depends upon the sediment size, but the maximum scour is independent of the sediment size. Ahmad conceded that for a wider range of materials, the silt factor must enter, since a gravel bed could hardly be expected to give the same result as a bed of fine sand, but for practical needs for sand beds consideration of the silt factor is not necessary. Obviously, more work is needed to settle the point.

An important assumption in the Inglis-Blench-Ahmad approach is that the maximum scour is dependent upon some mean flow intensity. The success of their approaches depends largely upon the choice of a mean flow

intensity value which is often very difficult to choose in case of natural flow.

Laursen's conclusion on local scour is that as long as there is appreciable movement of bed load, the maximum scour, which is a local phenomenon, depends only on the normal depth of flow and the length of the obstruction and is independent of the sediment size and the flow velocity. In other words, the flow intensity has insignificant effect on local scour. The design curve recommended by Laursen is shown as Fig. 3. Laursen's point of view concerning the effect of flow intensity on maximum scour is entirely opposite to those of Inglis-Blench-Ahmad's. It is very difficult to make comments on such a point until basic mechanics of local scour are discussed.

C. Controversies On Factors Affecting Maximum Local Scour

Owing to the complexity of the scour problem, investigators have not reached agreement on the following factors in connection with the maximum depth of scour:

1. Effect of material size

Inglis, based upon experiments with bed material ranging in size from 0.06 mm to 0.37 mm, concluded that gradation is a factor affecting the maximum scour. Ahmad, who used sand sizes of 0.35 mm and 0.695 mm, concluded that the rate of scour is influenced by the size of the material, but the maximum depth of scour is independent of the size of the bed material and possibly dependent only on major variations in bed material.

Laursen, who used bed material sizes ranging from 0.46 mm to 2.20 mm, stated that the bed material size does not affect the scour unless the mode of transport changes to suspended load.

2. Effect of flow velocity

Inglis's and Ahmad's study on scour indicated that the maximum scour depends upon local discharge (upon the local mean velocity of flow). Laursen has stated that the maximum scour depends mainly upon the flow depth and the length of the obstruction, and not noticeably upon the flow velocity, provided that the sediment transport from the approach channel is appreciable.

3. Effect of contraction ratio

Scour at bridge piers and abutments is considered by Laursen as a local phenomenon. According to Laursen for a given depth of flow, the scour depends upon the length of the obstruction. The flow diverted by the obstruction passes through the scour hole as a submerged spiral roller. The width of the scour hole which represents the influence of the diverted flow is about a value of 2.75 d_s (d_s = depth of scour below bed surface) projecting into the contracted channel. Ahmad has expressed the scour depth as a function of the average discharge intensity in the contracted section. Such a discharge intensity can be shown to depend upon discharge intensity of the approach flow and the contraction ratio. (Ahmad's analysis was based upon his laboratory data at a constant contraction ratio of 1/2, which may be high for alluvial channels).

D. Description Of Scour Phenomenon

The rate of scour caused by contracted flow decreases rapidly as the depth of scour increases. If the depth of scour is plotted against time, it displays two basic types of curves (Figs. 4a and 4b), depending on the amount of bed-load supply into the scour hole.

In the case of no bed-load supply, the scour history displays a trend as shown by Fig. 4a. After a certain period of time, the increase of scour is so small that the scour depth may appear to reach a limit. However, continuous increase of scour can be detected if the time of scour is prolonged appreciably. Although Fig. 5 indicates that the depth of scour increases linearly with the logarithm of time and that the scour depth approaches infinity as time approaches infinity, it is reasonable to assume, according to the concept of critical tractive force, that there exists a limit of scour at the time when the bed shear in the scour hole falls below a critical value. However, the maximum scour in such a case can not be readily detected by prolonging the scour time, because the depth of scour increases asymptotically to its maximum value only as time approaches infinity. An assumption can also be made that there exists a transition before the scour reaches its maximum limit.

Where dunes are moving into the scour hole, the scour history follows a general pattern as shown in Fig. 4b. The depth of scour fluctuates as the sand dunes pass through the scour hole.

In general, there exists three periods of scour:

(a) Transition of scour establishment is an early stage of scour. Within this period, the depth of scour increases rapidly with time and the rate of scour decreases rapidly as the amount of scour increases.

(b) Establishment of scour is a second stage of scour. Within this period of time, the average depth of scour increases with the logarithm of time. Several investigators, such as Laursen (14), Doddiah (15), and Ahmad (13) have attempted to analyze the relationship between depth of scour and time within this period.

(c) Transition to maximum scour is the latter stage in which the depth of scour approaches a maximum. When there is no bed-load supply into the scour hole, this period can not be defined easily by experiments. The existence of such a period is based upon the concept of critical tractive force. In case of appreciable bed-load supply moving as dunes, this period can be defined by experiments.

The preceeding classification depends upon the mode of the bed-load movement of the approaching flow. As long as the bed shear of the approach flow does not cause ripples to form, the scour history will be of the type shown in Fig. 4a, otherwise the scour history will be as shown in Fig. 4b.

As shown in Fig. 4b, the depth of scour, after reaching a maximum, decreases and eventually reaches an equilibrium depth of scour. Such a phenomenon can be explained as follows:

According to the principle of continuity, the sediment discharge at Section I (cross-sectional area a short distance upstream from abutment) plus the scouring capacity at Section II (cross-sectional area at the abutments) should equal the total transport capacity of the contracted flow. Which means that under a given transport capacity of the contracted flow, the scouring capacity will increase if the sediment supply decreases. As the depth of scour increases, the following changes are inevitable: the elevation of water surface at Section I decreases; hence, the sediment supply from Section I increases, and both the transport capacity and the scouring capacity of the contracted flow decreases. If the increase of sediment supply as a result of decrease of water surface at Section I is greater than the transport capacity of the contracted flow, the scour hole will be backfilled. At the stage of equilibrium depth of scour, the sediment supply, i.e., the transport capacity of the approaching flow, is equal to the transport capacity of the contracted flow.

E. Mechanics Of Scour

Assuming that the scour hole is shaped as a partial cone (see Fig. 2) and the angle of the inclination, θ, is approximately equal to the angle of repose of the bed material, an element of the volume of scour $\Delta\Psi_s$ for a unit cross-section can be expressed approximately as:

$$\Delta\Psi_s = \Delta d_s \cos\theta \frac{d_s}{\sin\theta} \cdot 1 \qquad (13)$$

in which

d_s is the depth of scour at time t

Δd_s is the increase of scour within a time interval Δt

the scouring capacity of the contracted flow is

$$\Delta Q_s = \frac{\Delta V_s}{\Delta t} = d_s \cot\theta \frac{\Delta d_s}{\Delta t} \tag{14}$$

Let q_{s1} be the intensity of sediment supply at Section I and c be the width of flow which is contracted as a result of the obstruction, and ξ is a variable denoting the distance perpendicular to the bank. The total sediment supply is

$$Q_{s1} = \int_0^c q_{s1} \, d\xi \tag{15}$$

Let the local transport capacity at the constriction be $q_{s2}(\xi, d_s)$. The total transport capacity at the constriction is

$$Q_{s2} = \int_a^c q_{s2} \, d\xi \tag{16}$$

in which a is the length of the constriction perpendicular to the main flow. According to the principle of continuity

$$Q_{s2} = Q_{s1} + \Delta Q_s \tag{17}$$

that is

$$\int_a^c q_{s2} \, d\xi - \int_0^c q_{s1} \, d\xi = d_s \cot\theta \frac{\Delta d_s}{\Delta t} \tag{18}$$

Both q_{s2} and q_{s1} depend upon local boundary shear, velocity distribution, and turbulence characteristics, all of which are functions of d_s and ξ .

It should be mentioned that as d_s increases q_{s1} increases, but q_{s2} decreases.

When the depth of scour reaches a maximum, $\frac{\Delta d_s}{\Delta t} = 0$. Eq (17) becomes

$$Q_{s1} = Q_{s2} \tag{19}$$

If $q_{s2}(d_s, \xi)$ and $q_{s1}(d_s, \xi)$ could be expressed explicitly as functions of d_s, and ξ, the scour depth could be expressed as a function of time by solving Eq (18). In view of the fact that information on mechanics of sediment transport related to such non-uniform and curvilinear flow is virtually nonexistent, Eq (18) can not be solved analytically at present.

F. Dimensional Analysis

In order to form a usable criterion for analysis of data, and to interpret the phenomenon of local scour, a dimensional consideration is given as follows:

The depth of scour d_s may depend upon the following variables:

- t time of scour
- Q total discharge
- h_n depth of the approach flow
- V_o velocity of the approach flow
- B channel width
- Q_s total sediment transport of the approach flow
- S energy gradient
- d characteristic size of the bed material
- $\Delta\gamma_s$ submerged specific weight of the bed material

ω representative fall velocity of the bed material

ρ density of water

g gravitational constant

μ dynamic viscosity of the water-sediment mixture

a length of the obstruction perpendicular to the flow

θ skew angle with respect to the flow direction

G the geometry of the obstruction

i.e.,

$$d_s = \phi_1(t, Q, h_n, V_o, B, Q_s, S, d, \Delta\gamma_s, \omega, \rho, g, \mu, a, \theta, G) \quad (20)$$

The fall velocity, ω, is used to include the factor of particle shape. Should the particle shape be considered an unimportant factor, either $\Delta\gamma_s$ or ω should be eliminated from Eq (20).

A further consideration of the problem indicates that some of the variables in Eq (20) are not independent variables. These dependent variables, except d_s, should be eliminated as follows:

Since

$$Q = V_o B h_n \quad (21)$$

$$Q_s = \phi_2 (S, Q, B, \rho, \mu, g, d, \Delta\gamma_s, \omega) \quad (22)$$

and

$$h_n = \phi_3 (S, Q, B, \rho, \mu, g, d, \Delta\gamma_s, \omega) \quad (23)$$

or

$$S = \phi_4 (h_n, Q, B, \rho, \mu, g, d, \Delta\gamma_s, \omega) \quad (24)$$

Q, Q_s, and S can be eliminated by substituting Eqs (21), (22), and (24) into Eq (20).

Therefore,

$$d_s = \theta_5 (t, h_n, V_o, B, d, \Delta\gamma_s, \omega, \rho, g, \mu, a, \theta, G) \quad (25)$$

or

$$\phi_6(d_s,\ t,\ h_n,\ V_o,\ B,\ d,\ \Delta\gamma_s,\ \omega\ ,\ \rho,\ g,\ \mu,\ a,\ \theta,\ G) = 0 \qquad (26)$$

If h_n , V_o , and ρ are selected as the repeating variables, Eq 26 can be arranged into dimensionless π-terms as follows:

$$\phi_7\left(\frac{d_s}{h_n}\ ,\ \frac{t\ V_o}{h_n}\ ,\ \frac{B}{h_n},\ \frac{d}{h_n},\ \frac{\rho V_o^{\,2}}{\Delta\gamma_s h_n}\ ,\ \frac{\omega}{V_o}\ ,\ \frac{V_o^{\,2}}{gh_n}\ ,\ \frac{\rho V_o h_n}{\mu}\ ,\ \frac{a}{h_n}\ ,\ \theta\ ,\ G\right) = 0 \qquad (27)$$

Under the assumption that the shape factor of the bed material is of minor importance on the depth of scour, either the term $\frac{\rho V_o^{\,2}}{\Delta\gamma_s h_n}$ or $\frac{\omega}{V_o}$ can be eliminated from Eq (27). Experience shows that ω is a very significant parameter in the study of sediment transport and does depend on shape of the particle. Therefore it is advantageous to retain $\frac{\omega}{V_o}$ and eliminate $\frac{\rho V_o^{\,2}}{\Delta\gamma_s h_n}$. Eq (27) becomes more meaningful, if it is written:

$$\frac{d_s}{h_n} = \phi_8\ \left(\frac{tV_o}{d}\ ,\ \frac{a}{h_n}\ ,\quad \theta,\ G\ ,\ \frac{V_o^{\,2}}{gh_n}\ ,\ \frac{B}{a}\ ,\ \frac{d}{h_n}\ ,\ \frac{\omega}{V_o}\right) = 0 \qquad (28)$$

In Eq (28) the terms are approximately given in the order of their importance on the depth of scour. The π-term $\frac{\Delta\gamma s}{\gamma}$ has been omitted from Eq (28). Eq (2) was used as a guide in planning the experiments and in analyzing the data.

V. EQUIPMENT AND PROCEDURE

A. Equipment

The equipment used in this study may be described under the headings:

1. Flumes
2. Flow systems
3. Sediment
4. Models
5. Measuring devices

1. Flumes

Two separate flumes were used in the experiments: (1) a tilting flume measuring 160 feet long, 8 feet wide, and 2 feet deep (referred to in this report as the 8-foot flume) and (2) a tilting flume measuring 80 feet long, 4 feet wide, and 2 feet deep (referred to in this report as the 4-foot flume). In addition, the 8-foot flume had a recessed box section, resting on the laboratory floor, 20 feet long, 8 feet wide and approximately $6\frac{1}{2}$ feet deep. The recessed box, located near the middle of the flume length, allowed for full vertical development of the scouring action around abutments placed in this section. A view of the 8-foot flume and the 4-foot flume are shown in Photo (5) and Fig. 10, respectively.

The 8-foot flume rests on a pair of 6-inch I-beams spaced 4 feet apart. The I-beams are supported by pairs of mechanical, screw jacks spaced from 8 to 10 feet apart along the length of

the flume. Solid, round, steel bars, used as guide rails for the instrument carriage, were mounted on top of each flume wall by means of adjustable bolts spaced at one foot intervals.

The 4-foot flume was similar in construction to the larger 8-foot flume with the exception that there was no recessed box section to provide for extensive vertical development of scouring action.

2. Flow Systems

The water supply for both the 8-foot and 4-foot flume was obtained from an underlying sump. Both flumes were provided with a manifold diffuser and a combination of wooden and wire mesh screens at the upper end of the flume to insure uniform distribution of flow.

After drawing sufficient water from the sump, the 8-foot flume utilized a closed recirculating system. The water-sediment mixture was then recirculated by a 7 cfs capacity or 14 cfs capacity centrifugal pump either separately or in combination. The 4-foot flume was fitted with a 5 cfs capacity pump which pumped directly from the sump--no recirculating system.

3. Sediment

River sand, having a median size of 0.56 mm (sieve analysis), and a mean fall velocity of 0.285 fps, was placed in the 8-foot flume to a depth of 0.7 ft. The size distribution of this sand (which was used throughout the experiments in the

8-foot flume) is shown in Fig. 6.

There were two sizes of sand used in the 4-foot flume: (1) the "filter" sand (runs 22-32, and 63-71) with a mean diameter of 0.65 mm and gradation as shown in Fig. 7, and (2) the "Black Hills" sand (runs 72-165) with a mean diameter of 0.56 mm and gradation as shown in Fig. 8.

4. Models

a. Orientation of crossing

1. Simple normal crossing is the case where the bridge crossing is normal to the main flow. Except in some runs, only one abutment model was placed in the flume.

2. Skew crossing is the case where the centerline of the roadway does not intersect the main flow at a right angle, but at an angle θ . The face of the abutment models was perpendicular to the roadway for all skew crossings.

b. Model geometry

Four types of abutments were tested: The vertical-board model (VB), the vertical-wall model (VW), the wing-wall model (WW), and the spill-through model (ST). All the models were made of 20-gage galvanized sheet metal. The lengths of the abutments were varied by adding extensions. The various abutment model shapes used in the 4-foot and 8-foot flumes are shown in Figure 9.

5. Measuring Devices

a. Orifice meter

Discharge delivered to the 8-foot flume by the 7-cfs pump was measured by a 10-inch stainless steel orifice located in the 12-inch supply line; whereas, discharge supplied by the 14-cfs pump was measured by a side-contracted orifice located in the 19-inch supply line. Differential manometers were used in both cases to register the pressure difference across the orifice plates. Discharge delivered to the 4-foot flume was measured by an orifice in an 8-inch supply line. A V-notch weir, located in the tail box at the end of the 4-foot flume, was used as a second discharge measuring device.

b. Point gage

Water-surface and bed-surface elevations at any point in the two flumes were measured by means of carriage mounted point-gages. The point-gages were equipped with verniers to measure to the nearest 0.001 ft. The carriages traveled along the flume on guide rails which were mounted on the side walls of the flume. The point-gages were also fitted to slide transversely across the flume on rails mounted on the carriage. Steel tapes fixed on the walls of the flume and on the carriage were used respectively for longitudinal and transverse location of the point-gage readings.

c. Sonic depth sounder

An instrument termed a Sonic Depth Sounder (17), see Fig. 10, was used to measure the variation in depth of scour with time. In this instrument ultrasonic sound waves produced by an electrically pulsed piezoelectric crystal were used to measure the distance from the transducer face to the sand bed. The crystal on being electrically pulsed vibrated at its natural frequency for a short period (a few cycles) which resulted in a short burst of sound energy which traveled through the water to the sand bed. Most of the sound was then reflected back to the transducer. The time interval between the start of the sound wave from the transducer and the return of its echo from the stream bed was proportional to the distance between the face of the transducer and the bed surface. The Sonic Depth Sounder measured this time interval and converted it to a distance which was recorded automatically, see Fig. 12.

d. Bubbler gage

A pressure recording bubbler system with a servo manometer, designed by the United States Geological Survey Instrumentation Research and Development Unit, was used as an indicator of slope for the 8-foot flume (18). The device was connected through plastic tubing to two taps 100 ft apart in the flume wall. The pressure difference (and thus the slope of the water surface) between the two

points with respect to time was measured and recorded by the bubbler gage. This system was based on the manometer principle with a flotation unit as an indicating device. A recorder connected to the flotation unit recorded the water-surface slope with time, see Fig. 11.

e. Sediment sampler

At the downstream end of the flume a total sediment sampler was used for measuring the sediment concentration. The sampler which sampled a vertical section of the water-sediment mixture at a time could be moved transversely across the flow to determine an average sediment concentration.

f. Miscellaneous instruments

An engineers' level and a rod were used for setting the flume slope, adjusting the rails, and determining all reference elevations. Confetti and potassium permanganate were used to observe eddies and flow patterns.

B. Procedure

Experimental procedure involved gathering data on backwater (drop across the embankment, Δh_s), depth of scour, cross-sectional area of the scour hole for different discharges, embankment length, flow depths, orientation of bridge crossings, and model types.

The general test procedure was as follows: (a) the desired flume slope was set approximately; (b) an equilibrium flow condition for a given discharge was established. The normal depth of flow under these conditions was determined and recorded; (c) abutment model was placed in the flume and

necessary data were taken; and (d) when the scour hole reached equilibrium the flow was stopped, the scour hole was contoured, and photographs of the contoured hole were taken.

1. Establishing Normal Flow

After setting the required flume slope, the desired discharge was established. A constancy in the water-surface slope and bed slope were considered as a criterion for equilibrium. Measurements of elevation along the centerline of the water surface and of the bed surface were taken every 2 feet along the length of the flume by means of a point gage. The tailgate was adjusted to obtain the desired depth. The difference between the average water surface and the average bed surface under equilibrium conditions was used as the normal depth of flow.

2. Placing Models

After an equilibrium condition had been established, the flow was stopped. Water was allowed to drain out through a drain valve located at the bottom of the recess box in the vicinity of the test section. A hole was dug in the bed at the test section and the abutment model was installed. Cracks between the model and the flume wall were sealed with modeling clay. After the bed material sand was backfilled around the model and tamped to its original elevation, the required normal flow discharge was re-established.

3. Collection of Data

The following data were taken:

a. The drop of water surface, Δh_s, across the embankment was determined by a point-gage at a time immediately after the beginning of each experiment, Δh_{si} (see Table I) and also when the scour had reached equilibrium, Δh_{sf} (see Table I).

b. The history of scour was obtained by use of the Sonic Depth Sounder (see Fig. 12); and by point-gage readings taken at selected intervals. Data were generally taken until the scour hole reached equilibrium.

c. Cross-section of scour perpendicular to the flow was measured with the point gage at the section of maximum scour, after the flow had been stopped.

4. Contouring the Scour Hole

The bed surface was contoured at 0.2-ft intervals after the flow had been stopped. The contoured mound and scour hole were recorded by photographs as shown in Fig. 13.

5. Photography

In addition to photos, taken of the contoured scour holes, pictures were also taken of the physical testing set-up including the flumes, models, the various measuring devices, and phenomenon concerned with flow patterns and scour at the abutments. A representative group of photos illustrating the contoured scour holes and other aspects of the study are grouped in Appendix A.

Several hundred feet of moving pictures (16 mm color film) were taken in an attempt to illustrate particularly the flow pattern and scouring action in the vicinity of the abutment. Some time-lapse photography was included showing the development of the scour hole and accompanying movement of scoured material out of the scour hole in the form of bed load.

VI. PRESENTATION OF DATA

Data obtained directly from laboratory measurements are tabulated in Appendix C, Table I. They can be classified into three categories:

A. Data Pertaining to Normal Flow

B. Data Pertaining to Scour

C. Data Pertaining to Backwater

A. Data Pertaining to Normal Flow

As mentioned earlier in this report, information on the normal flow is needed for studying the backwater and scour.

Before the installation of the abutment model, the flow had been run until an equilibrium condition was reached. History of the slope was recorded and plotted. Profiles of water surface and bed surface were taken frequently. In some cases concentration of sediment transport was measured--see page 106. The flow was considered normal when the water surface was approximately parallel to the bed profile, and the average depth of flow remained constant.

B. Data Pertaining to Scour

Depth of scour was measured with respect to the average normal bed surface by a point-gage and/or by the Sonic Depth Sounder. At the beginning of the run, the scour rate was quite high. During this period of time, the point-gage readings were taken at 3 to 5 minute intervals. Later, as the scouring action diminished, the point-gage readings were taken at intervals of 15 to 30 minutes.

C. Data Pertaining to Backwater

At the beginning of this research, considerable thought and time were given to determining the backwater, h_1^*, in an alluvial channel. It was reasoned that the backwater might be considerably less than that of a corresponding rigid-boundary channel, since any scour at the constriction would apparently reduce the backwater. However, obtaining a reasonable and consistent value of backwater, h_1^*, with point-gage measurements taken along the profile of the water surface in the area, upstream from the abutment, was quite difficult. The difficulty was attributed to the continually varying opening ratio, during the scouring process, and to the fluctuation of the water surface due to the changing pattern of the surface of the alluvial bed. Fluctuation of the water surface, due to surface waves, for instance, was often greater than the anticipated magnitude of the backwater.

Due to the unreliability of backwater values, h_1^*, determined by point-gage measurements of the fluctuating water surface profile, the attempt to measure the value, h_1^*, was abandoned in favor of, Δh_s, the drop across the embankment. Although the drop across the embankment value varied as the scouring action proceeded, reliably consistent values could be obtained with a point-gage. In addition, it was felt that the value of, Δh_s, drop across the embankment, was related to h_1^*, and gave some indication of the magnitude of the backwater to be expected upstream from the constriction.

VII. ANALYSIS OF DATA

A. Analysis of Normal Flow

Data on discharge and depth of flow are reasonably good for the experiments in the 4-foot flume. The slope of the 4-foot flume, however, was kept small in order to avoid bed load movement. For example, for bed material of 0.56 mm in size, the critical shear, T_c, is approximately 0.007 lb./sq. ft. Assuming the flow depth is 0.5 ft, the maximum slope should be

$$S = \frac{0.007}{62.4 \times 0.5} = \frac{0.007}{30.8} \approx 0.00023$$

which is so small that it cannot be measured accurately in a flume 80 feet in length. Hence, for convenience, the 4-foot flume was maintained at a zero slope; consequently, normal flow could not be established.

In the 8-foot flume, the flow generally carried appreciable bed load. The bed form changed appreciably with the change of flow condition. Considerable time was required to establish normal flow. In addition, the presence of sand waves caused considerable difficulty in determining the average depth of flow.

If the bed slope could have been maintained constant for all discharges, a plot of the discharge against the depth of flow, known as a rating curve, would be adequate for determining the accuracy of the data pertaining to the normal flow. Data of unreliable runs would not adhere to the rating curve. However, since the bed slope in the 8-foot flume could not be maintained constant, such a technique of checking normal flow condition was not possible.

Data of normal flow can be examined according to such characteristics as described by Liu and Hwang (4). However, due to the fact that the same sand mixture was used for several months by another project after the completion of Run 54 (September 10, 1958) and before Run 288 started (July 27, 1959), it was found that the mean size had been increased from 0.56 mm to approximately 0.60 mm owing to washing out of fine material. Variables pertaining to normal flow in the 8-foot flume have been grouped into two dimensionless parameters:

$$\frac{V*d}{\nu} \quad \text{and} \quad \frac{\frac{V}{V*}\frac{T_b}{\Delta\gamma_s d}\,S^{\lambda}}{\left(\frac{R_b}{d}\right)^{m} F_n^{N}}$$

in which λ, m, and N vary with the bed configuration and the mean size of the bed material. For the dune bed case, the exponents have the following values:

	λ	m	N
d = 0.56 mm	0.286	0.132	0.700
d = 0.60 mm	0.284	0.136	0.700

Fig. 14 is a plot of these two parameters for d = 0.56 mm. Fig. 15 is a similar plot for d = 0.60 mm. All runs shown on Fig. 14 had subcritical flow with dunes on the bed. In Fig. 15 those runs (No.312--314, 316--318, 319--324, 331--333) which had subcritical flow with dunes are along the upper line, those which were nearly critical with long bars on the bed are along the lower line. The lower family of runs can be considered as a case of transition. The slope measurements for all transition cases were not accurate, particularly for runs 288, 290, and 291.

If the analysis of normal flow is continued according to the approach given by Liu and Hwang, the mean velocity of flow over a dune bed can be written as for:

d = 0.56 mm

$$V = 20\, h_n^{0.54}\, S^{0.33} \tag{25}$$

and for d = 0.60 mm

$$V = 22.5\, h_n^{0.57}\, S^{0.34} \tag{26}$$

for the case of transition with d = 0.60 mm

$$V = 33\, h_n^{0.57}\, S^{0.34} \tag{26a}$$

The change of discharge coefficient from 22.5 to 33 signifies that a bed consisting of long bars offers less resistance to flow than a bed consisting of dunes. Eqs 25, 26, and 26a are obtained directly from Fig. 14 and 15 by writing equations for the straight lines and reducing them to terms of h_n, and S, and the discharge coefficient. Velocities computed according to Eq 25, 26, and 26a have been compared with those computed according to the continuity principle and shown in Fig. 16. Data pertaining to runs 288, 290, and 291 have been deleted for the reason stated previously. Fig. 16 indicates that the Liu-Hwang formula yields satisfactory results once the bed configuration and the size of the bed material are known.

Computations for normal flow in the 8-ft flume are tabulated in Table II - Appendix C. Some data on total load were measured and recorded, page 106. It was found that total sediment transport varied considerably due to sediment wave movement, and that a large number of measurements are necessary to determine more accurately the sediment load.

The bed material used in the 8-ft flume was coarse enough so that in most cases the total load was essentially the bed load only. Existing methods of computing bed load by Straub and by Kalinske were used. However, the computed bed loads deviated appreciably from the measurements.

B. Analysis of Scour Data

This portion of the analysis will be divided into several parts:

1. Equilibrium depth of local scour
2. Maximum depth of local scour
3. History of local scour
4. Cross section and volume of local scour

1. Equilibrium depth of local scour

Although it is difficult to define, the effective value of the discharge intensity, q, has been used by Inglis, Blench, and Ahmad in predicting scour. Correlation of depth of scour and discharge intensity, based upon laboratory data, has been extended to prototype data by Blench (12) and by Izzard and Bradley (16). Despite considerable scattering of the data, there seems to be a fair correlation between scour and discharge intensity. (Note - no distinction was made by previous investigators between equilibrium scour, maximum scour, and scour). The reader should be reminded that it is difficult to determine the depth of scour during a flood, and consequently their correlation is only approximate.

In general, the Inglis-Blench-Ahmad approach can be expressed as

$$D_{SE} = d_{SE} + h_n = K\ q^{2/3} \tag{27}$$

in which D_{SE}, d_{SE} are the equilibrium depth of scour measured from the water surface and the bed surface respectively; K a coefficient, and q an effective discharge intensity. Eq 27 can be changed into the following form

$$\frac{d_{SE}}{h_n} + 1 = KF^{2/3}\ g^{1/3} \left(\frac{1}{M}\right)^{2/3} \tag{28}$$

in which

$F_n = \frac{V_n}{\sqrt{gh_n}}$, the Froude number of the normal flow

$M = \frac{b}{B}$, the opening ratio

(b = width of opening in constriction, B = width of channel). The use of the opening ratio, M, in Eq 28 results from the assumption that the discharge intensity through the contracted opening, i.e., q_b, is the effective discharge intensity. The foregoing approach stresses the argument that the effective discharge intensity or the flow velocity is the important factor in determining the final depth of scour.

Laursen has claimed that the final depth of scour is primarily a function of flow depth and length of embankment and not of flow velocity, provided that the flow is transporting an appreciable amount of bed load. Laursen has recommended

the curve on Fig. 3 for design purposes. Although Laursen's approach simplifies greatly the design procedure, his conclusion may be oversimplified. For example, it is a well known fact that wherever there is a concentration of flow, the discharge intensity is higher and the depth of scour is greater. Such a fact seems to support partially the validity of Eq. 27.

Experiments were made in this study to determine the effect of velocity on the equilibrium depth of scour. The depth of flow was maintained constant at 0.5 ft and conditions associated with two mean velocities, 1.2 fps and 2.1 fps, were investigated. As shown in Fig. 17, higher velocity caused greater scour. In addition, tests were made by varying Froude number from 0.3 to approximately 1.0 to determine the effect of Froude number, hence, the effect of velocity on d_{SE}. As shown in Fig. 18, $\frac{d_{SE}}{h_n}$ increases with Froude number F_n. It can be seen from these data that $\frac{d_{SE}}{h_n}$ is proportional to $F_n^{1/3}$. As indicated on Fig. 3, Laursen's design curve is essentially an envelope for Froude numbers less than 0.5.

Data obtained in this study indicate that for a constant Froude number, $\frac{d_{SE}}{h_n}$ is proportional to $\left(\frac{a}{h_n}\right)^{0.4}$, in which a is the length of the embankment. Consequently, $\frac{d_{SE}}{h_n}$ for vertical wall models, can be plotted against

$$F_n^{1/3} \left(a/h_n\right)^{0.4}$$ as shown in Fig. 18

An equation representing the average can be written as

$$\frac{d_{SE}}{h_n} = 2.15 \left(\frac{a}{h_n}\right)^{0.4} F_n^{1/3} \qquad (29)$$

Regarding Fig. 18 and Eq. 29, it should be pointed out that:

(a) Because $\frac{d_{SE}}{h_n}$ is proportional $F_n^{1/3}$, the effect of Froude number on depth of scour is not of primary importance. For example, a variation of F_n from 0.1 to 0.5 would change $F_n^{1/3}$ from 0.46 to 0.79. However, inclusion of the Froude number in Eq 29 properly indicates the effect of velocity on equilibrium scour.

(b) The application of Fig. 18--Eq 29 to prototype structures, even though parameter variation may include field conditions, should be used with considerable caution since model-prototype relationship knowledge is still lacking in this area.

(c) Fig. 18 is based upon laboratory data that resulted from considering relatively long periods of scour. In view of the fact that the duration of a flood in natural channels corresponds generally to only a few minutes of flow in the laboratory, the use of Fig. 18 for engineering purposes would result in an uneconomical design. Thus, it seems desirable to modify Fig. 18 and Eq 29 according to prototype data, so that a more economical criterion can be formulated. An alternative would be to use the information on scour history which will be discussed later in this report, and determine the depth of scour according to a suitable time scale.

The technique used for analyzing the vertical-wall and vertical-board data can also be applied to other types of abutments such as wing-wall and spill-through. Although suitable exponents of F_n and $\frac{a}{h_n}$ can be chosen so that figures similar to Fig. 18 can be obtained for the wing-wall and spill-through types, such an effort is not fully justified due to the limited amount of data. The relation for wing-wall and spill-through models has been shown in Fig. 19 below the line representing Eq 29 which is for the vertical-wall and vertical-board models. In general, values of d_{SE} for either WW or ST models are less than those for the vertical-wall or vertical-board models. In the prototype case, the type of abutment may account for only minor variation of d_{SE} because of the relatively long embankment.

Computed parameters related to scour are tabulated in Table III of Appendix C for the vertical-wall and vertical-board, wing-wall, and spill-through models.

2. Maximum depth of local scour

Maximum scour, d_{SM}, pertaining to vertical-wall and vertical-board models caused by flow carrying appreciable bed load have been plotted against $F_n^{1/3} \left(\frac{a}{h_n}\right)^{0.4}$ as shown in Fig. 20. In general, d_{SM} is larger than d_{SE} as expected. An equation fitting the data can be written as

$$\frac{d_{SM}}{h_n} = 0.3 + 2.15 \left(\frac{a}{h_n}\right)^{0.4} F_n^{1/3} \qquad (30)$$

In case the scour is caused by flow carrying no bed load, the depth of scour should asympotically approach a limit, d_{SL}, as time approaches infinity. In order to obtain such a limiting scour, a scour hole of a given depth, similar to those developed by the flow, was preshaped. Depth and discharge of the flow were adjusted until particles at the bottom of the scour hole began to move. The limiting scour, d_{SL}, was determined in this manner for various flow conditions and abutment lengths (Runs 101--287) and reported in Table I, Appendix C. When the approach velocity was large, the upstream bed was covered by cloth to prevent the approaching flow from moving the bed particles. Limiting scour conditions are shown in Fig. 21 in which T_o is the tractive force pertaining to the approach channel, and T_c is the critical tractive force. For $d_{50} = 0.56$ mm, $T_c = 0.007$ lb/sq. ft, and where $T_o/T_c > 1$, the bed of the approach channel was covered by cloth.

Data in Fig. 21 can be replotted as shown in Fig. 22 to obtain a straight line relationship. In Fig. 22, M appears to be an important factor. A comparison between Fig. 18 and Fig. 22 indicates that the scour caused by flow carrying bed load is a local phenomenon, while the scour caused by flow carrying no bed load is related to the over-all geometry of the constriction. Additional research is needed to clarify this paradox.

3. History of local scour

The classification of scour history shown as Fig. 4 is mainly for the convenience of discussing the final scour. Due to the fact that scour in natural streams seldom lasts long enough to reach d_{SE}, d_{SM}, or d_{SL}, the engineering problem is to estimate the depth of scour within certain flood periods.

Data on scour history have been plotted on semi-logarithmic coordinates on Figs. 5, 23, and 24.

In the beginning period of scour (designated as the transition of scour establishment in this report), the depth increases rapidly with time and the rate of scour decreases rapidly with increase in amount of scour. As in many other transitional phenomena, it is difficult to analyze this case. The depth of scour and the rate of scour in this period depend to a large extent upon the initial bed configuration and the characteristics of the local flow. During the second period of scour (designated as the establishment of scour in this report), the depth of scour can be expressed empirically as a function of t according to the following formula, which is a form of the equation given in reference (13):

$$d_s = d_{SM}\left[1 - e^{-c\frac{t}{t_o}\Big/\left(1-\frac{t}{t_m}\right)}\right] \qquad (31)$$

in which

d_s is the average depth of scour at time t.

d_{SM} is the maximum scour

t_o is a time factor

t_m is the time required for d_s to reach d_{SM}

$c = e^{A_o(1-y)^{1/2}}$

$y = \frac{d_s}{d_{SM}}$

and

A_o is a coefficient depending upon the model geometry, the flow condition, and the bed material.

When the flow carries appreciable bed load, t_m is finite. When the flow carries no bed load, t_m is infinite and d_{SM} is defined as d_{SL} such that Eq. 31 reduces to

$$d_s = d_{SL} \left(1-e^{-c\frac{t}{t_o}}\right) \qquad (32)$$

Fig. 23 is a typical example indicating that the depth of scour, d_s, caused by flow carrying bed load can be represented by Eq. 31. Fig. 24 indicates that the depth of scour, d_s, caused by flow carrying no bed load can be represented by Eq. 32. In Figs. 23 and 24, the time scale is in minutes, therefore, the horizontal location of the equation to fit the data determines the time factor t_o. Curvature of the curves representing Eq. 31 and Eq. 32 depends upon A_o. All three parameters, t_o, t_m, and A_o may depend upon the

characteristics of the flow, the properties of the bed material, and the geometry of the constriction.

Preliminary analysis indicates that for a given bed material and geometry of constriction, A_o depends upon F_n and M as shown in Fig. 25. Owing to the fact that Eqs 31 and 32 were developed during the last stage of the analysis of data, the information obtained during the tests is not sufficient to evaluate the parameters t_o, t_m, and A_o.

It is possible that Eq 31 and Eq 32 are also applicable to other cases of scour such as those caused by an impinging jet, flow over a spillway, and flow from a sluice gate. Additional research is needed in order to complete the analysis on the rate of scour.

4. Cross-section and volume of local scour

A photograph showing the contour of the scour hole at the end of a test when $d_s = d_{SM}$ is given as Fig. 13. The cross-section of the scour hole was measured at the end of the test period at the constricted section. In the case of scour caused by flow carrying appreciable bed load, it was found that the scour area varied considerably with time. Fig. 26 shows a typical example of such a case. It is reasonable to assume that the volume of scour also varies considerably with time. Analysis showed that there is no correlation between the scour area at $d_s = d_{SM}$, the flow parameters, and the

abutment geometry. However, there is some correlation if an average scour area over a long period of time is used.

The cross-sectional profile intersects a horizontal line at an average angle of 27° 30' near the vertical-wall model, and at an average angle of 22° in case of the spill-through model--the angle depending on the flow pattern resulting from the shape of the abutment. The angle of repose in air for the same material is about 30°.

C. Backwater in an Alluvial Channel

In report (1), data on h_1* and Δh_s in rigid channels were studied extensively. The effect of scour on the backwater was quite difficult to determine quantitatively because the magnitude of h_1* , measured in the laboratory, was of the same order of magnitude as the surface fluctuation caused by sand waves. Sometimes h_1* appeared to be negative or the entire water-surface profile was shifted higher or lower than the normal water-surface profile. Such higher or lower water surface was caused by the change of water volume in the flume when the discharge was re-established after the installation of the abutment. As a result the depth of flow, the mean velocity, the bed roughness, and the bed slope were all changed slightly, although the discharge was kept constant. Such slight change of the flow characteristics may not affect appreciably the depth of scour, but affect h_1* considerably.

In order to determine the maximum h_1* at the beginning of scour, attempts were made to stabilize the bed by covering the constriction

area with cloth. However, due to the instability of the cloth on the bed, and the difference in roughness between the cloth and the sand grains, the water-surface profile was affected. Backwater data determined by this method were deemed unsatisfactory and the procedure was discontinued.

In place of measuring the backwater, h_1^*, along the centerline of the constriction, the change in water surface elevation on the upstream and downstream side of the abutment, Δh_s, were made. Data on Δh_s seem to be more consistent than either the water-surface profile or the backwater, h_1^*. For the purpose of studying the effects of an alluvial bed on Δh_s, new criteria for determing Δh_s in rigid channels have been obtained by using data reported in a previous report (11), and are presented as Figs. 27, 28, and 29. Data on Δh_s in alluvial channels are compared with those in a rigid channel, as shown in Fig. 30.

All measured Δh_s values in alluvial channels seem to be considerably less than those found in rigid channels. For the conditions tested, it might be said that Δh_s in an alluvial channel is about sixty per cent of that in a rigid channel. Such a ratio will change if the bed material is changed. For example, if the material is so coarse that it can effectively resist any scour, the channel can be considered as being rigid. A quantitative general criterion cannot be given in this report because existing data are not sufficient to evaluate the erodability of the bed material.

It should be noted that in an alluvial channel, the problem of both high backwater and excessive scour can exist during one flood. At the beginning of the flood, the water level may reach a dangerous level.

As scour at abutments and piers develops, the flood may endanger the foundation of the bridge. More research is needed in order to determine the correlation of h_1^*, Δh_s, and the depth of scour as a function of flow condition, bed material size, and abutment geometry.

VIII. SUMMARY AND CONCLUSIONS

The objectives of this research were twofold:

A. To study the depth of scour under various flow conditions and constriction geometry.

B. To determine the effect of scour on the maximum backwater.

Valuable information and accurate data have been obtained satisfying the first objective. However, on account of difficulties mentioned earlier, only qualitative information was obtained pertaining to the second objective.

Throughout the study, the normal flow condition prior to the installation of abutment models was used as a reference in measuring the depth of scour, and certain other variables associated with the experiments.

Bed-load measurements for the normal flow did not check with computations based upon bed-load formulas, proposed by such authors as Kalinske, Meyer-Peter, and Straub. On the other hand, velocity measurements agreed satisfactorily with computations based upon the formula proposed by Liu and Hwang, provided that the bed configuration and the bed material size were known.

There are three major controversial factors affecting maximum local scour:

A. The effect of sediment size

B. The effect of flow velocity

C. The effect of opening ratio

The effect of sediment size on scour was not considered in this study. The effect of flow velocity on scour is appreciable. The effect of opening ratio on scour is not fully understood--such an effect may be secondary compared to that of the flow depth. When the flow carries appreciable bed load, the opening ratio has no appreciable effect on the depth of scour. However, when the flow carries no bed load, the limiting maximum scour is found to be a function of the opening ratio.

For convenience, the history of scour may be divided into three periods:

A. Transition of scour establishment

B. Establishment of scour

C. Transition to maximum scour

A general empirical equation has been found to describe the second period (see Eq 31). This equation is valid regardless of whether the flow carries bed load or not.

Owing to the lack of such information as velocity distribution, pressure distribution, and sediment movement in the vicinity of the constriction, the mechanics of scour could not be studied thoroughly. Further research on the mechanics of scour is recommended. The approach used in this report is empirical.

There were two flumes used for the experiments: (1) an 8-ft wide flume used mainly to evaluate the scour caused by flow carrying bed load--in this system, a natural sediment mixture was used, and (2) a 4-ft wide flume used mainly to study scour caused by flow carrying no bed load.

The maximum depth of scour can be classified as:

A. Maximum scour, d_{SM}

B. Equilibrium depth of scour, d_{SE}

C. Limiting depth of scour, d_{SL}

The maximum scour, d_{SM}, depends to a certain extent upon initial flow conditions. In case the flow does not carry bed load, the maximum scour is denoted as the limiting scour. The equilibrium depth of scour may exist if the flow carries appreciable bed load, and is usually less than the maximum depth of scour. In the laboratory, the time required to reach maximum scour or equilibrium scour is on the order of one to three days.

Both the equilibrium depth of scour and the maximum depth of scour are functions of the Froude number, the normal depth of flow, and the length of the embankment (see Fig. 18 and Fig. 20 for vertical-wall models). The limiting depth of scour is a function of the Froude number and the contraction ratio (see Fig. 22). Model geometry and size of the bed material may change such correlations considerably. Information on d_{SM}, d_{SE}, and d_{SL} obtained in the laboratory represents the ultimate maximum depth of scour. In order to use such information for engineering purposes, it is desirable to know the time scale and to utilize Eq 31 which expresses scour as a function of time. Further research is needed to evaluate the constants in Eq 31.

The volume of scour and cross-section area of scour at right angles to the flow vary considerably with time due to the movement of sand waves through the constriction.

Because of inherent difficulties, the backwater caused by a constriction in an alluvial channel could not be measured very satisfactorily. However, data on the difference of water surface elevation across the embankment are fairly consistent. For the sediment involved in the tests, the water-surface drop across the embankment is approximately 60 per cent of that in a rigid channel. It is expected, however, that this ratio varies with the bed material.

Although considerable information and a better understanding of scour caused by flow at bridge crossings have been obtained as a result of this research, an understanding of the mechanics of scour, and prototype measurements of scour and backwater are still lacking. It is recommended that field studies should be made to verify the laboratory results contained in this report and that additional theoretical research be encouraged to develop the mechanics of local scour.

ACKNOWLEDGMENTS

The authors wish to acknowledge the following officials and personnel who have assisted this research in various capacities: Mr. Carl F. Izzard, Chief, Hydraulic Research Branch, U. S. Bureau of Public Roads, who made this research possible; Mr. Joseph N. Bradley, former Research Engineer, U. S. Bureau of Public Roads, who offered valuable comments, suggestions, and assistance in carrying out this research; Mr. Dasel E. Hallmark, Research Engineer, U. S. Bureau of Public Roads, who has reviewed this report; Dr. Maurice L. Albertson, Director of Colorado State University Research Foundation, who initiated this research program and has reviewed this research from time to time; Dr. A. R. Chamberlain, Acting Dean of Engineering and Chief of Civil Engineering Section, who has contributed his effort to administer this research project, and Mr. R. V. Asmus, and his shop personnel, who have helped to maintain the equipment to make the testing program possible. Acknowledgment is also due to the following graduate students who have contributed their time and talent in this program: Mr. Ramesh Malhotra, Mr. H. Y. Hwang, Mr. S. S. Fan, and Mr. Nobu Yotsukura.

H. K. Liu supervised this research and was responsible for the preparation of this report. F. M. Chang has contributed considerably in the analysis of data and in the preparation of tables and figures. M. M. Skinner, Assistant Research Engineer, was responsible for carrying out the experiments and the final preparation of this report.

BIBLIOGRAPHY

1. Liu, H. K., Bradley, J. N., and Plate, E. J., "Backwater Effects of Piers and Abutments," Colorado State University. Civil Engineering Section. CER57HKL10, 1957.

2. Strickler, A., "Beiträge zur Frage der Geschwindegkeitsformel und der Rauhigkeritszahlem Für Ströme, Kanäle und geschlossene Leitungen" Eidg. Wasserwirtschaftsamt Berne, Mitteilung, 1923.

3. Einstein, H. A., and Barbarossa, N. L., "River Channel Roughness", Trans. ASCE., Vol. 117, 1952. p. 1121.

4. Liu, H. K., and Hwang, S. Y., "Discharge Formula for Straight Alluvial Channels," J. Hyd. Div. ASCE, Nov. 1959, Proc. No. 2260.

5. Liu, H. K., "Mechanics of Sediment-Ripple Formation," Journal of Hyd. Div. Vol. 83, HY 2, Proc. ASCE, April 1957.

6. Laursen, E. M., "Scour at Bridge Crossings," Journal of Hyd. Div. Proc. ASCE, No. 2369, Feb. 1960.

7. Straub, L. G. "Approaches to the Study of Mechanics of Bed Movement," Proc. Hydraulics Conference, State University of Iowa, Iowa City, Iowa, 1940.

8. Laursen, E. M., "The Total Sediment Load of Streams," Journal of Hyd. Div. Vol. 84, No. HY1, Pt. 1, Proc. ASCE, Feb. 1958.

9. Etcheverry, B. A., "Land Drainage and Flood Protection," Copyright, 1931, McGraw-Hill Book Co., Inc.

10. Khosla, Rai., Bahadur, A. N., Bose, N. K., and Taylor, E. McKenzie., "Design of Weirs on Permeable Foundations" Central Board of Irrigation, India, Publication No. 12, Simla, Sept. 1936, p.131.

11. Inglis, C. C., "The Behavior and Control of Rivers and Canals," Research publication No. 13, pt. I and II. Central Waterpower Irrigation and Navigation Research Station, Poona, India, 1949. pp. 327-348.

12. Blench, T., "Regime Behavior of Canals and Rivers," Butterworths Scientific Publications, London, 1957.

BIBLIOGRAPHY - Cont'd.

13. Ahmad, Mushtag., "Experiments on Design and Behavior of Spur Dikes," Proc. Minnesota International Hydraulics Convention, 1953. University of Minn., Minneapolis, Minn.

14. Laursen, E. M., "Observations on the Nature of Scour," Proc. 5th Hydraulics Conference, 1952. State University of Iowa, Iowa City, Iowa.

15. Doddiah, Doddiah, Albertson, M. L., Thomas, J. R., "Scour from Jets," Proc. Minnesota International Hydraulics Convention, 1953, p. 161. University of Minn. Minneapolis, Minn.

16. Izzard, Carl F. and Bradley, Joseph N., "Field Verification of Model Tests of Flow Through Highway Bridges and Culverts," Proc. 7th Hydraulics Conference, Bulletin 39, Studies in Engineering, State University of Iowa, Iowa City, Iowa.

17. Gray, Earl E., and Karaki, S. S., "Dual Channel Stream Monitor," Final report to Agricultural Research Service, Beltsville, Maryland, Aug. 1960, CER60SSK46.

18. U. S. Geological Survey, "Pressure Recording Bubbler System," Instrumentation Research and Development Unit, Columbus, Ohio.

FIGURES

Fig. 1 - Criterion for Ripple Formation

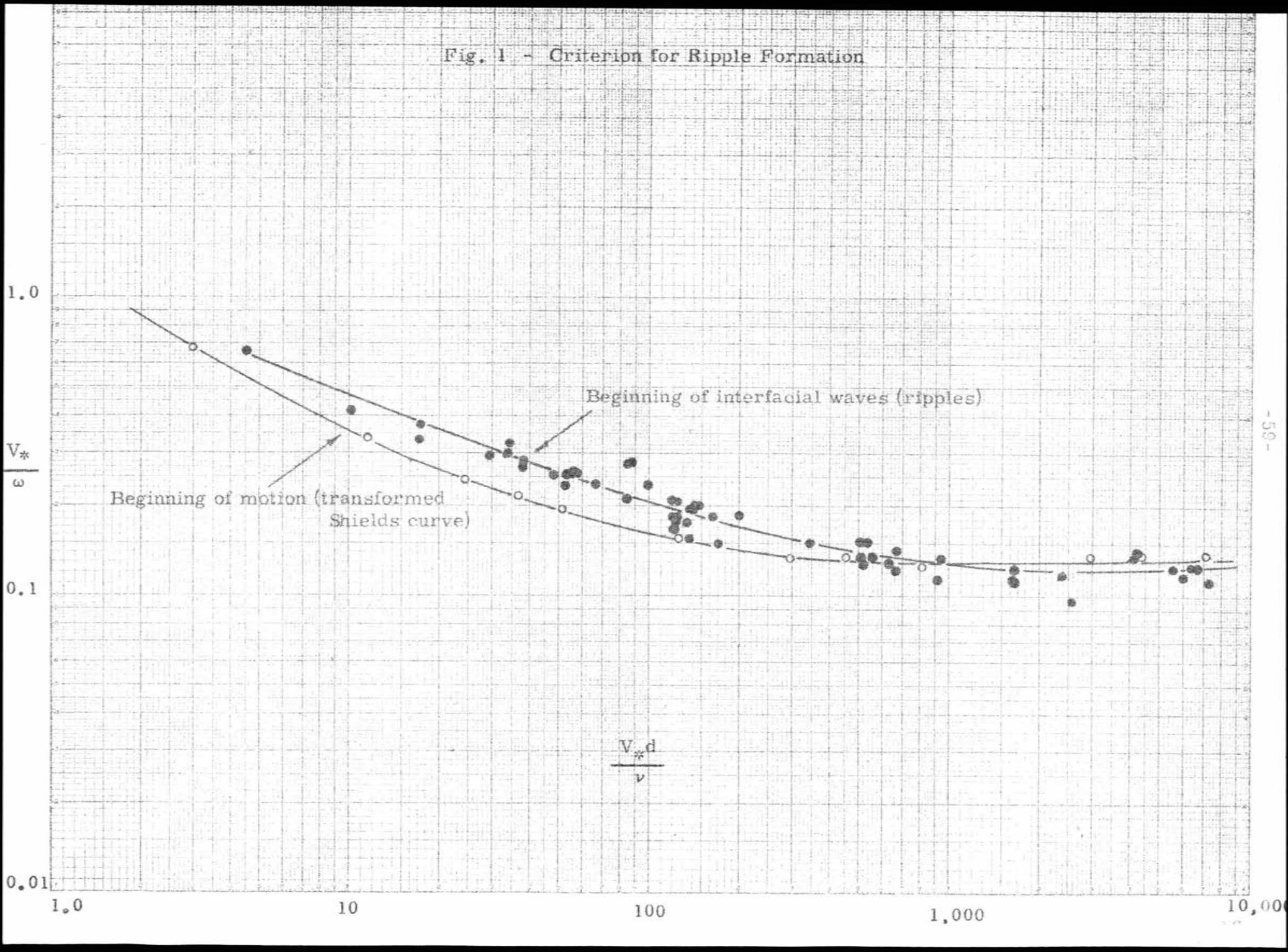

Fig. 2 - Side View of Scour Hole

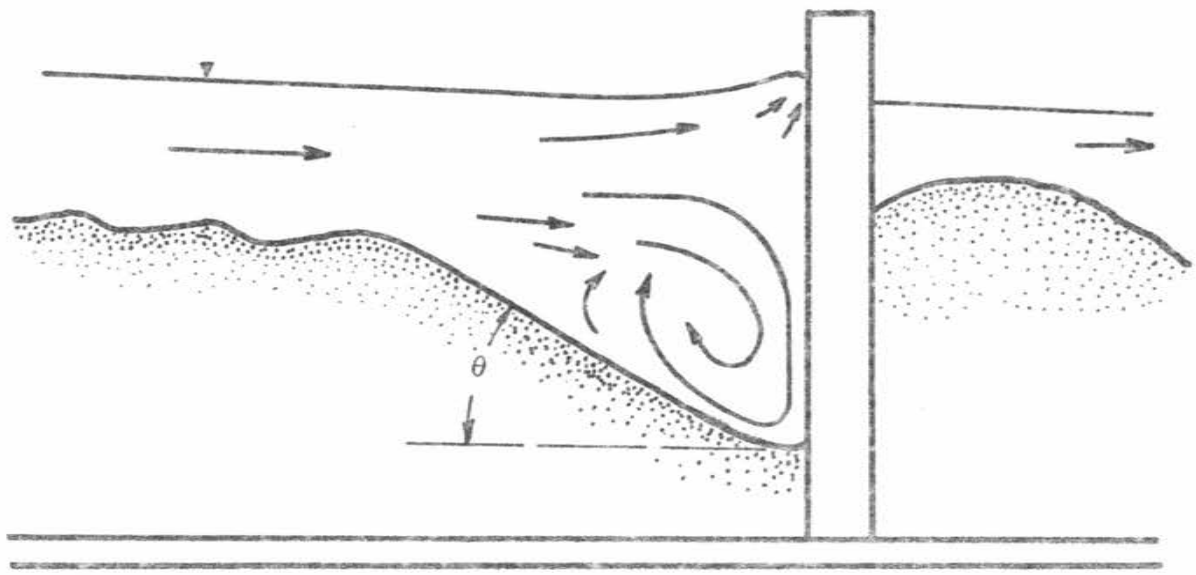

Fig. 3 - Comparison of Laursen's Curve with CSU Data

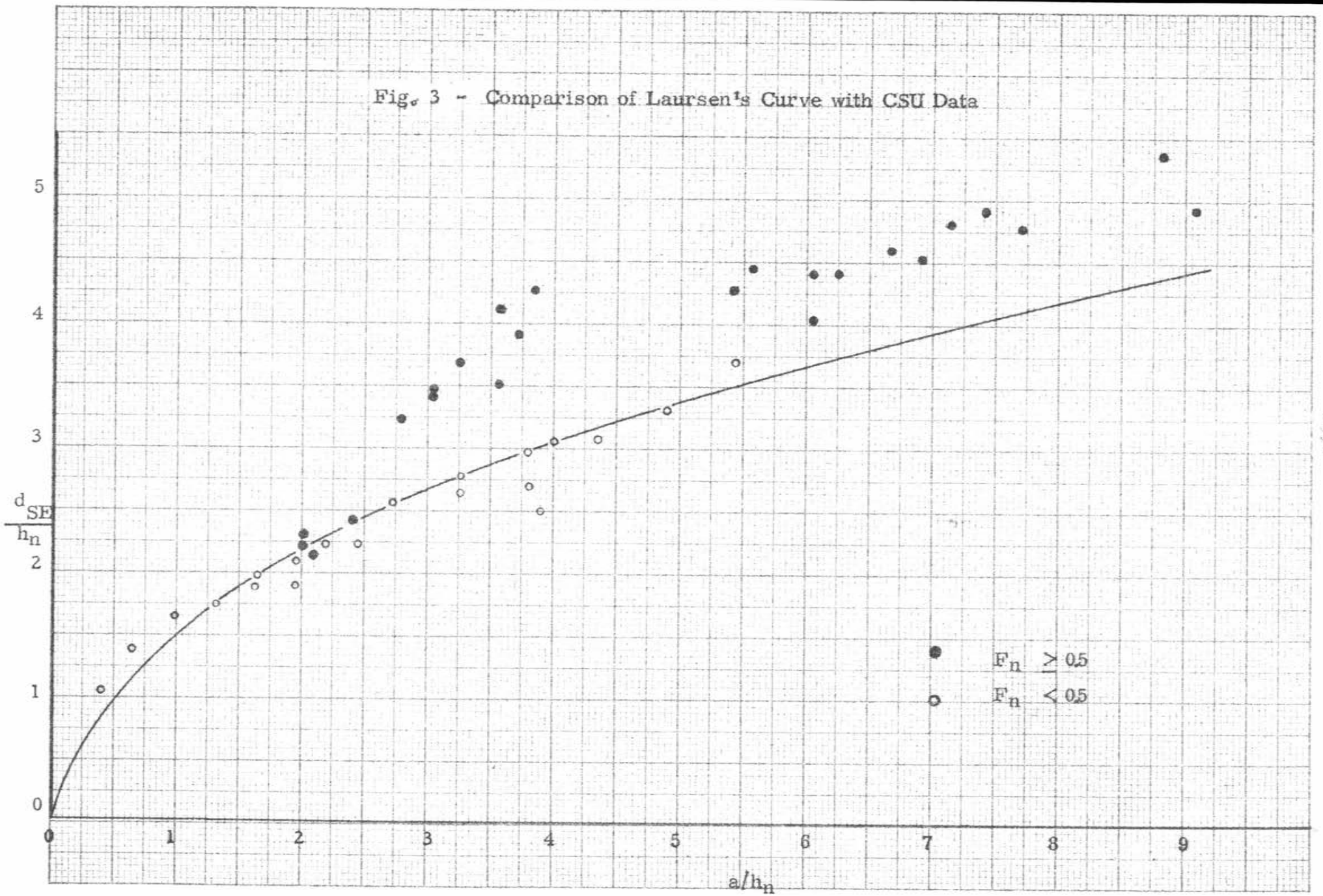

Fig. 4a - History of Scour - No Sediment Supply

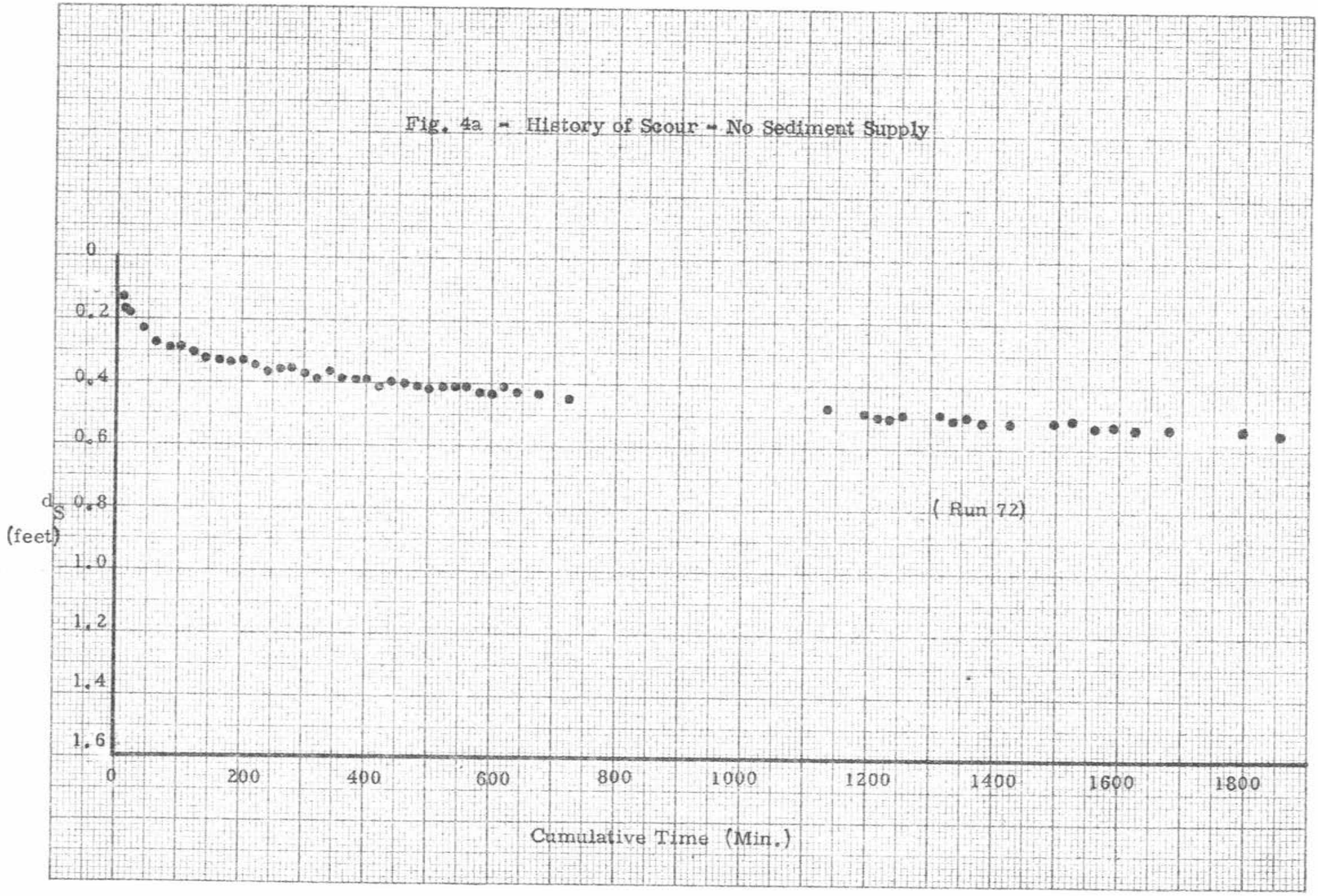

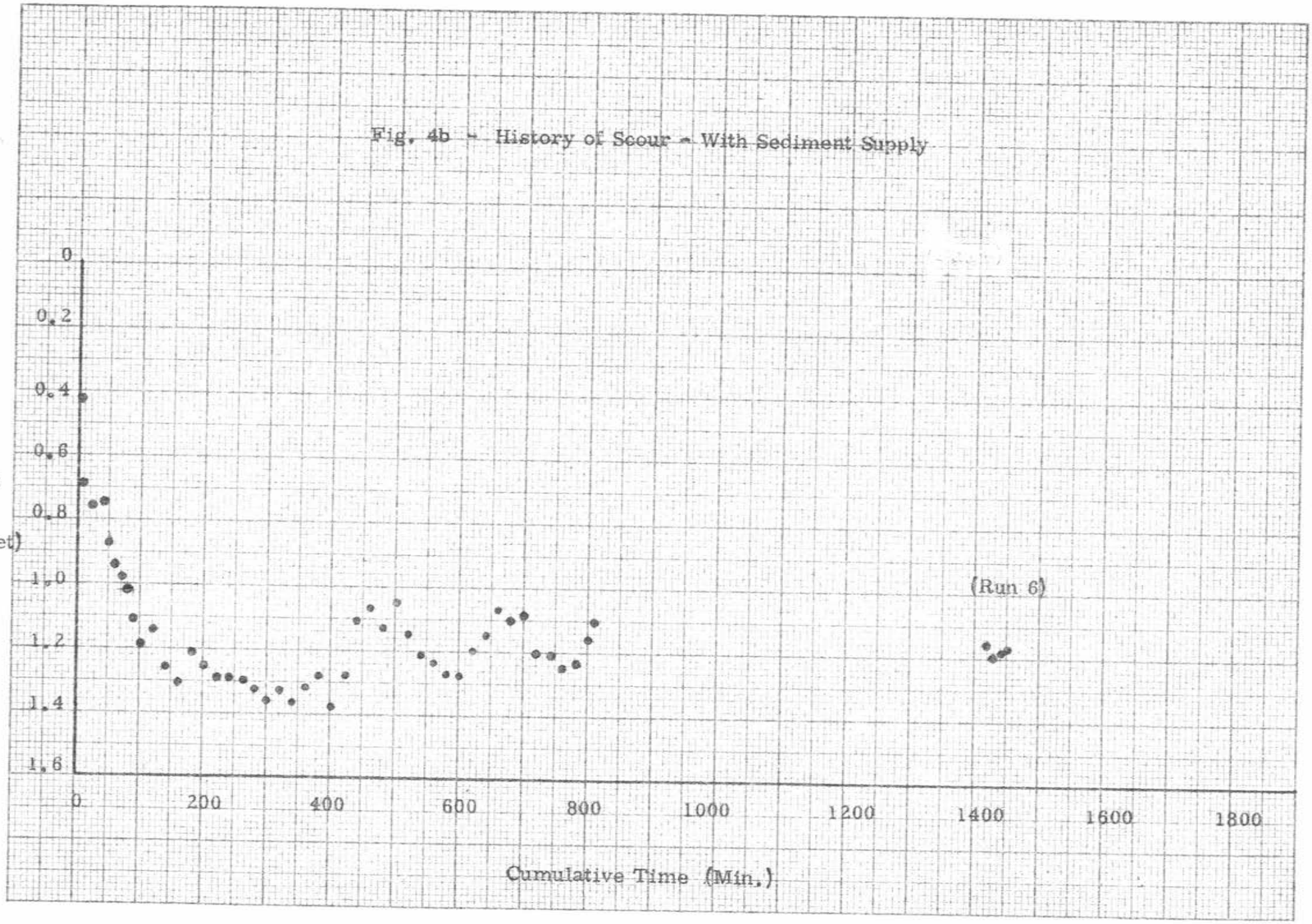
Fig. 4b - History of Scour - With Sediment Supply
0
0.2
0.4
0.6
0.8
1.0
1.2
1.4
1.6
(Run 6)
0
200
400
600
800
1000
1200
1400
1600
1800
Cumulative Time (Min.)

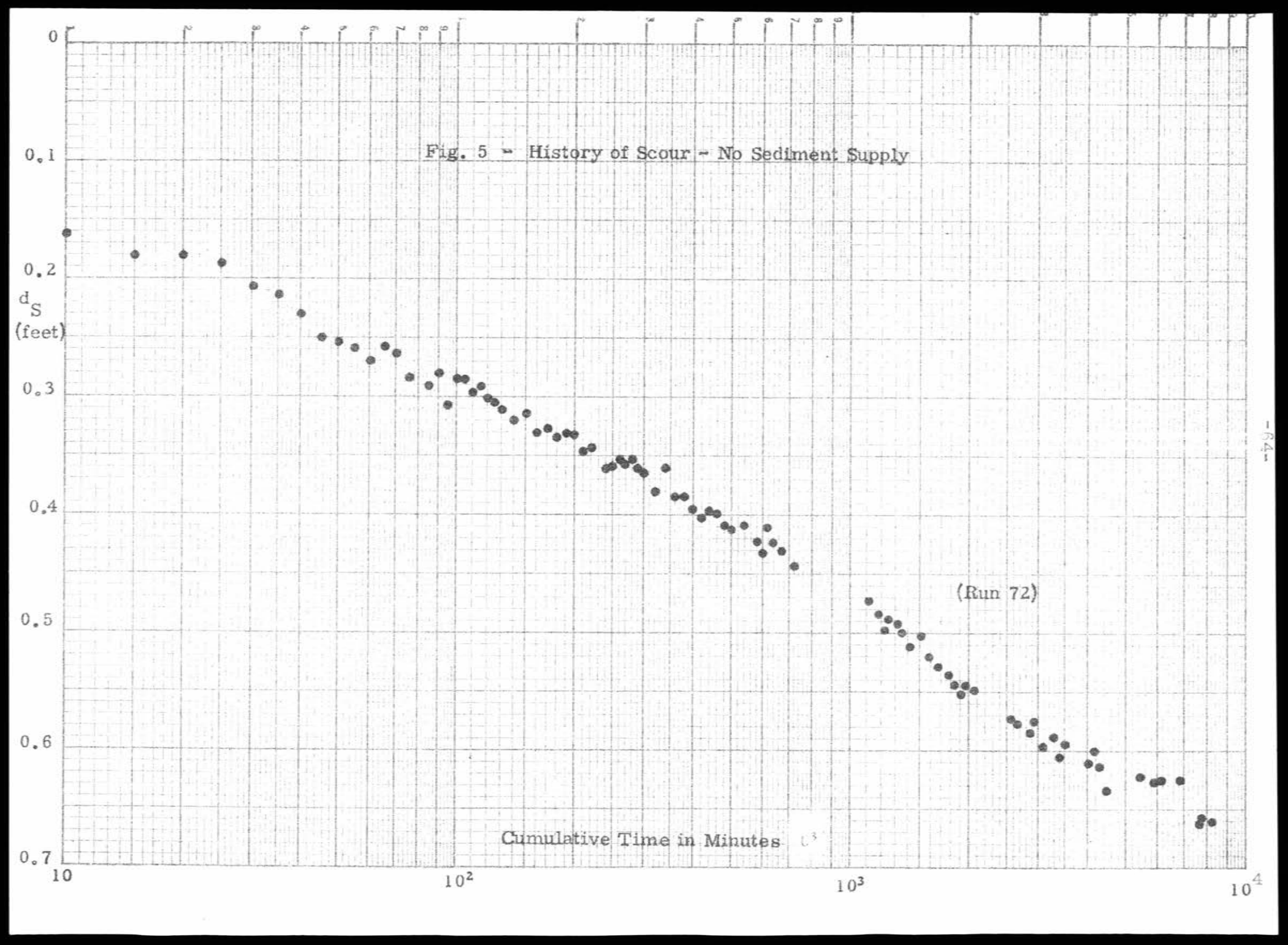

Fig. 5 - History of Scour - No Sediment Supply

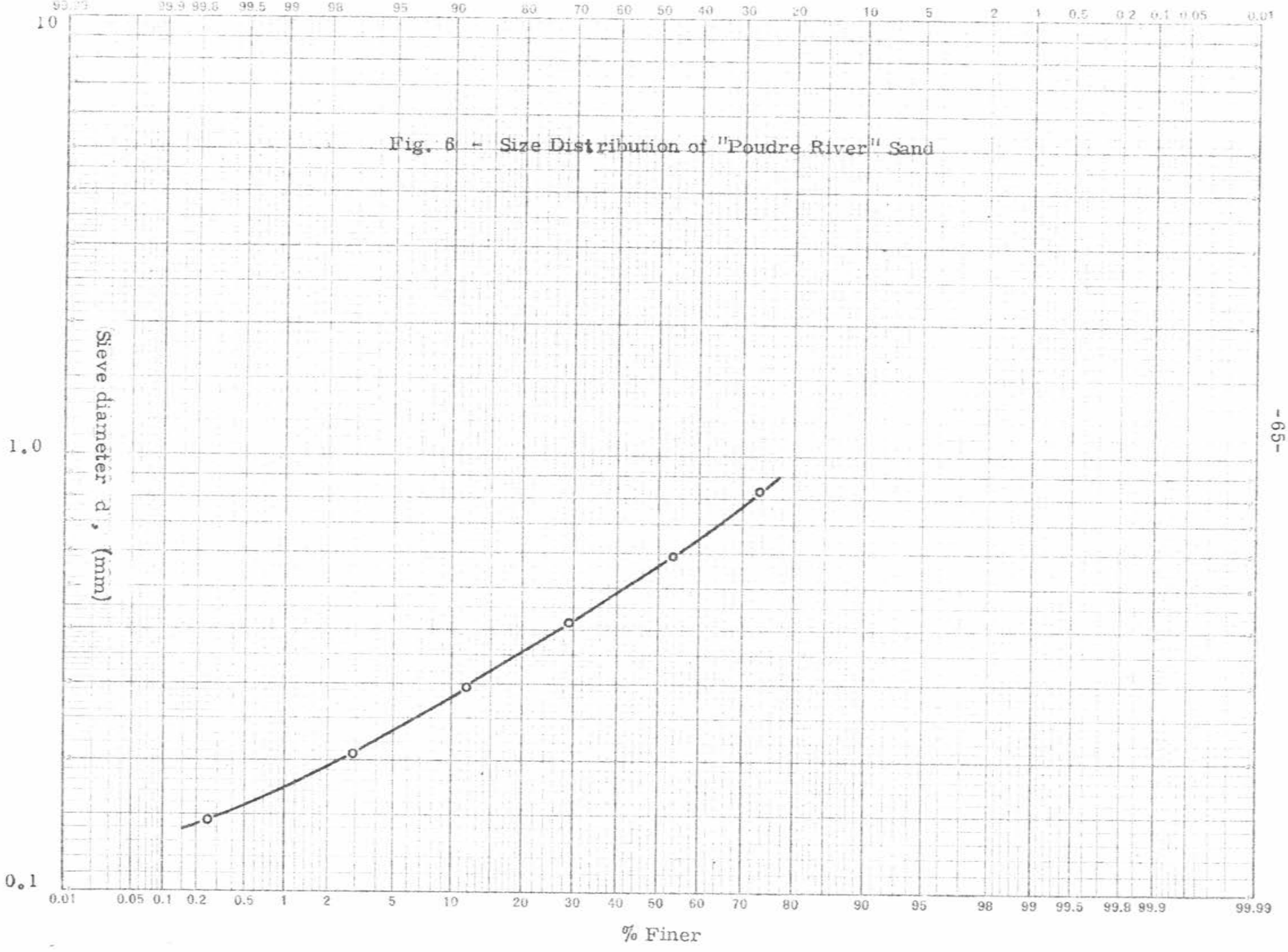

Fig. 6 – Size Distribution of "Poudre River" Sand

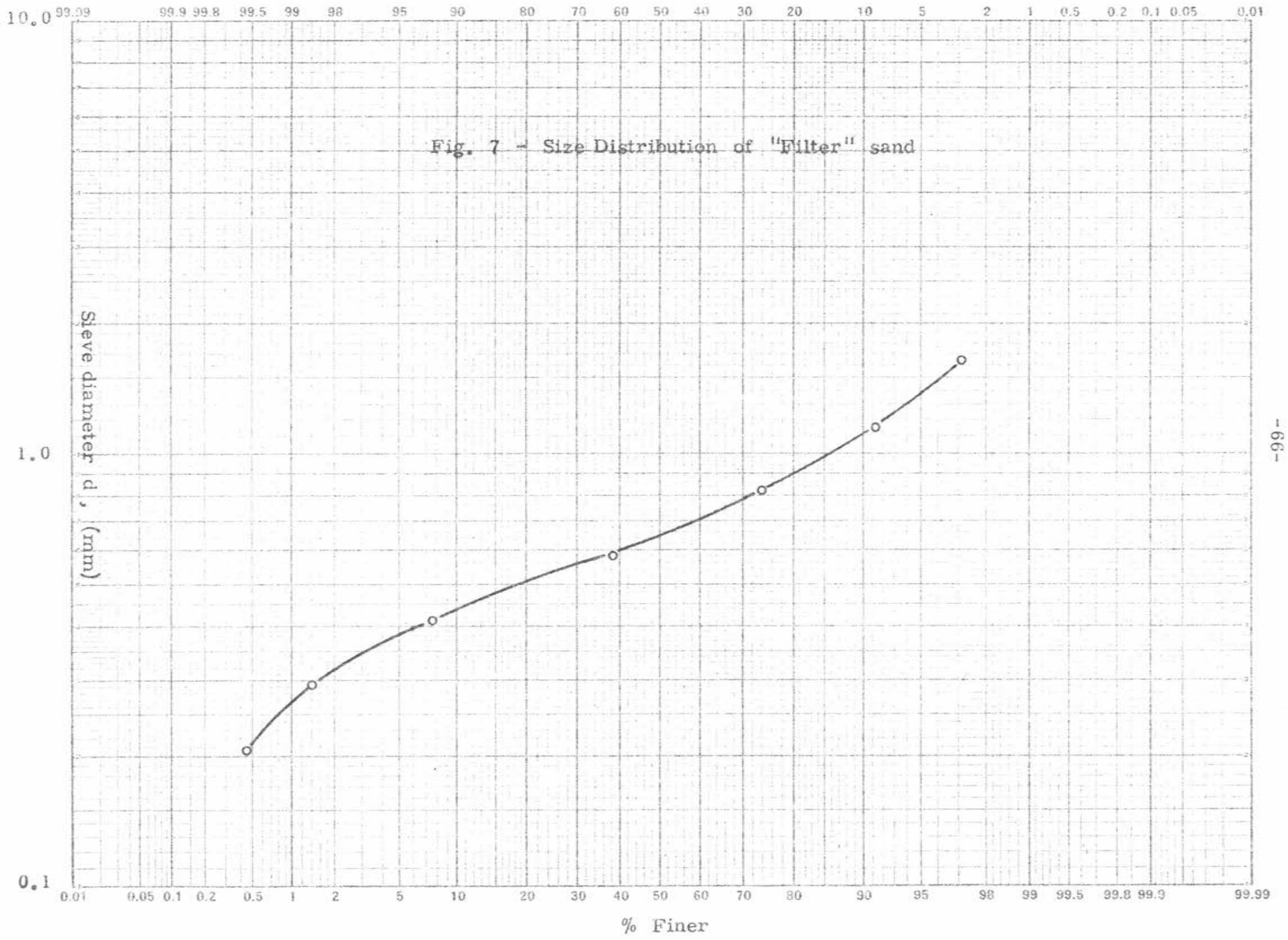

Fig. 7 - Size Distribution of "Filter" sand

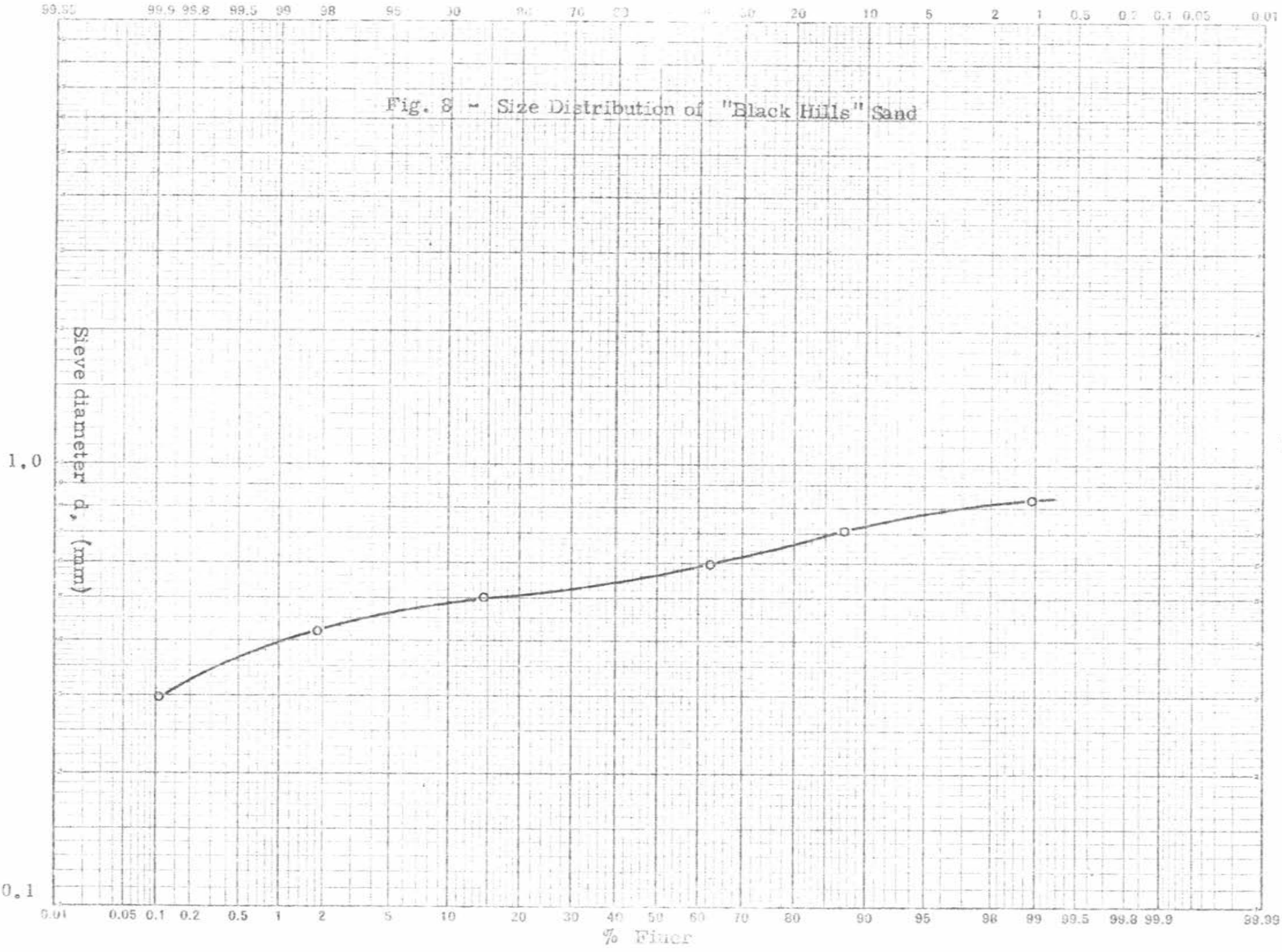

Fig. 8 - Size Distribution of "Black Hills" Sand

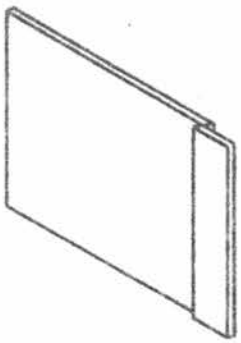

Vertical Board

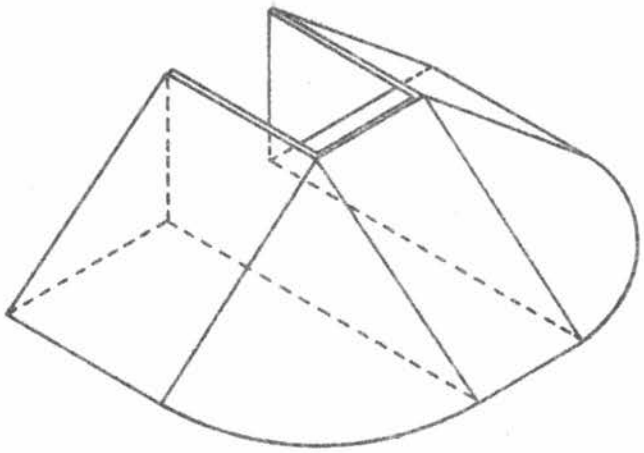

Spill-through

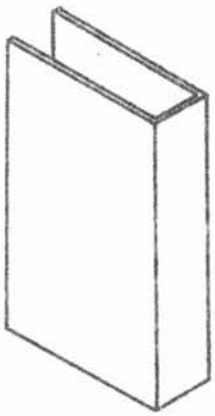

Vertical Wall

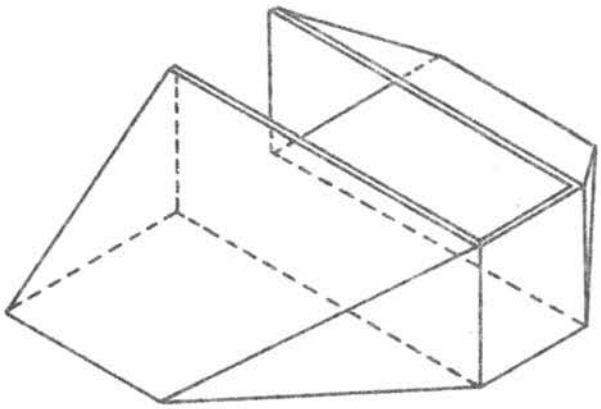

Wing-wall

Fig. 9 - Definition Sketch of Abutment Models

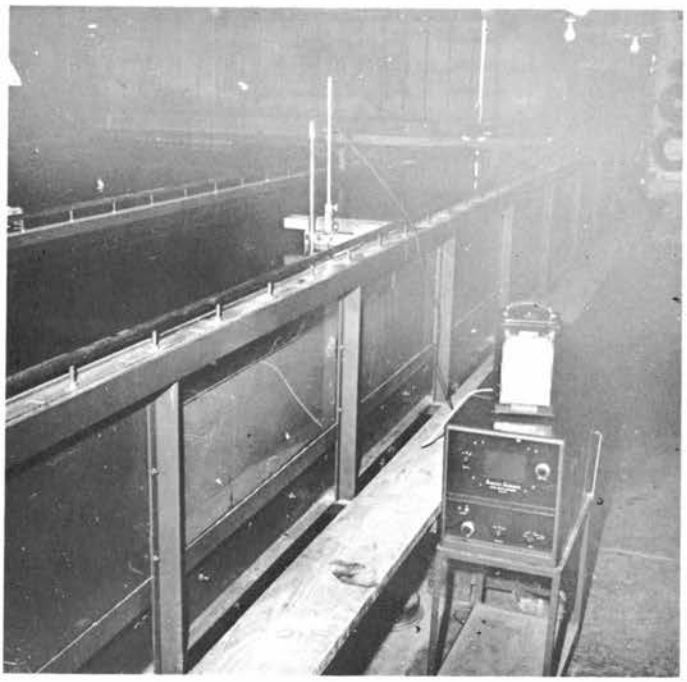

Fig. 10 - Sonic Depth Sounder

Fig. 11 - Slope vs Time (Recorded by Bubbler Gage)

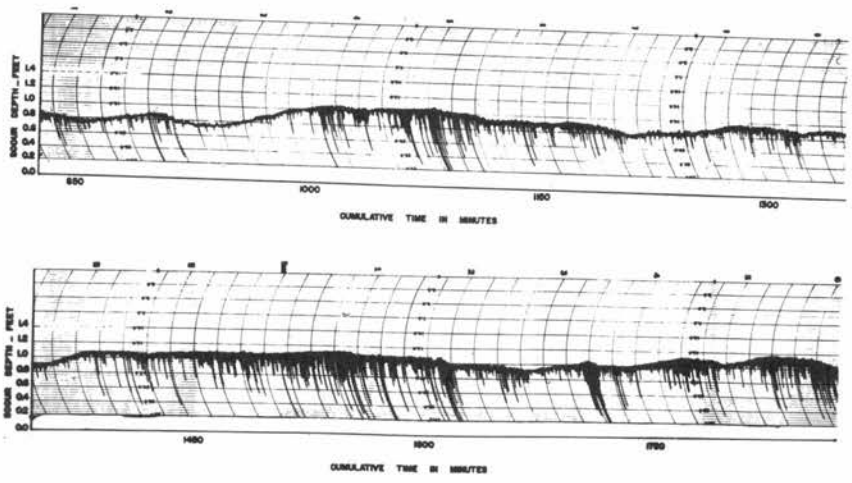

Fig. 12 - History of Scour Recorded by Sonic Depth Sounder

Flow direction

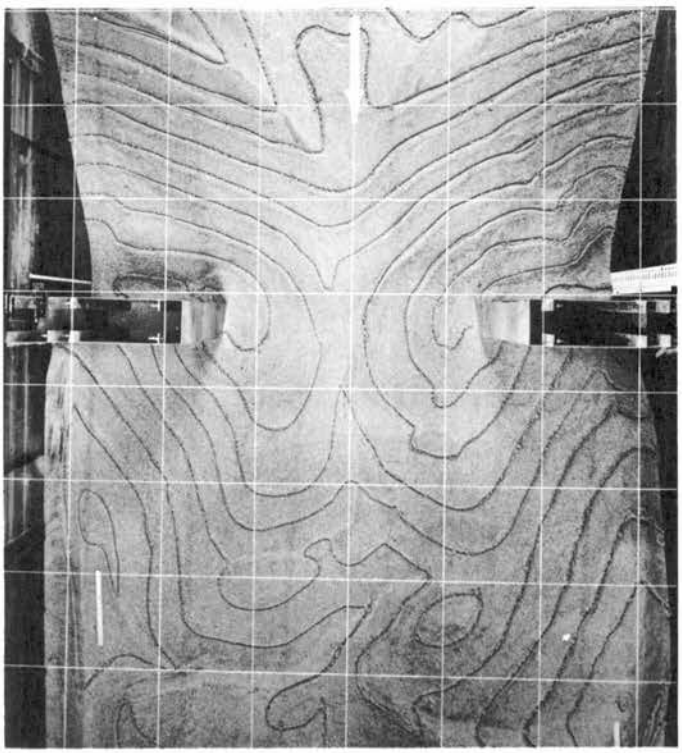

Fig. 13 - Contoured Scour Holes

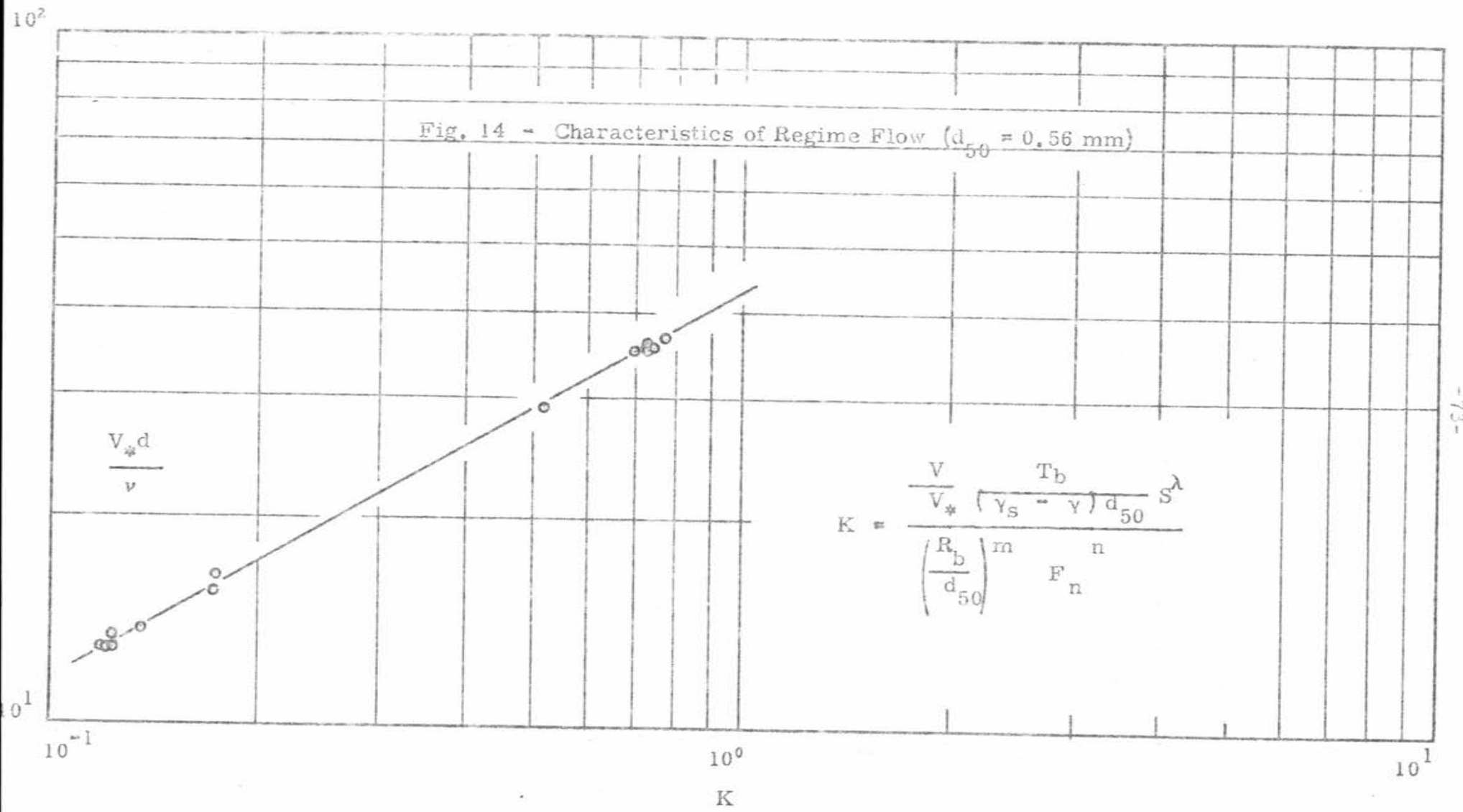

Fig. 14 - Characteristics of Regime Flow (d_{50} = 0,56 mm)

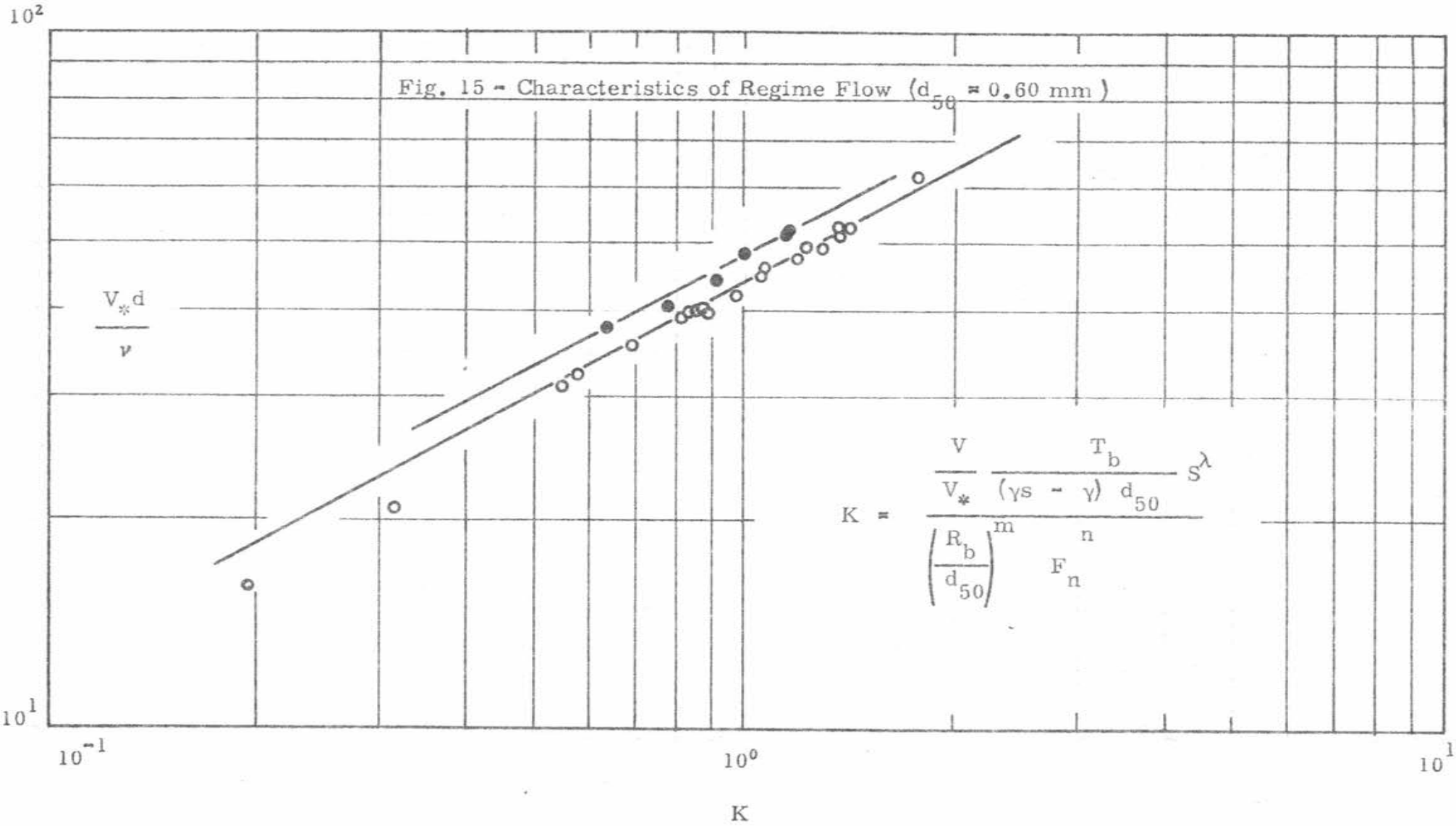

Fig. 15 - Characteristics of Regime Flow (d_{50} = 0.60 mm)

Fig. 16 - Mean Velocity of Regime Flow

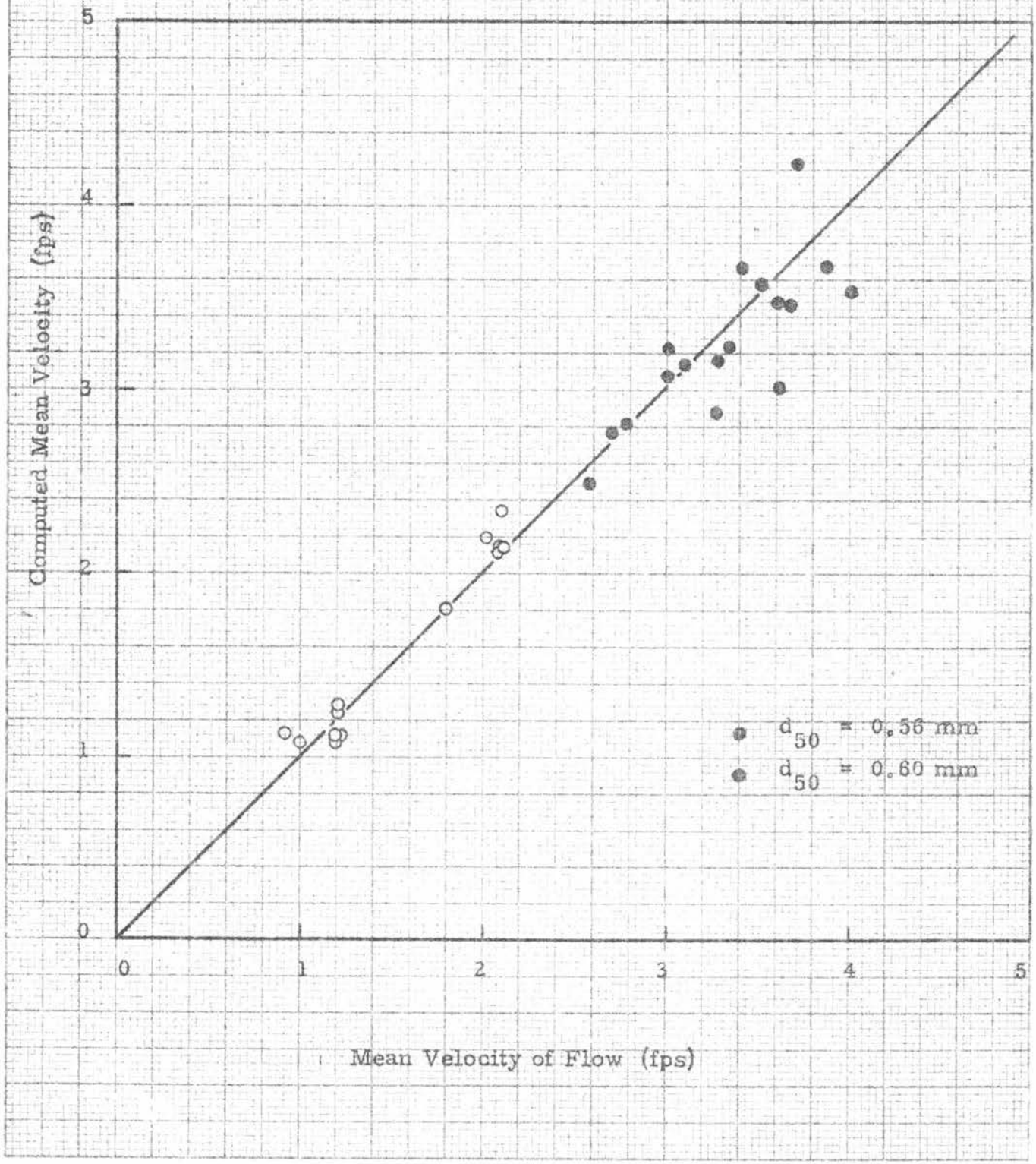

Fig. 17 - Effect of Velocity on Scour
(with sediment supply)

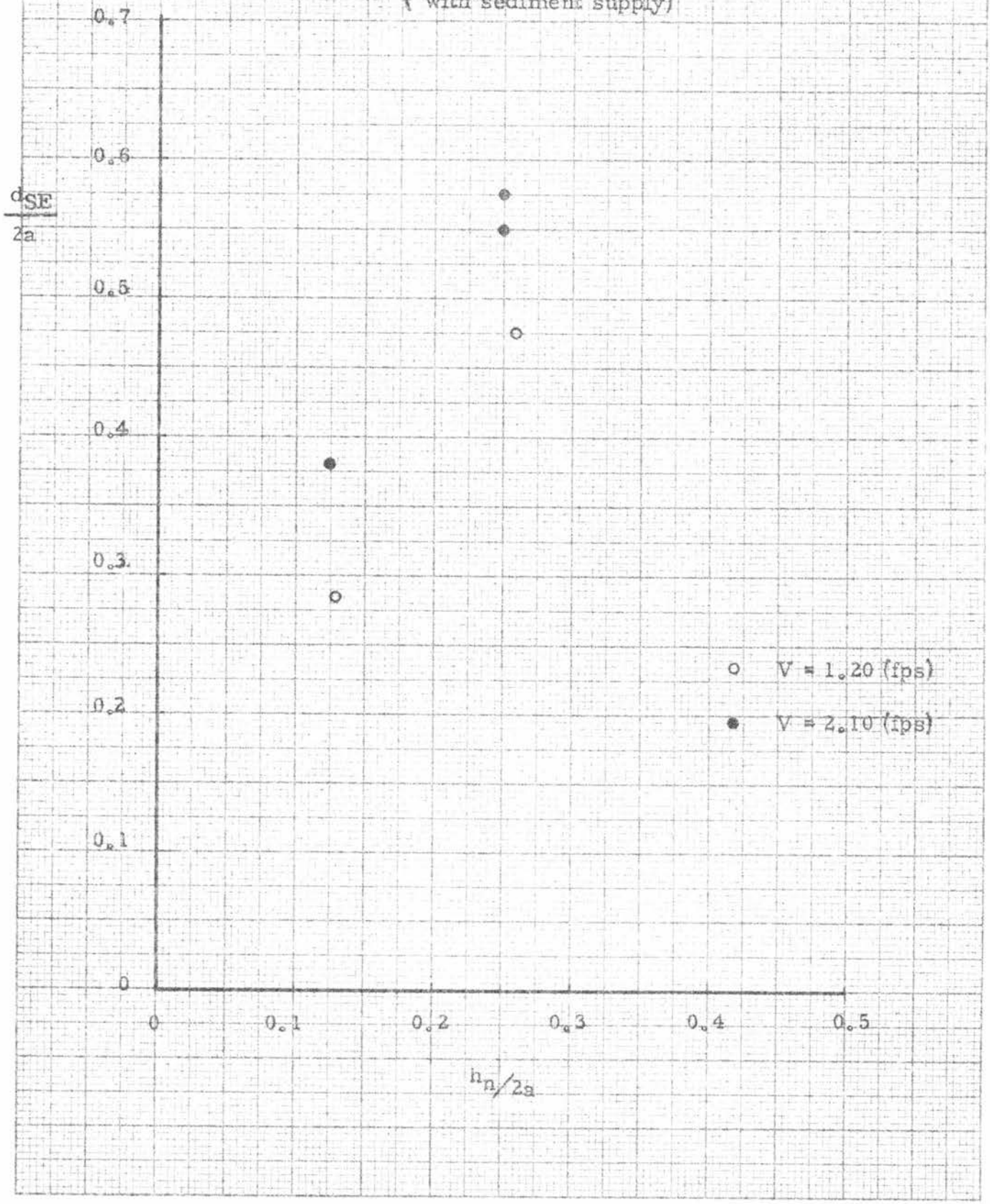

Fig. 18 - Criterion For Equilibrium Depth of Scour
(with sediment supply)

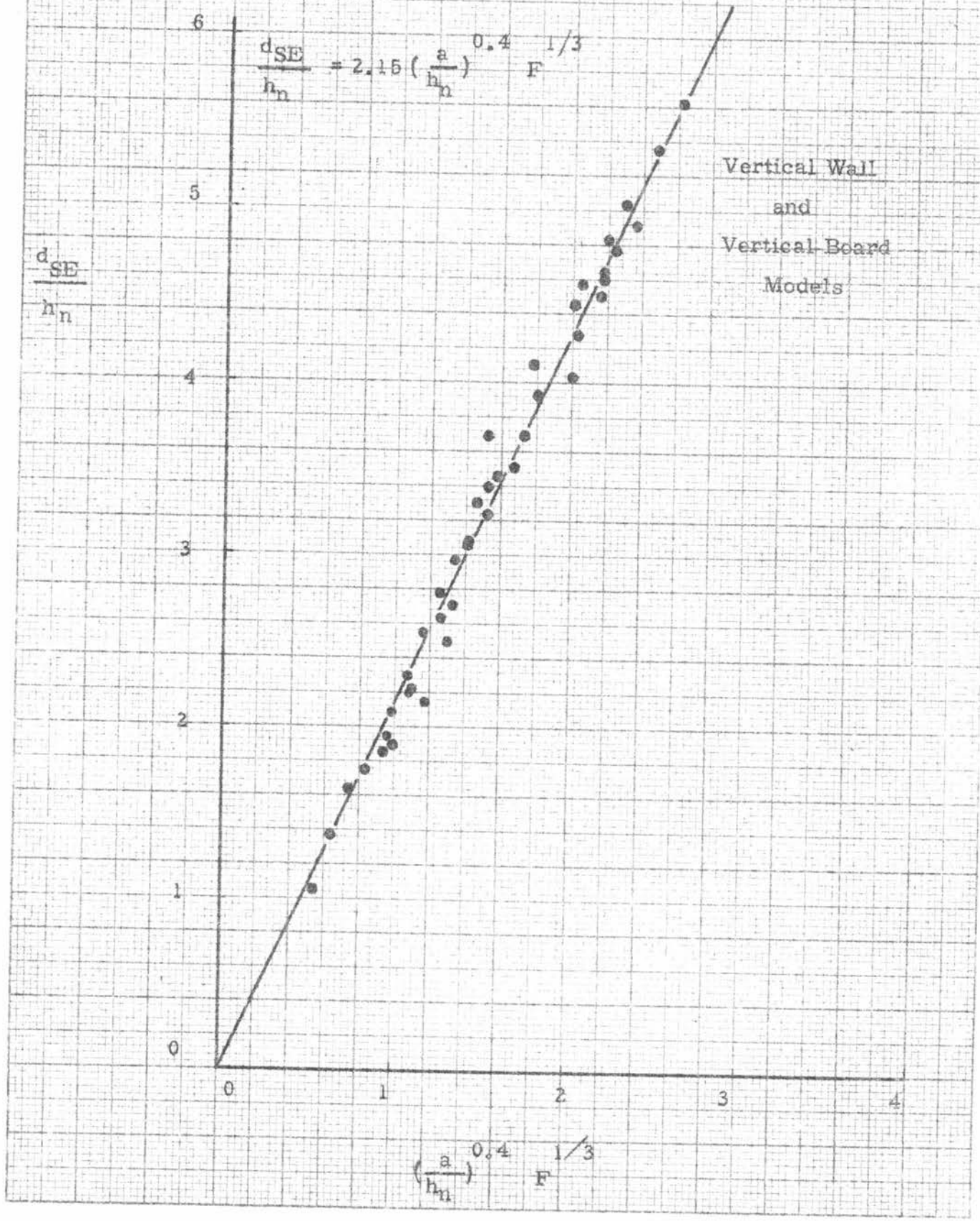

Fig. 18 - $\frac{d_{SE}}{h_n}$ vs $\left(\frac{a}{h_n}\right)^{0.4} F^{1/3}$

(with sediment supply)

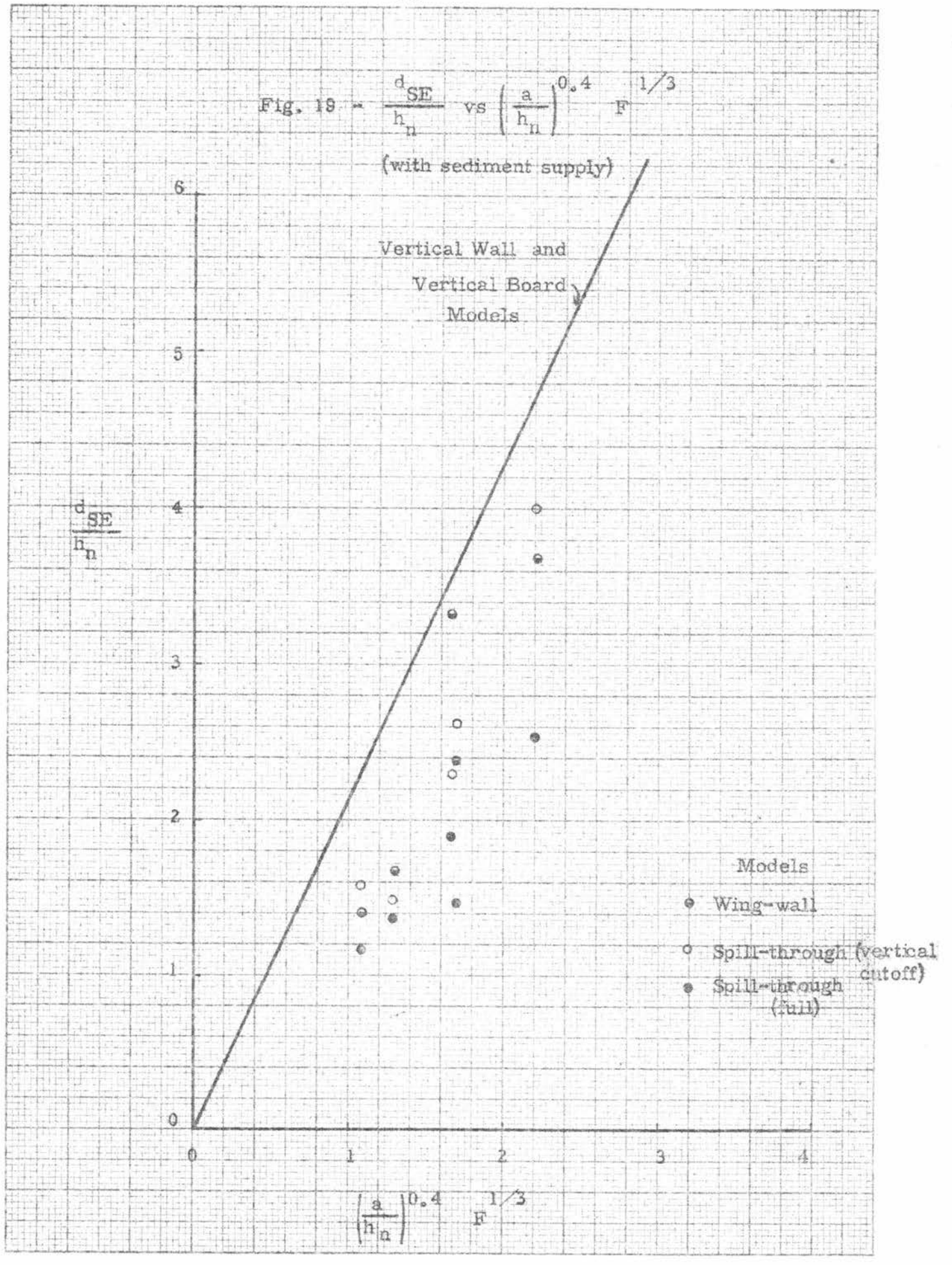

Fig. 20 - Criterion For Maximum Depth of Scour
(with sediment supply)

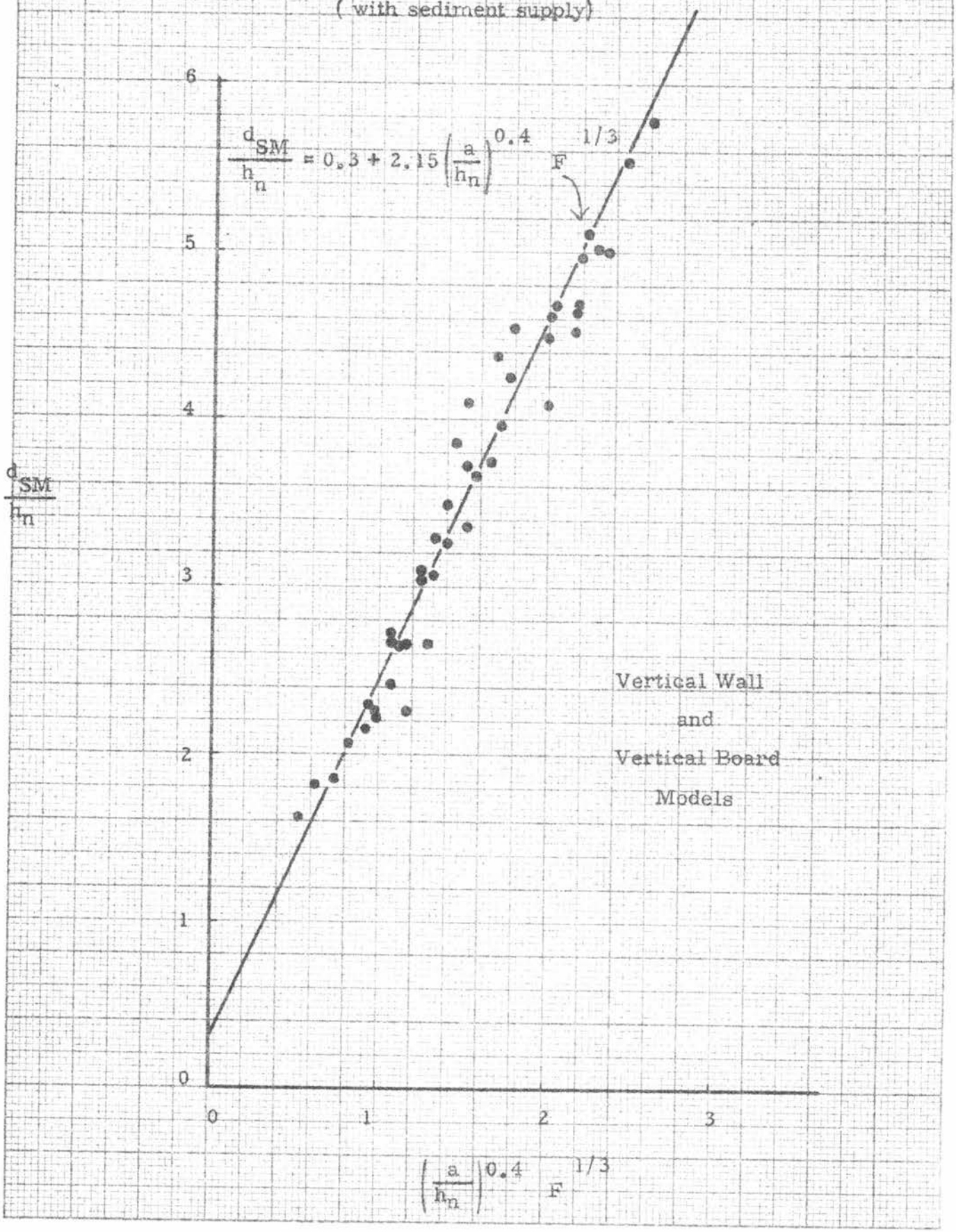

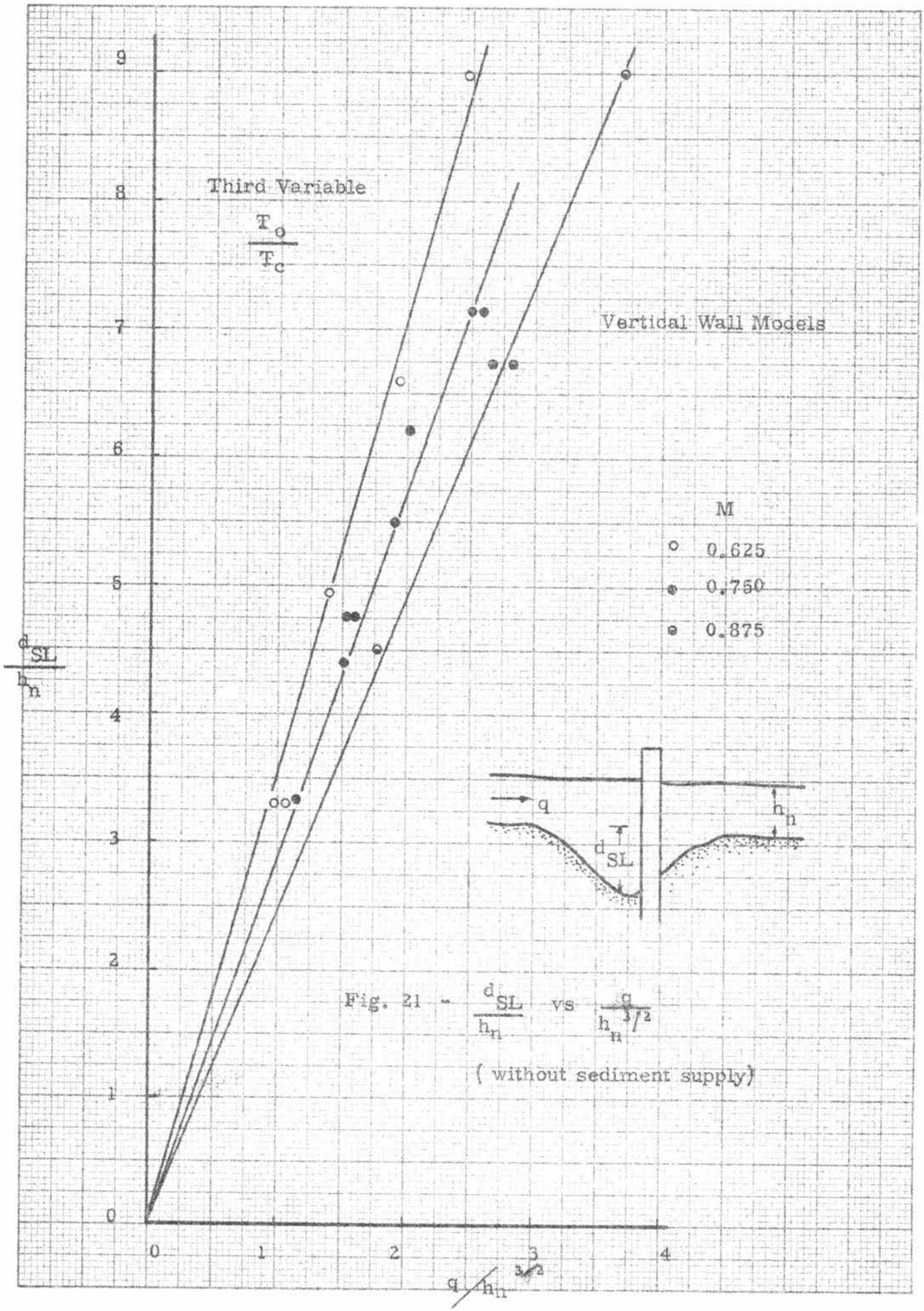

Fig. 21 - $\frac{d_{SL}}{h_n}$ vs $\frac{q}{h_n^{3/2}}$

(without sediment supply)

Fig. 22 - Criterion For Limiting Depth of Scour
(without sediment supply)

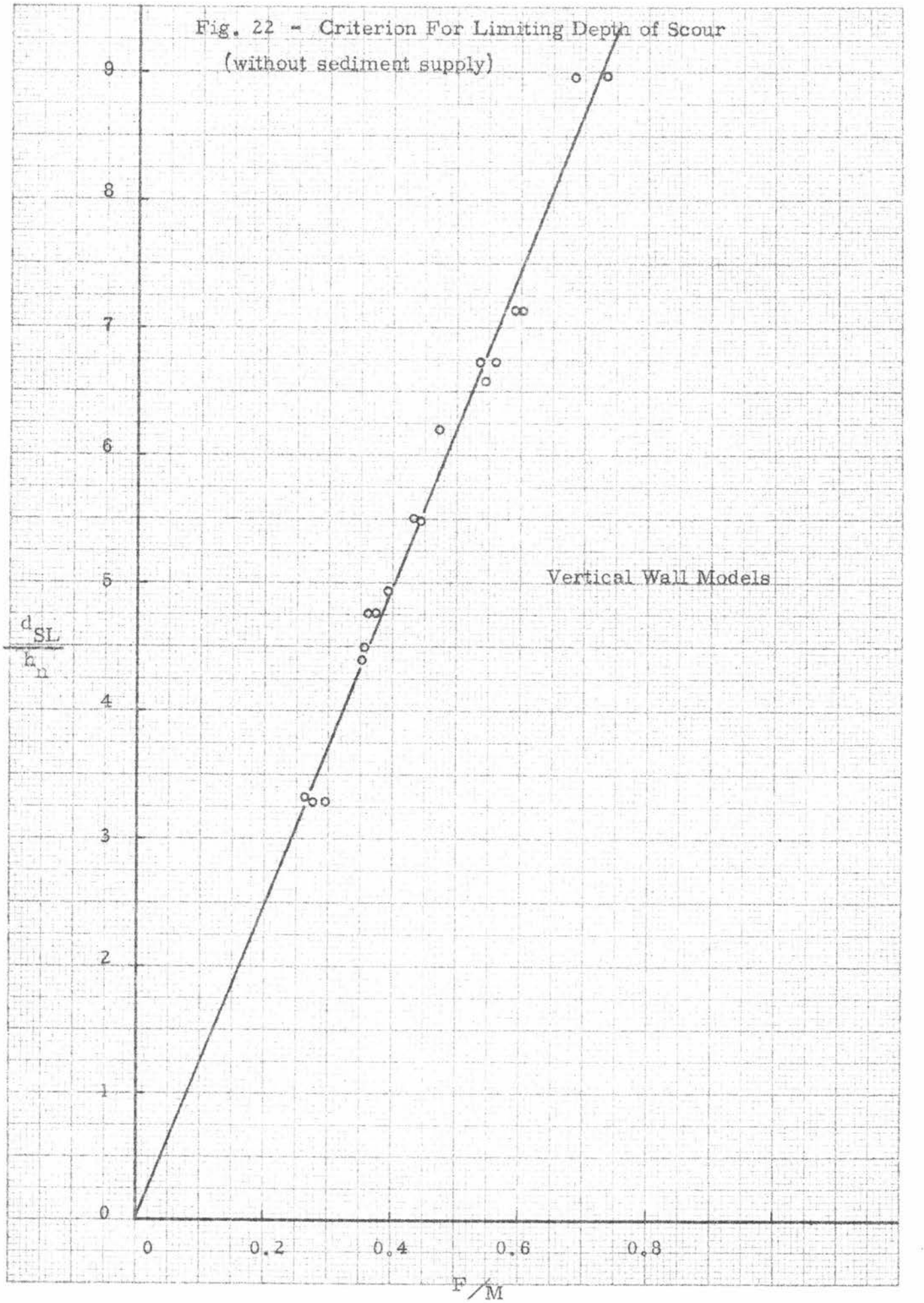

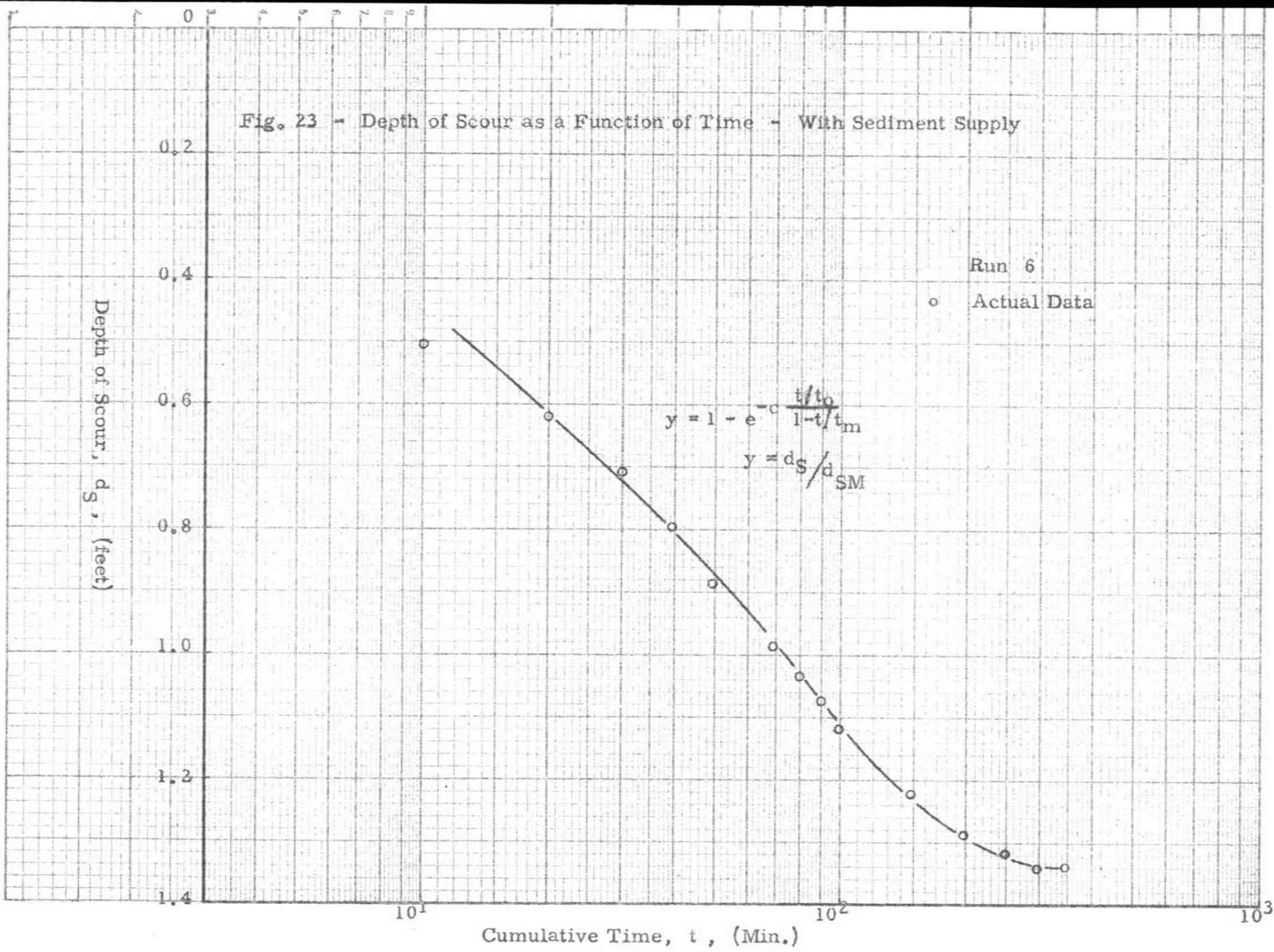

Fig. 23 - Depth of Scour as a Function of Time - With Sediment Supply

Fig. 24 - Depth of Scour as a Function of Time - Without Sediment Supply

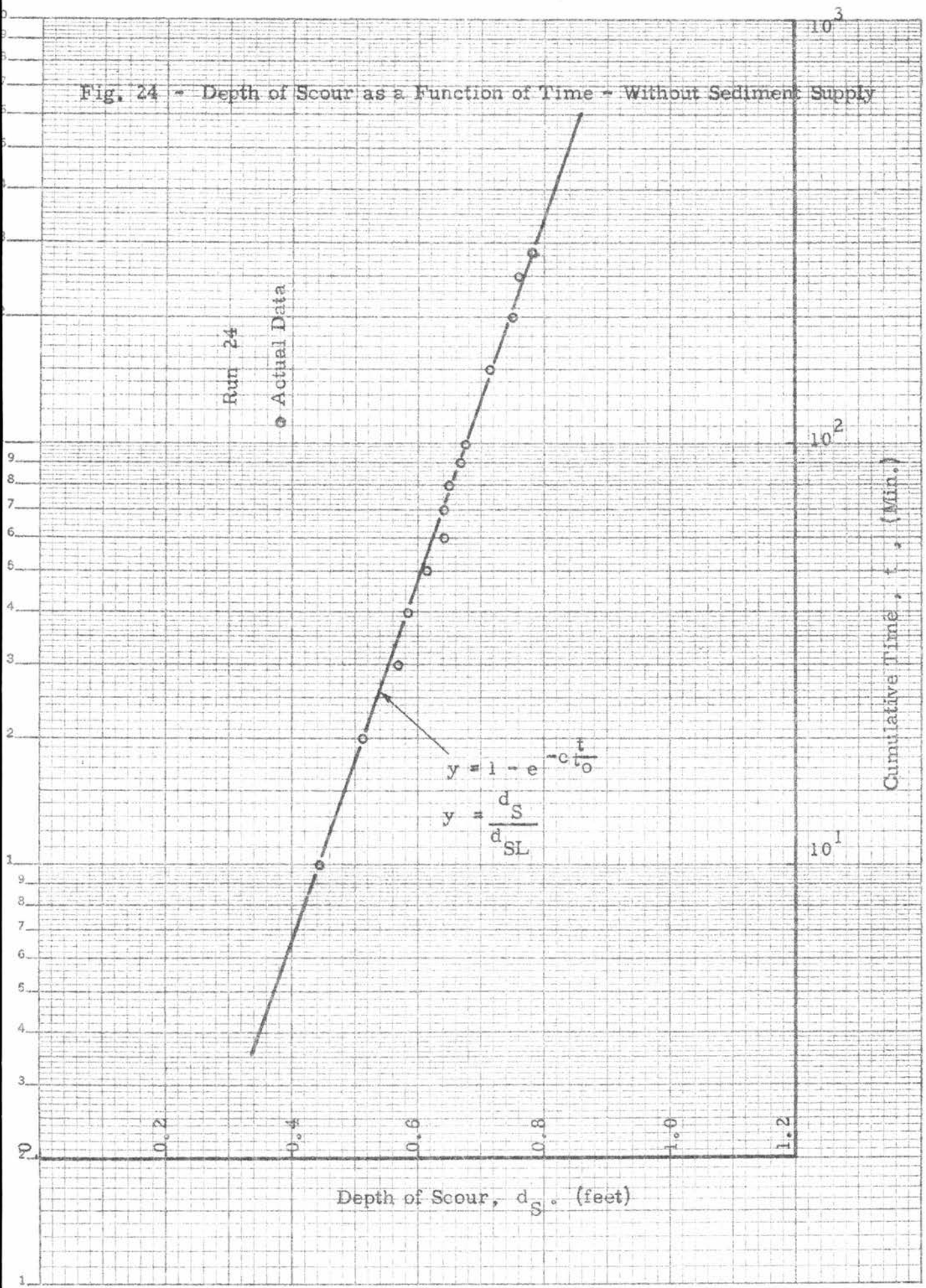

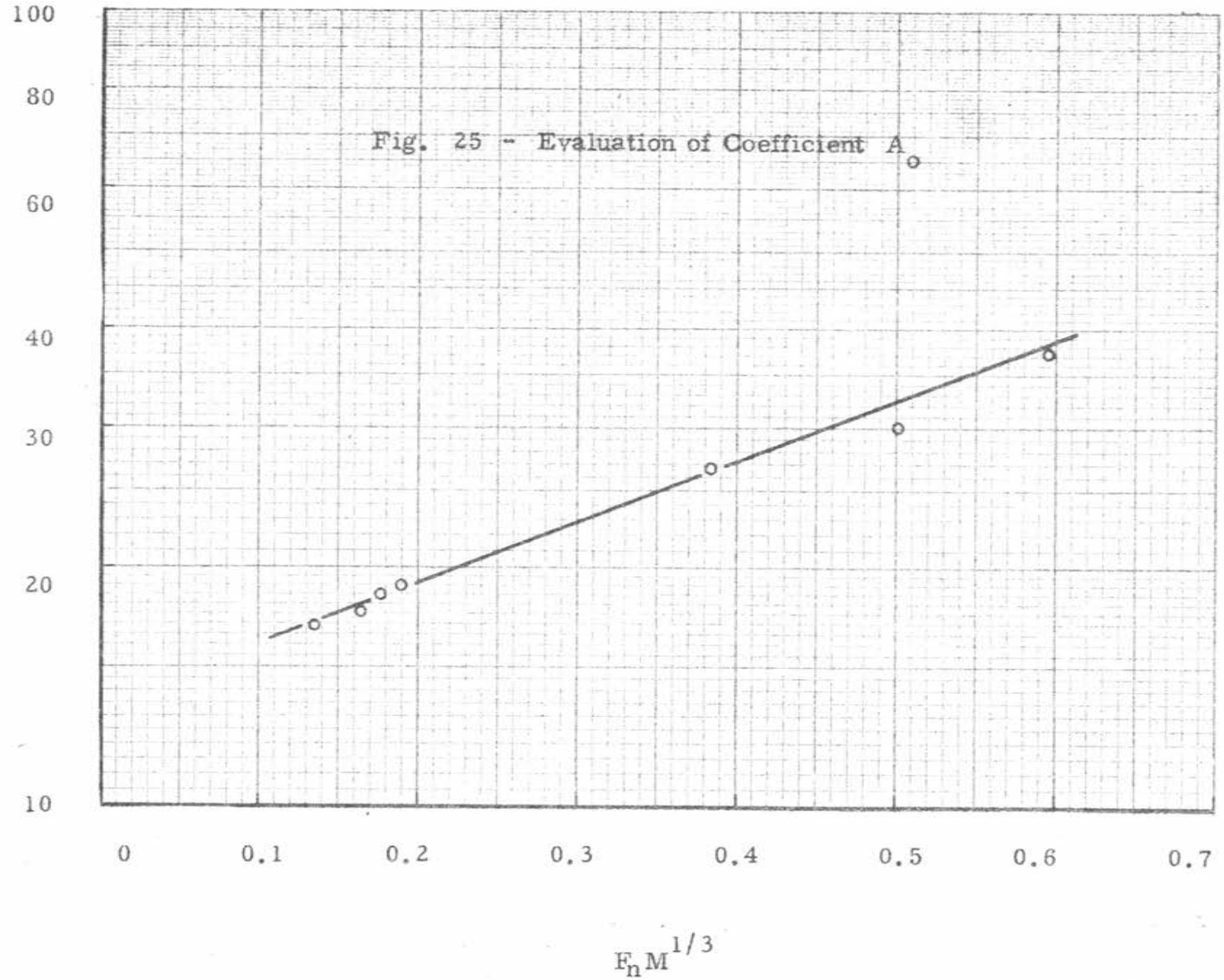

Fig. 25 - Evaluation of Coefficient A_o

Fig. 26 - Scour Area vs Time
(with sediment supply)

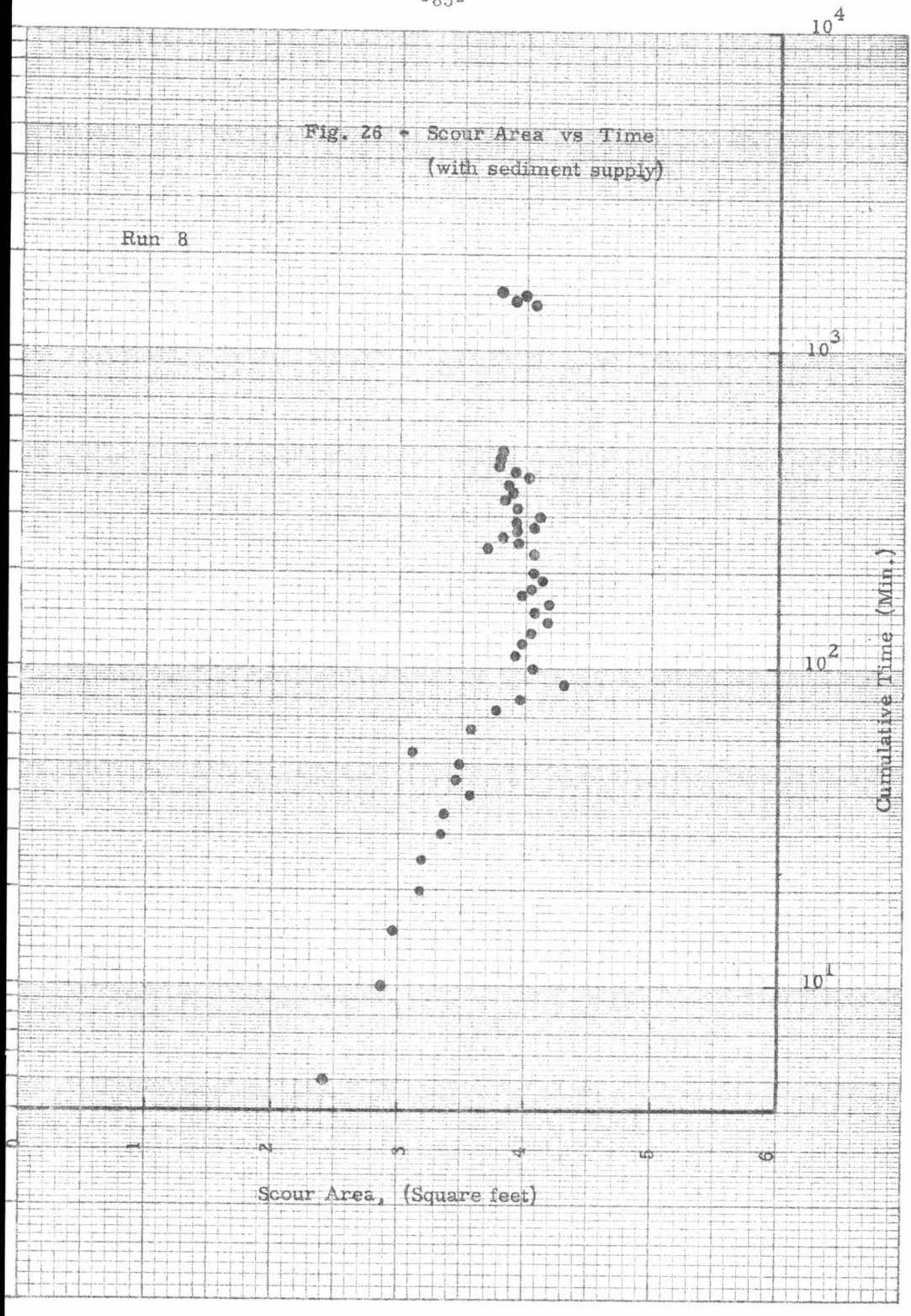

Fig. 27 + Δh_s in a Rigid Channel (Vertical Board and Vertical Wall Models)

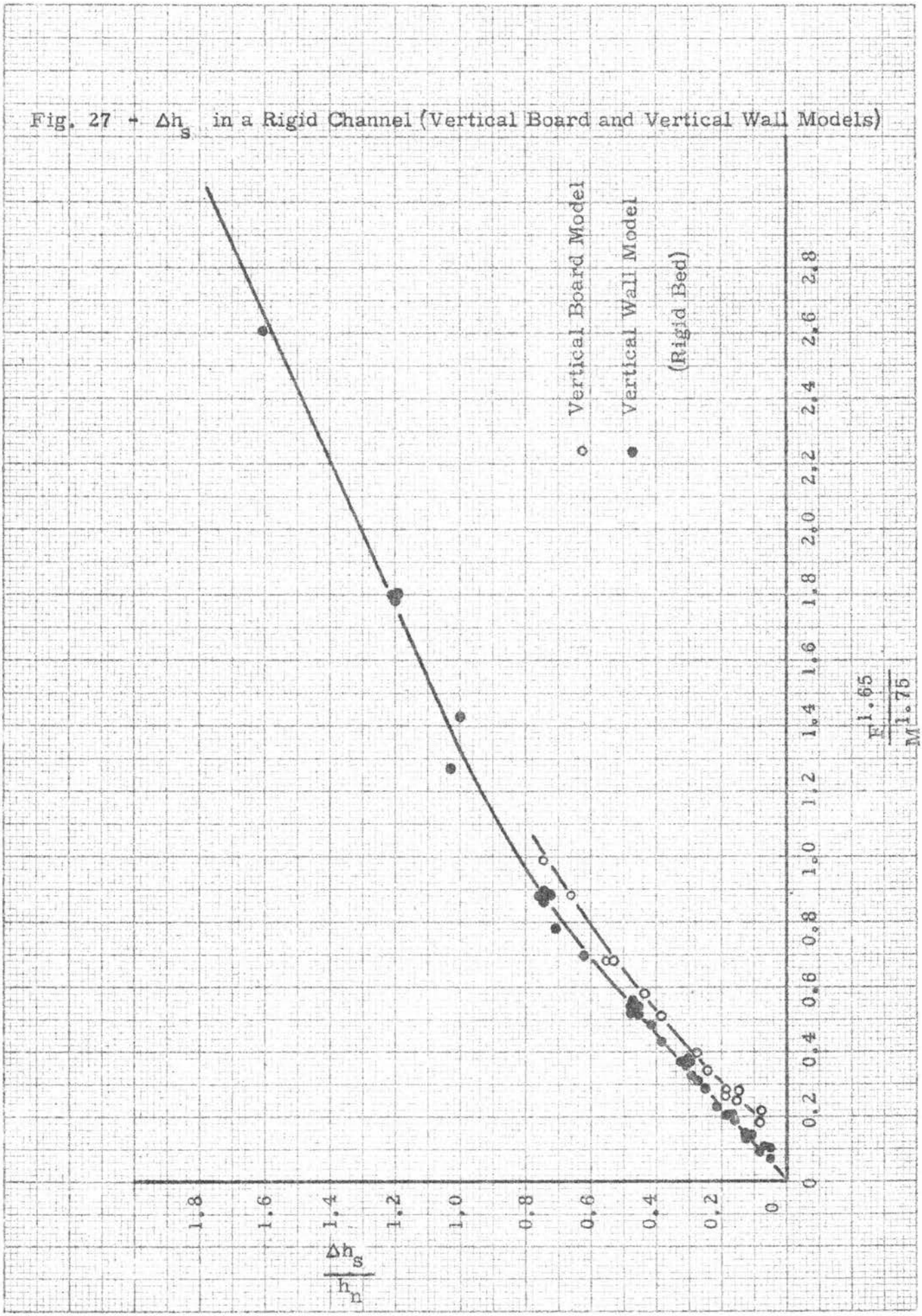

Rigid Bed

Fig. 28 - Δh_s in a Rigid Channel (Wing Wall Models)

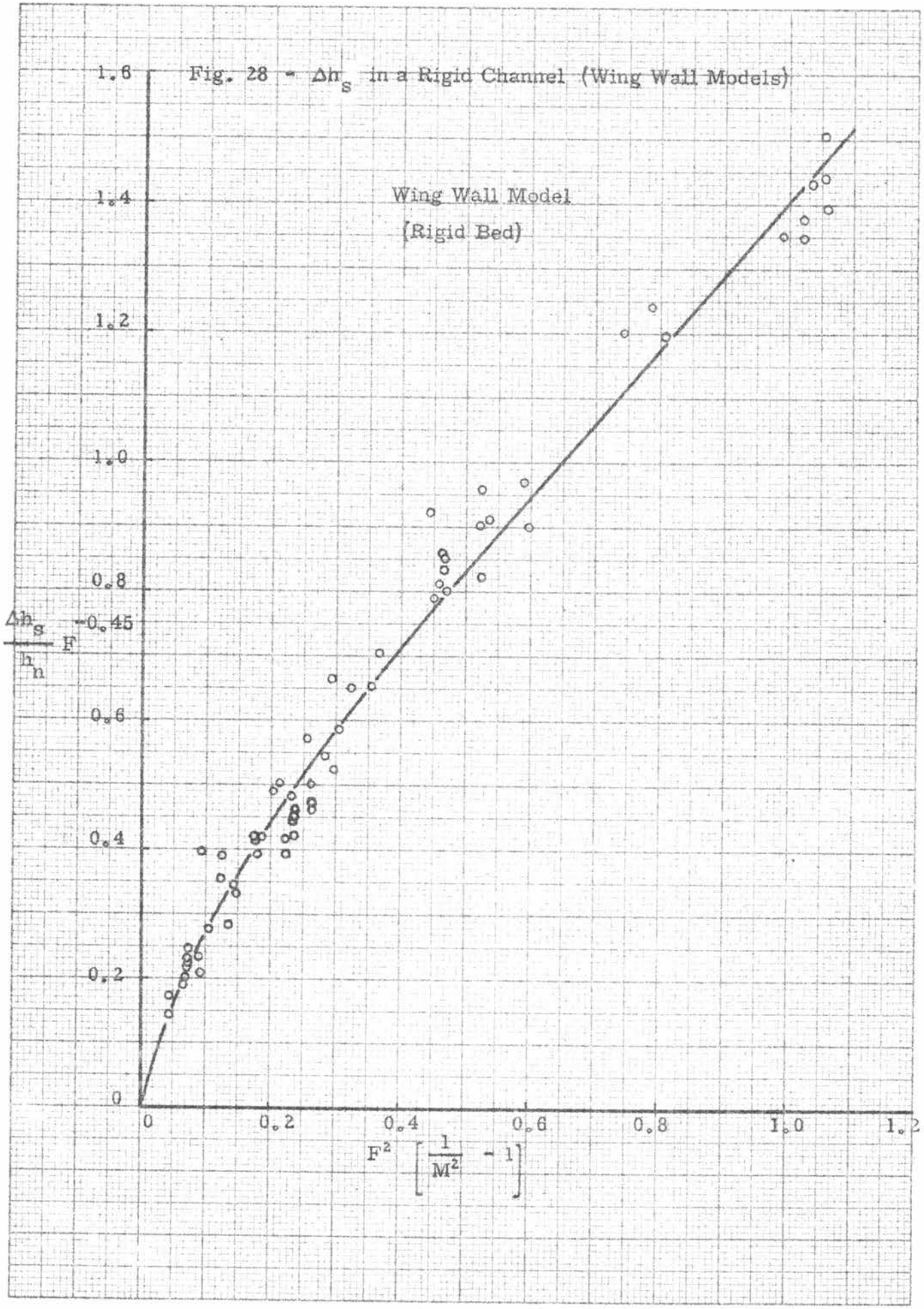

Fig. 29 - Δh_s in a Rigid Channel (Spill-Through Models)

(Rigid Bed)

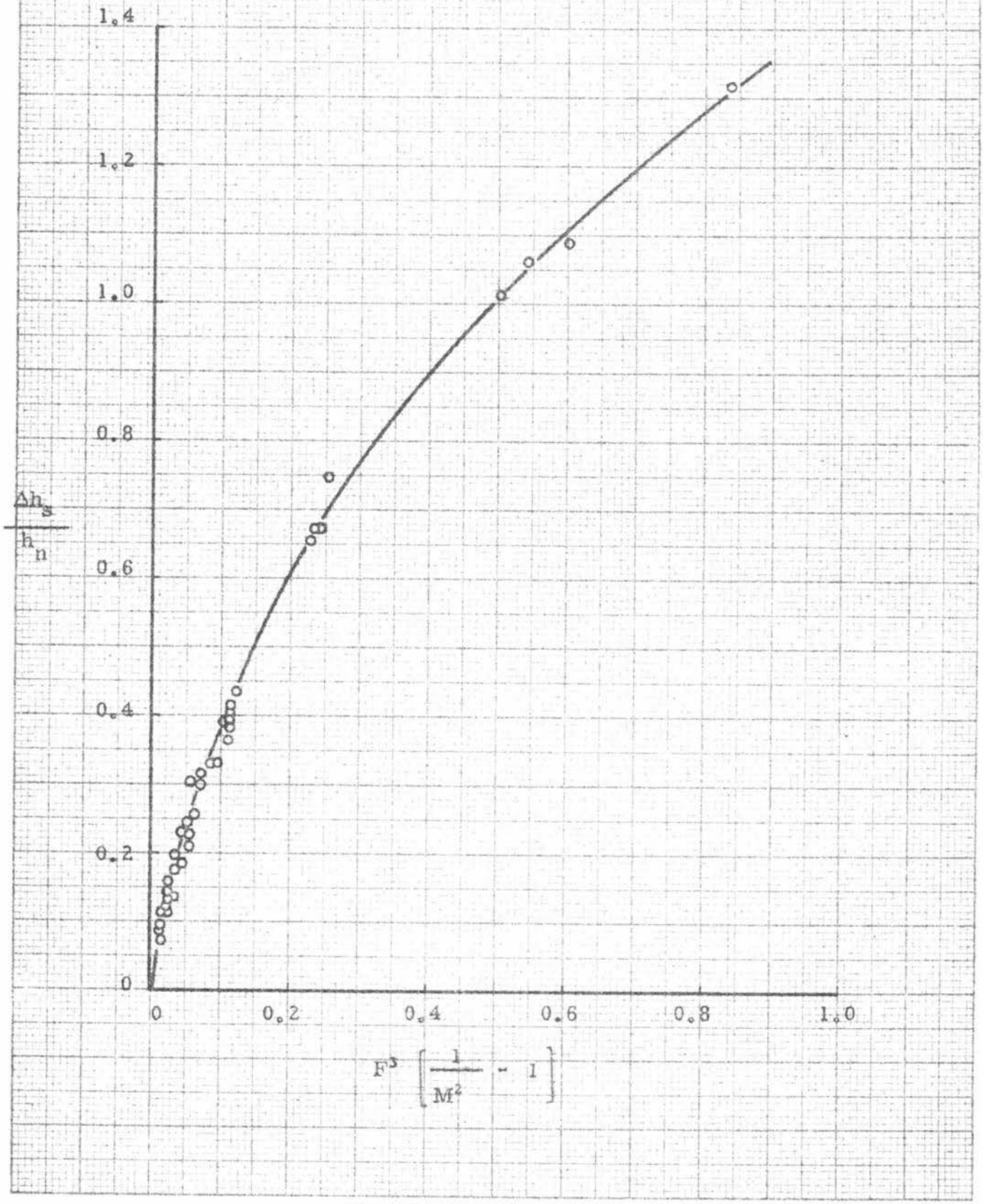

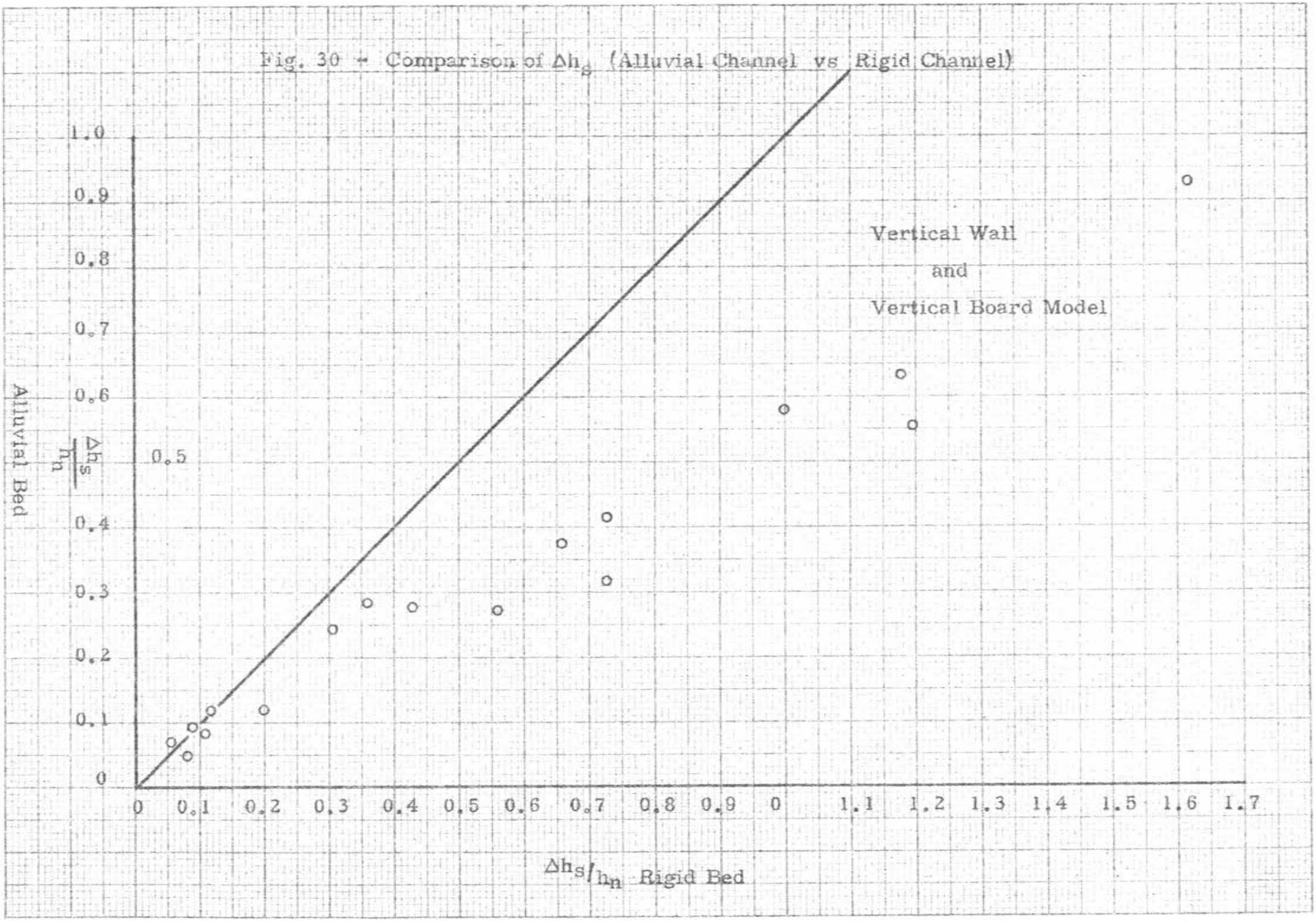
Fig. 30 - Comparison of Δh_s (Alluvial Channel vs Rigid Channel)
Vertical Wall
and
Vertical Board Model
Alluvial Bed
$\frac{\Delta h_s}{h_n}$
$\Delta h_s / h_n$ Rigid Bed
0
0.1
0.2
0.3
0.4
0.5
0.6
0.7
0.8
0.9
1.0
1.1
1.2
1.3
1.4
1.5
1.6
1.7

APPENDICES

Appendix A - Photographs

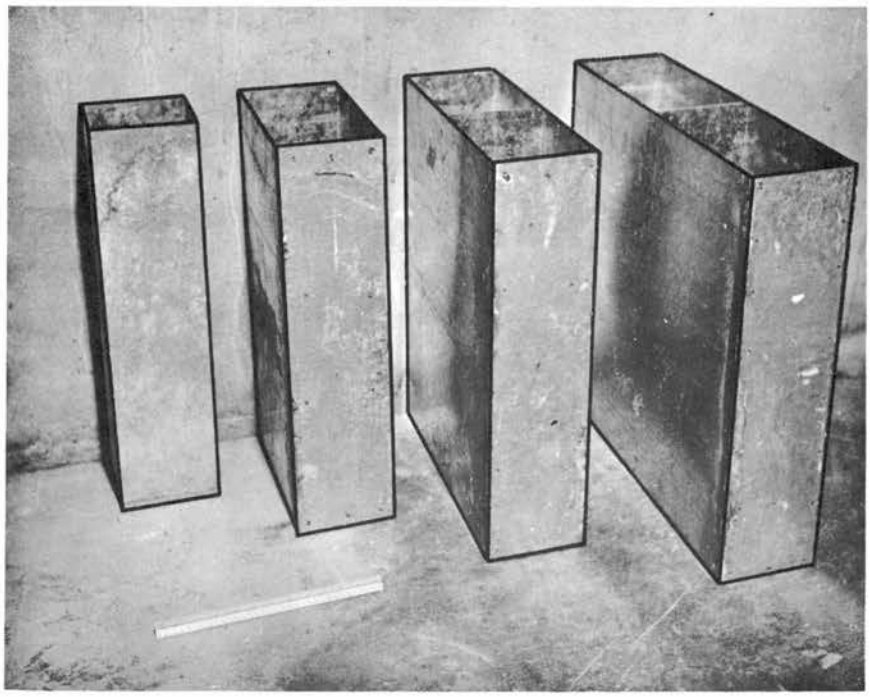

Photo 1 - Vertical-Wall Models

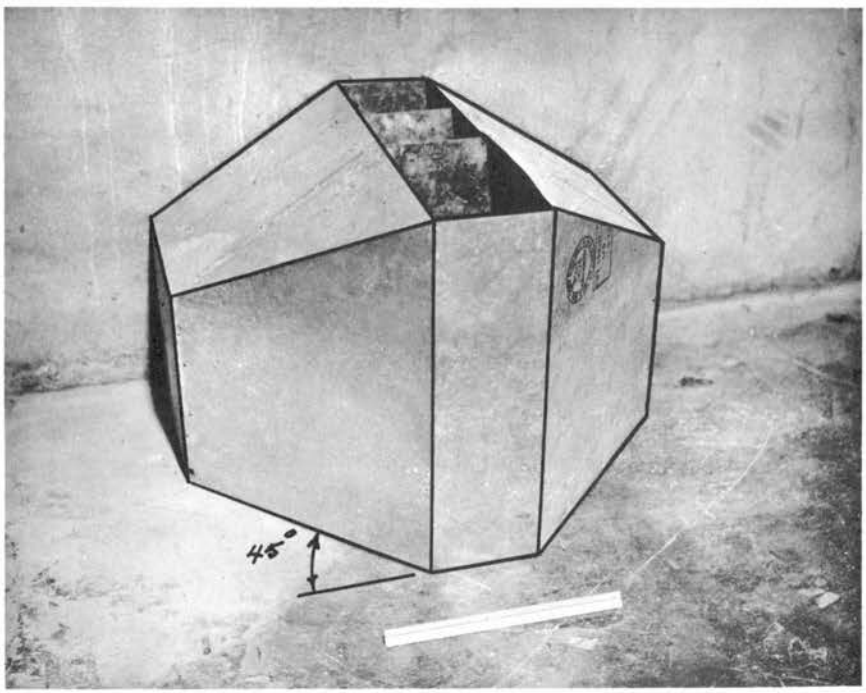

Photo 2 - 45^0 Wing-Wall Model
Side-slope = 1-1/2:1

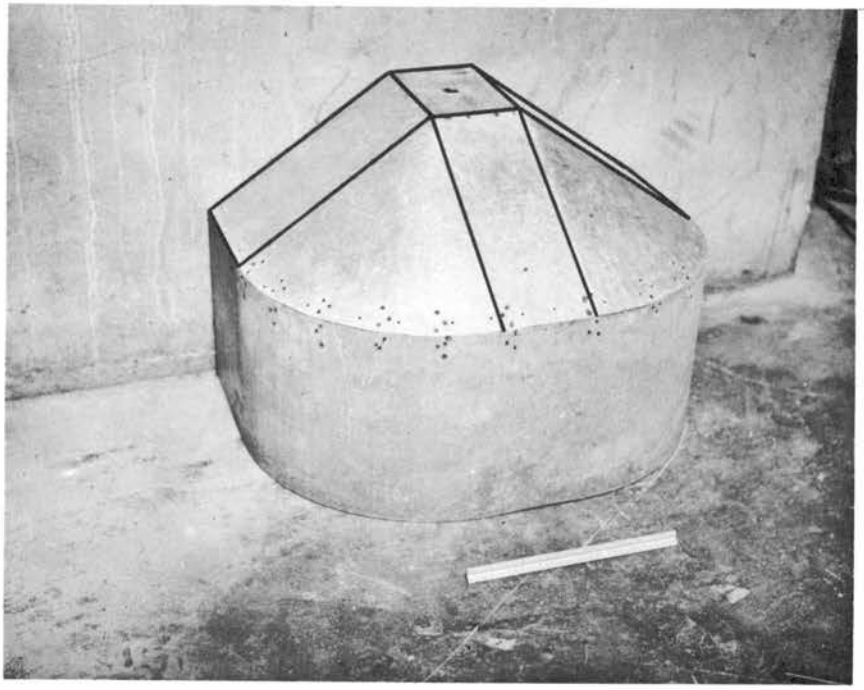

Photo 3 - Spill-through Model
Side-slope = 1-1/2:1

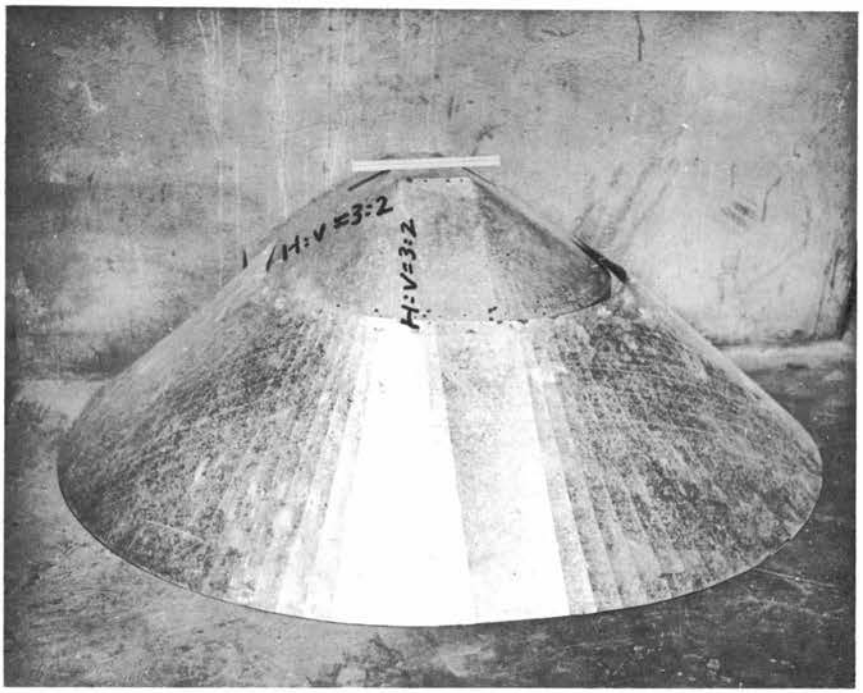

Photo 4 - Full Spill-through Model
Side-slope = 1-1/2:1

Photo 5 - Bed of a Normal Run

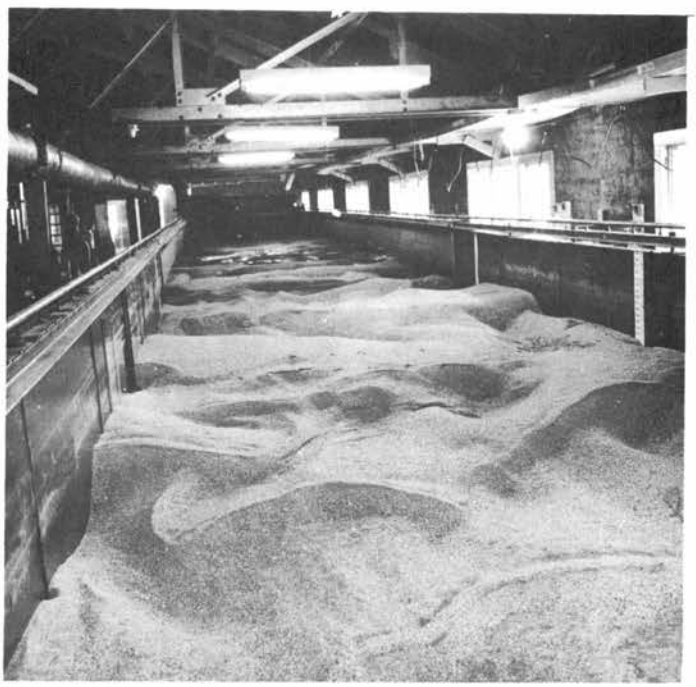

Photo 6 - Bed of a Normal Run

Flow direction

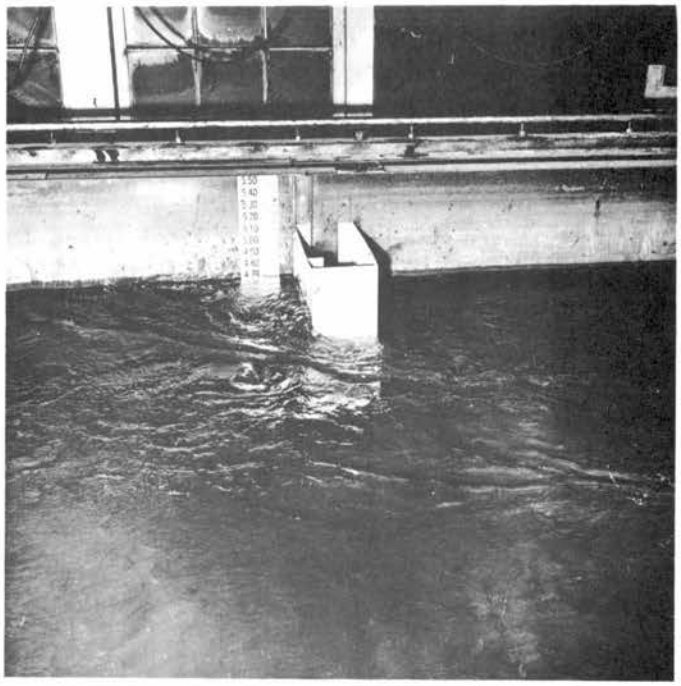

Photo 7 - Model Installed for Scour Test

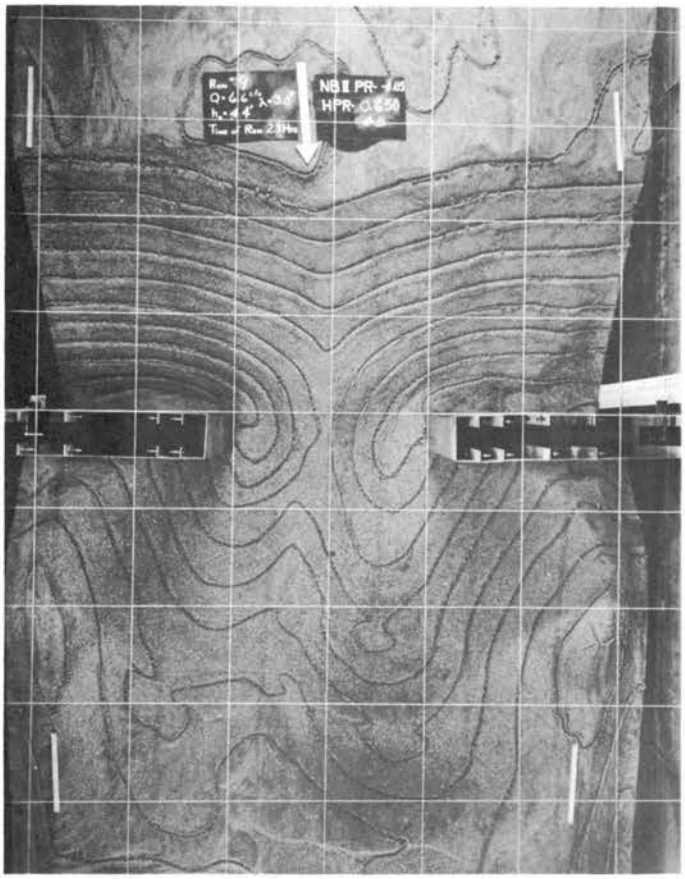

Photo 8 - Example of Scour Hole Interference

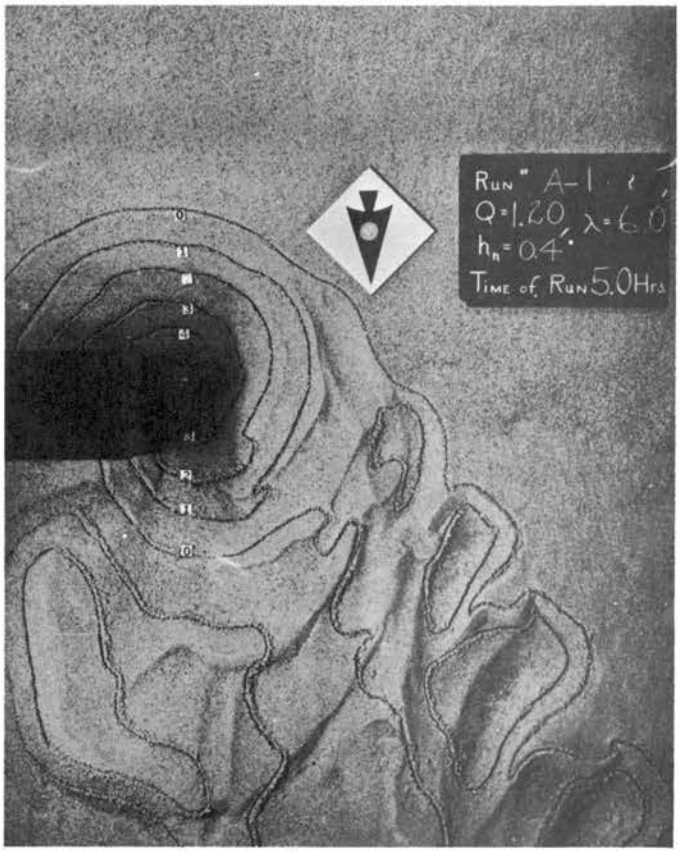

Photo 9 -

Contoured Scour Hole;
1-foot VW-Model,
M = 0.750

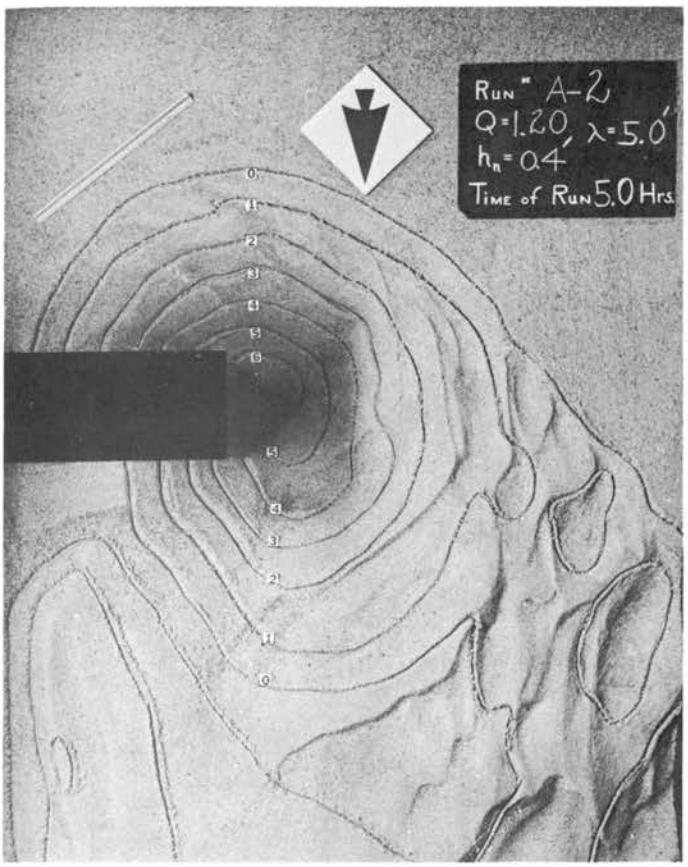

Photo 10 -

Contoured Scour Hole
1-1/2 foot VW-Model
M = 0.625

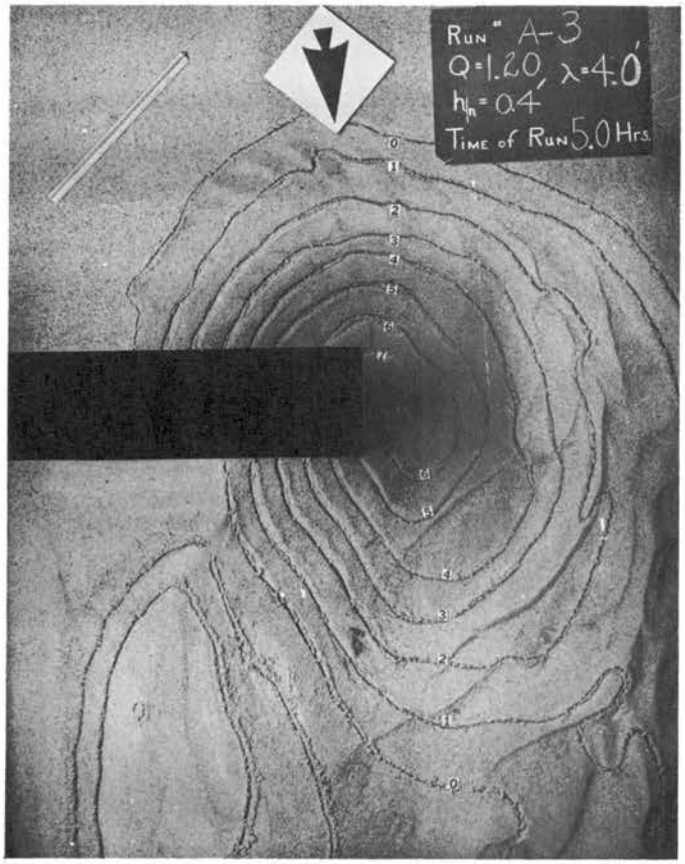

Photo 11 -

Contoured Scour Hole;
2-foot VW Model,
M = 0.500

Photo 12 -

Contoured Scour Hole;
1-foot Wing-wall Model
M = 0.750

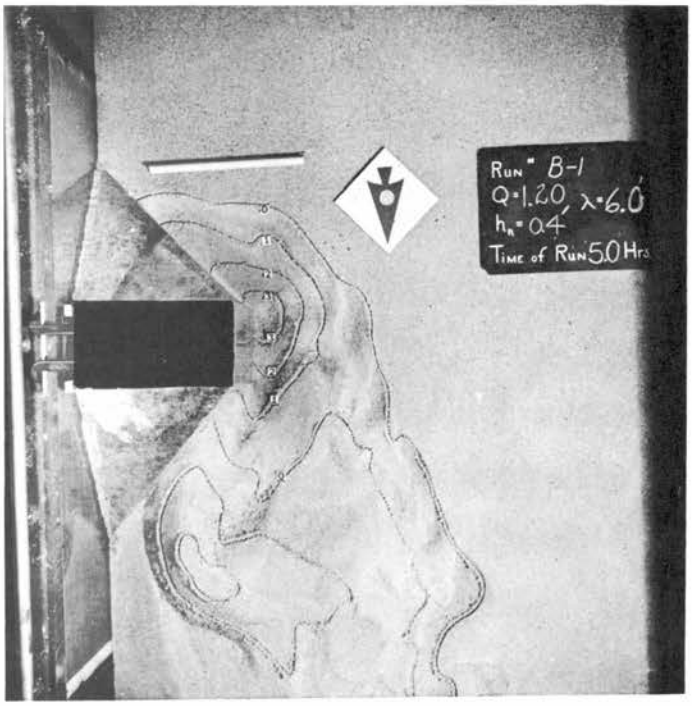

Photo 13 -

Contoured Scour Hole;
1-1/2 foot Wing-wall Model,
M = 0.625

Photo 14 -

Contoured Scour Hole;
2-foot Wing-wall Model,
M = 0.500

Photo 15 -

Contoured Scour Hole;
VW-Model
Skewed Downstream

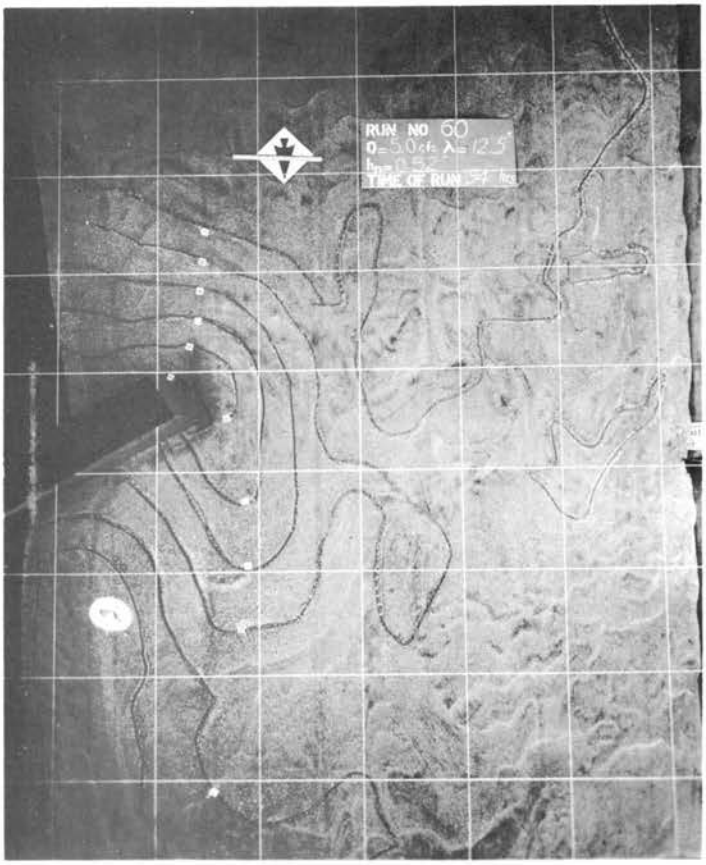

Photo 16 -

Contoured Scour Hole;
VW-Model
Skewed Upstream

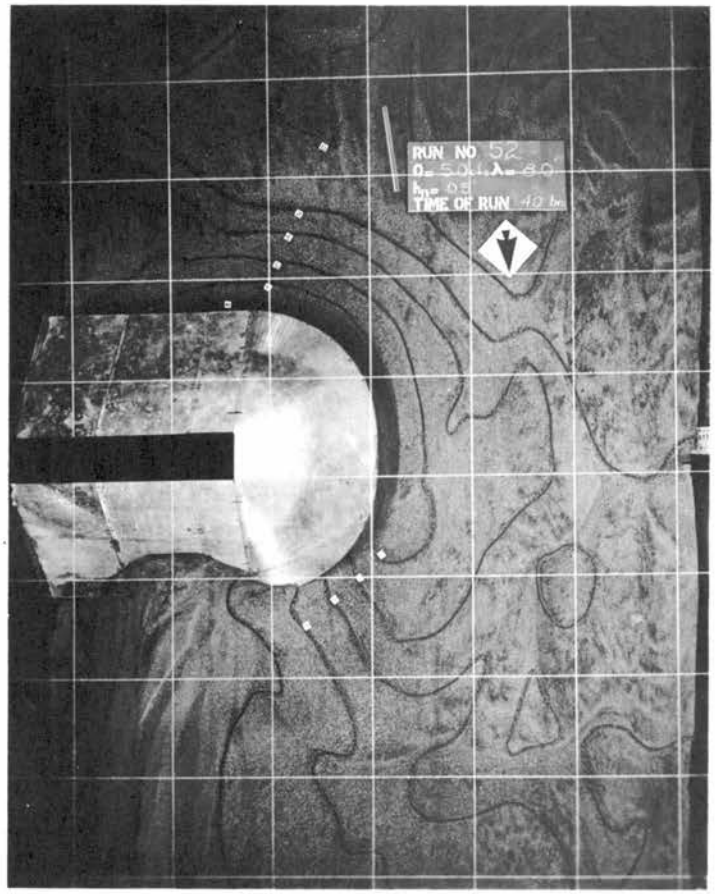

Photo 17 -

Contoured Scour Hole;
Spill-through Model
with Vertical Cut-off

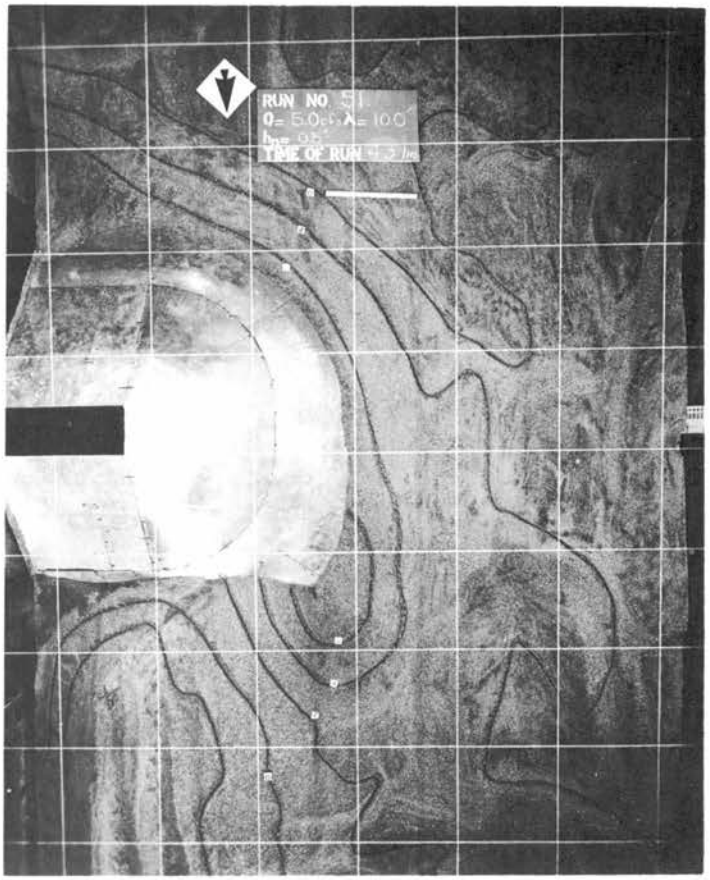

Photo 18 -

Contoured Scour Hole;
Full Spill-through Model

Appendix B - Scour Rate Curves

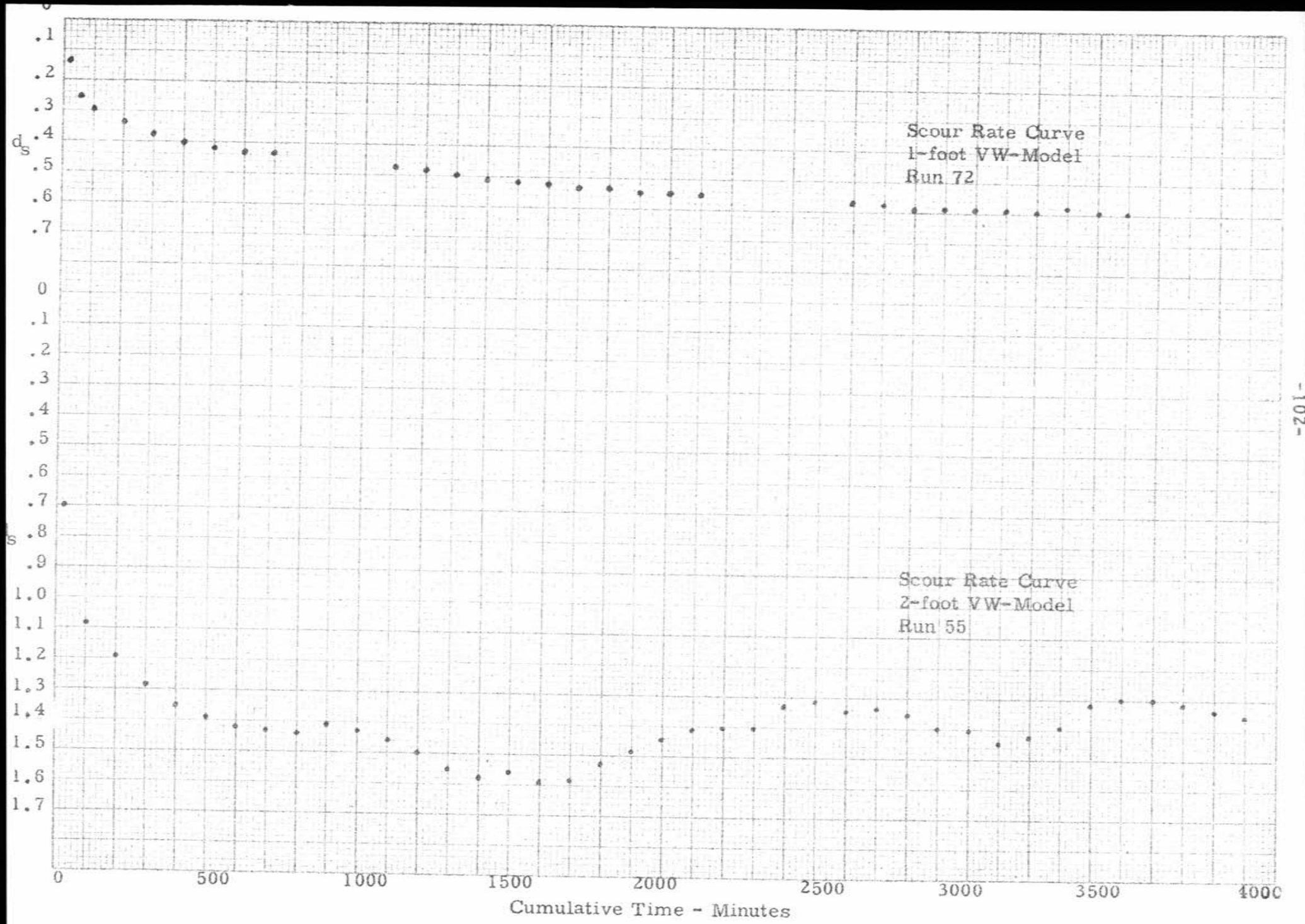
Scour Rate Curve
1-foot VW-Model
Run 72
Scour Rate Curve
2-foot VW-Model
Run 55
d_s
d_s
.1
.2
.3
.4
.5
.6
.7
0
.1
.2
.3
.4
.5
.6
.7
.8
.9
1.0
1.1
1.2
1.3
1.4
1.5
1.6
1.7
0
500
1000
1500
2000
2500
3000
3500
4000
Cumulative Time - Minutes

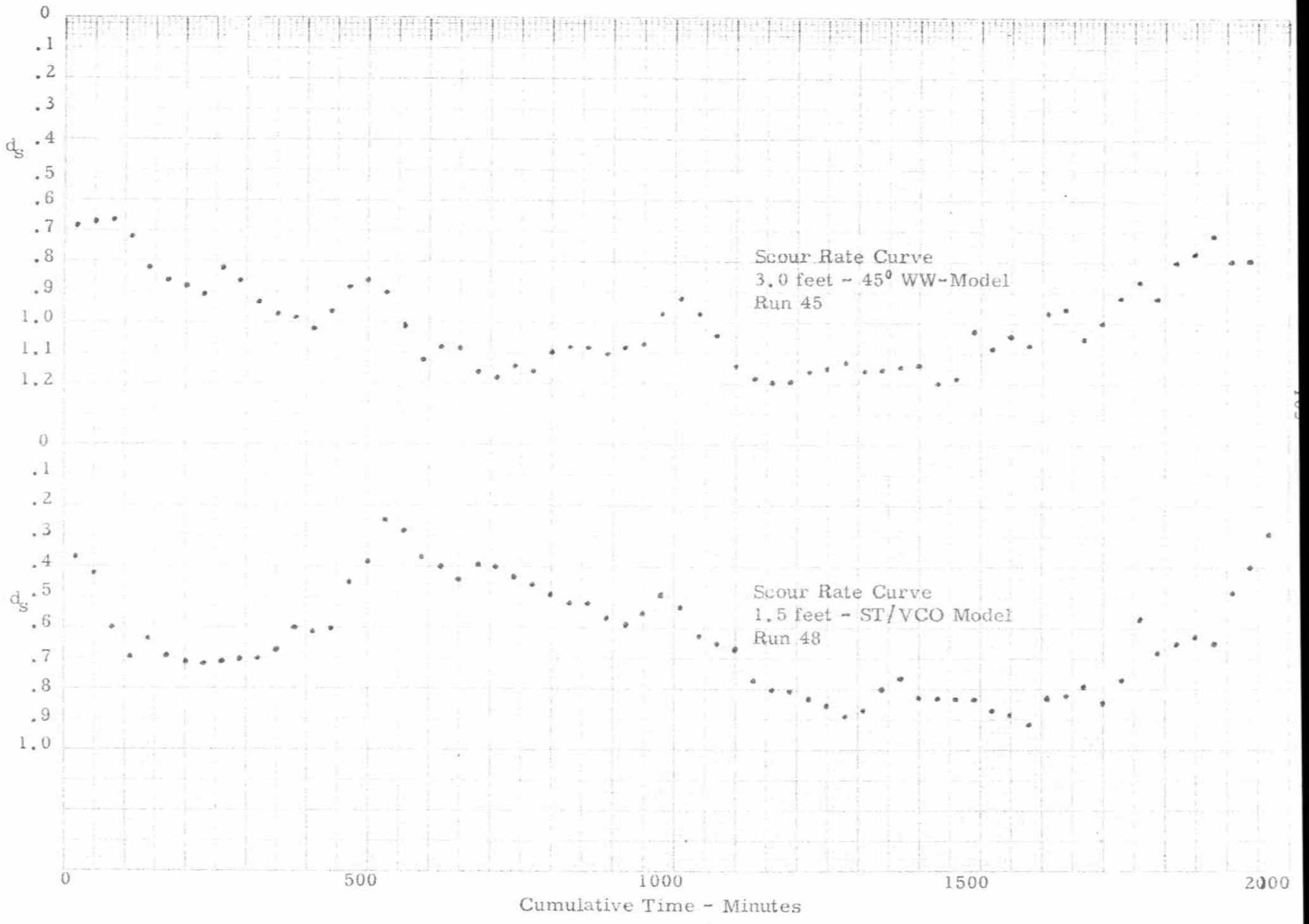
0
.1
.2
.3
.4
.5
.6
.7
.8
.9
1.0
1.1
1.2
d_s
Scour Rate Curve
3.0 feet - 45° WW-Model
Run 45
0
.1
.2
.3
.4
.5
.6
.7
.8
.9
1.0
d_s
Scour Rate Curve
1.5 feet - ST/VCO Model
Run 48
0
500
1000
1500
2000
Cumulative Time - Minutes

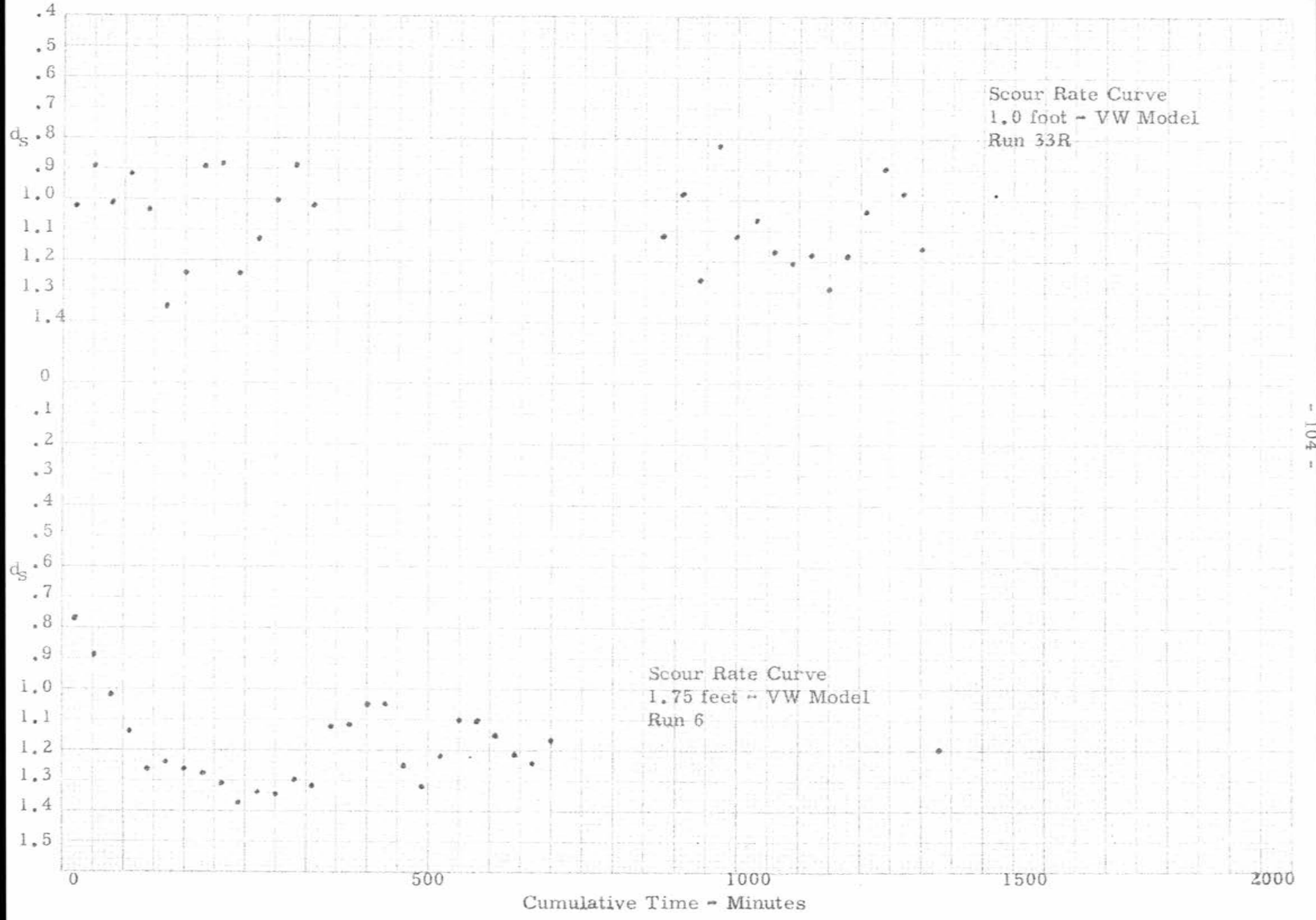
Scour Rate Curve
1.0 foot - VW Model
Run 33R
Scour Rate Curve
1.75 feet - VW Model
Run 6
d_s
d_s
.4
.5
.6
.7
.8
.9
1.0
1.1
1.2
1.3
1.4
0
.1
.2
.3
.4
.5
.6
.7
.8
.9
1.0
1.1
1.2
1.3
1.4
1.5
0
500
1000
1500
2000
Cumulative Time - Minutes

Appendix C - Tables

SUMMARY OF EXPERIMENTS

Runs 1-19; investigation of scour and backwater, 8-foot flume, vertical-wall models, model placed on each side of flume (except runs 15 and 16), some interference of scour holes (runs 4, 5, 6, 7, 8, 9, 12, 13, 14 and 18) due to double-model arrangement, total sediment load ≈ 600 - 800 ppm, equilibrium runs with sediment supply.

Runs 20-21; comparison of scour depth for a rectangular and a circular pier of equal width, 8-foot flume, rectangular and circular pier, pier placed near center of flume, equilibrium runs with sediment supply.

Runs A-1 through C-5; qualitative effect of abutment geometery on location and degree of scour, 4-foot flume, vertical-wall, wing-wall, and spill-through models, clear-water supply and flow velocity kept small to prevent movement of bed material, bed material = "filter" sand, 5-hour runs, time-lapse photography of development of scour hole (16 mm - color movie film).

Runs 33-62; to study scour and backwater, 8-foot flume, vertical-wall, wing-wall, and spill-through models, equilibrium runs with sediment supply.

Runs 63-71; qualitative effect of abutment geometery on location and degree of scour, 4-foot flume, vertical-wall, wing-wall, and spill-through models, clear-water supply and no movement of bed material, 5-hour runs.

Runs 72-77; trial and comparison of "Black Hills" sand, 4-foot flume, vertical-wall models.

Runs 101-165; determination of limiting scour, 4-foot flume, vertical-wall, wing-wall, and spill-through models, clear-water supply, upstream bed covered to prevent bed-load movement into scour hole, flow conditions varied until noticeable scouring (movement) of bed material was observed in pre-shaped scour hole.

Runs 166-237; determination of limiting scour, 8-foot flume, wing-wall and spill-through models, recirculating flow, bed not covered, flow varied until movement of material in pre-shaped scour hole observed.

Runs 238-287; determination of limiting scour, model abutment on flood plain (see sketch)*, 8-foot flume, vertical-wall models, recirculating flow, bed not covered, flow varied until movement of material in pre-shaped scour hole observed.

Runs 288-318; scour and backwater investigation for high-velocity flow, 8-foot flume, vertical-wall and vertical-board models, no restriction on sediment supply or bed-material movement.

Runs 319-333; scour and backwater, 8-foot flume, wing-wall and spill-through models, no restriction on sediment supply or bed-material movement.

*

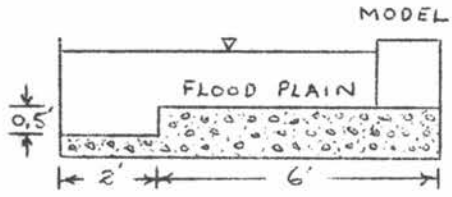

TABLE I. BASIC EXPERIMENTAL DATA

Run No.	Model Type	Model Length a (ft)	Number of Models p	Width of Flume B (ft)	Total Discharge Q (cfs)	Slope of Bed S	Median Size of Bed Mat'l d_{50}	Normal Depth of Flow h_n (ft)	Time of Test t (min)	Maximum Scour Depth d_{SM} (ft)	Equilibrium Scour Depth d_{SE} (ft)	Limiting Scour Depth d_{SL} (ft)	Water Surface Drop Across Embankment: Initial Δh_{si} (ft)	Water Surface Drop Across Embankment: Final Δh_{sf} (ft)	Opening Ratio $M = \frac{B-pa}{B}$	Mean Velocity of flow V (ft/sec)	Froude Number F_n
1	VW	0.50	2	8	4.5	0.00250	0.56	0.43	1204	1.643	1.560	- -	0.035	0.032	0.875	1.310	0.353
2	"	0.75	"	"	6.6	0.00253	"	0.46	1540	1.058	0.898	- -	0.113	0.040	0.812	1.795	0.467
3	"	1.00	"	"	"	"	"	"	1070	1.113	1.013	- -	0.130	0.055	0.750	"	"
4	"	1.25	"	"	"	"	"	"	1400	1.218	1.173	- -	0.127	"	0.687	"	"
5	"	1.50	"	"	"	"	"	"	1835	1.403	1.213	- -	0.065	0.069	0.625	"	"
5A	"	"	"	"	"	"	"	"	1580	1.428	1.273	- -	- -	- -	"	"	"
6	"	1.75	"	"	"	"	"	"	1455	1.413	1.243	- -	0.101	0.047	0.562	"	"
6A	"	"	"	"	"	"	"	"	1435	1.513	1.363	- -	- -	- -	"	"	"
7	"	2.00	"	"	"	"	"	"	1560	1.613	1.413	- -	0.146	0.055	0.500	"	"
8	"	2.25	"	"	"	"	"	"	1505	1.783	1.523	- -	- -	- -	0.437	"	"
9	"	2.50	"	"	"	"	"	"	1410	1.893	1.693	- -	- -	- -	0.375	"	"
10	"	0.50	"	"	13.0	0.00230	"	0.77	1190	1.405	1.050	- -	0.085	- -	0.875	2.110	0.424
11	"	0.75	"	"	"	"	"	"	1420	1.425	1.260	- -	0.160	- -	0.812	"	"
12	"	1.00	"	"	"	"	"	"	1555	1.593	1.340	- -	0.150	- -	0.750	"	"
13	"	1.50	"	"	"	"	"	"	605	1.743	1.610	- -	- -	- -	0.625	"	"
14	"	2.00	"	"	"	"	"	"	130	1.800	1.700	- -	- -	- -	0.500	"	"
15	"	3.00	1	"	"	"	"	"	595	2.046	1.920	- -	0.290	- -	0.625	"	"
16	"	1.50	"	"	"	"	"	"	1410	1.716	1.460	- -	0.157	- -	0.812	"	"
17	"	1.00	2	"	10.0	0.00270	"	0.62	425	1.343	1.150	- -	0.178	- -	0.750	2.015	0.452
18	"	1.50	"	"	"	"	"	"	545	1.683	1.380	- -	0.169	- -	0.625	"	"
19	"	0.25	"	"	"	"	"	"	315	1.003	0.650	- -	- -	- -	0.937	"	"
20	□ pier	0.80	1	"	9.6	0.00200	"	0.64	100	0.970	0.900	- -	- -	- -	0.900	1.878	0.414
21	○ pier	0.80	"	"	9.5	0.00160	"	0.78	85	0.500	0.420	- -	- -	- -	"	1.522	0.304
22(A-1)	VW	1.00	"	4	1.2	0	0.65	0.40	300	- -	- -	- -	0.023	0.019	0.750	0.750	0.209
23(A-2)	"	1.50	"	"	"	"	"	"	"	- -	- -	- -	0.033	0.023	0.625	"	"
24(A-3)	"	2.00	"	"	"	"	"	"	"	- -	- -	- -	0.044	0.024	0.500	"	"
25(B-1)	WW	1.00	"	"	"	"	"	"	"	- -	- -	- -	0.023	0.017	0.750	"	"
26(B-2)	"	1.50	"	"	"	"	"	"	"	- -	- -	- -	0.031	0.017	0.625	"	"
27(B-3)	"	2.00	"	"	"	"	"	"	"	- -	- -	- -	0.035	0.018	0.500	"	"
28(C-1)	ST	1.75	"	"	"	"	"	"	"	- -	- -	- -	0.030	0.018	0.563	"	"
29(C-2)	"	"	"	"	"	"	"	"	"	- -	- -	- -	0.030	0.019	"	"	"
30(C-3)	"	"	"	"	"	"	"	"	"	- -	- -	- -	0.033	0.022	"	"	"
31(C-4)	"	"	"	"	"	"	"	"	"	- -	- -	- -	0.028	0.020	"	"	"
32(C-5)	"	"	"	"	"	"	"	"	"	- -	- -	- -	0.029	0.018	"	"	"
33	VW	1.00	"	8	8.5	0.00370	0.56	0.50	390	1.338	1.150	- -	- -	- -	0.875	2.130	0.531
33R	"	"	"	"	8.4	0.00340	"	"	1440	1.365	1.100	- -	0.085	0.067	"	2.100	0.524
34	"	2.00	1	"	"	0.00335	"	"	1200	1.631	1.520	- -	- -	0.054	0.750	2.100	0.524
35	"	1.00	"	"	4.8	0.00050	"	0.51	1600	1.160	1.130	- -	0.051	0.023	0.875	1.190	0.294
36	"	2.00	"	"	"	0.00044	"	"	"	1.515	1.500	- -	0.061	0.029	0.750	1.200	0.297
37	"	0.50	"	"	"	0.00045	"	0.50	1160	0.750	0.710	- -	0.035	0	0.937	1.210	0.302
38	"	1.50	"	"	"	0.00068	"	"	1400	1.070	1.040	- -	0.047	0.030	0.812	"	0.302
39	"	2.50	"	"	4.0	0.00046	"	"	1900	1.550	1.350	- -	0.041	0.023	0.687	1.000	0.250
40	"	3.00	"	"	"	"	"	0.54	7100	1.757	1.730	- -	0.028	0.024	0.625	0.925	0.222
41	"	2.00	"	"	5.0	0.00069	"	0.52	2975	1.350	1.140	- -	0.043	0.034	0.750	1.201	0.294
42	"	1.00	"	"	"	"	"	"	3660	1.070	0.950	- -	0.025	0.019	0.875	"	"
43	"	3.00	"	"	"	"	"	"	5420	1.520	1.380	- -	0.062	0.048	0.625	"	"
44	WW	1.50	"	"	"	"	"	"	1620	0.885	0.775	- -	0.045	0.013	0.812	"	"
45	"	3.00	"	"	"	"	"	"	2180	1.200	1.060	- -	0.046	0.030	0.625	"	"
46	VW	1.00	"	"	"	"	"	"	3200	- -	- -	- -	0.039	0.034	0.875	"	"
47	"	3.00	"	"	"	"	"	"	4860	- -	- -	- -	0.068	0.047	0.625	"	"
48	ST	1.50	"	"	"	"	"	"	2900	0.920	0.780	- -	0.037	0.033	0.812	"	"
49	"	"	"	"	"	"	"	"	5300	0.500	0.400	- -	0.040	0.029	"	"	"
50	"	3.00	"	"	"	"	"	"	2745	1.305	0.940	- -	0.069	0.033	0.625	"	"
51	"	"	"	"	"	"	"	"	2580	0.900	0.700	- -	0.053	0.036	"	"	"
52	"	4.00	"	"	"	"	"	"	2345	1.200	1.020	- -	0.055	0.035	0.500	"	"
53	"	"	"	"	"	"	"	"	3515	1.050	0.820	- -	0.058	0.043	"	"	"
54	VW	2.00	"	"	"	"	"	"	7300	1.560	1.420	- -	0.027	0.033	0.750	"	"
55	"	"	"	"	7.0	0.00038	"	0.70	6045	1.610	1.430	- -	0.053	0.026	"	1.250	0.264
56	"	1.00	"	"	"	0.00050	"	"	7020	1.110	1.040	- -	0.052	0.021	0.875	"	"
57	"	2.00	"	"	5.0	0.00070	"	0.51	4500	1.265	0.980	- -	0.047	0.027	0.750	1.230	0.304
58	"	"	"	"	"	"	"	"	5760	1.420	1.170	- -	- -	0.036	"	"	"
59	"	"	"	"	"	"	"	"	4600	1.215	1.050	- -	0.022	0.017	"	"	"
60	"	"	"	"	"	"	"	"	5600	1.650	1.060	- -	0.039	0.034	"	"	"
61	LC	2.00	1	"	"	"	"	0.52	1440	- -	0.400	- -	- -	- -	"	1.200	0.295
62	VW	"	"	"	"	"	"	- -	1460	0.990	0.570	- -	- -	- -	"	- -	- -
63	"	1.50	"	4	1.2	0	0.65	0.40	9300	0.920	- -	- -	- -	- -	0.625	0.750	0.209
64	WW	1.25	"	"	"	"	"	"	300	0.370	- -	- -	- -	- -	0.687	"	"
65	"	1.00	"	"	"	"	"	"	"	0.280	- -	- -	- -	- -	0.750	"	"

TABLE I. BASIC EXPERIMENTAL DATA (cont'd)

Run No.	Model Type	Model Length a (ft)	Number of Models p	Width of Flume B (ft)	Total Discharge Q (cfs)	Slope of Bed S	Median Size of Bed Mat'l d_{50}	Normal Depth of Flow h_n (ft)	Time of Test t (min)	Maximum Scour Depth d_{SM} (ft)	Equilibrium Scour Depth d_{SE} (ft)	Limiting Scour Depth d_{SL} (ft)	Water Surface Drop Across Embankment: Initial Δh_{si} (ft)	Water Surface Drop Across Embankment: Final Δh_{sf} (ft)	Opening Ratio $M = \frac{B-pa}{B}$	Mean Velocity of flow V (ft/sec)	Froude Number F_n
66	WW	1.75	1	4	1.2	0	0.65	0.40	320	0.550	- -	- -	- -	- -	0.533	0.750	0.209
67	ST	1.37	"	"	"	"	"	"	300	0.220	- -	- -	- -	- -	0.656	"	"
68	"	"	"	"	"	"	"	"	"	0.210	- -	- -	- -	- -	"	"	"
69	"	1.87	"	"	"	"	"	"	"	0.390	- -	- -	- -	- -	0.531	"	"
70	"	"	"	"	"	"	"	"	"	0.420	- -	- -	- -	- -	"	"	"
71	VW	1.00	"	"	"	"	"	"	2300	0.770	- -	- -	- -	- -	0.750	"	"
72	"	"	"	"	"	"	0.56	0.50	8545	0.660	- -	- -	- -	- -	"	0.600	0.150
73	"	"	"	"	"	"	"	0.25	6720	0.990	- -	- -	- -	- -	"	1.200	0.424
74	"	"	"	"	"	0.00100	"	"	8180	0.850	- -	- -	- -	0.009	"	"	"
75	"	"	"	"	2.1	"	"	0.46	5560	1.350	- -	- -	- -	- -	"	1.130	2.940
76	"	"	"	"	1.7	0.00250	"	0.24	1235	0.940	- -	- -	- -	- -	"	1.810	0.657
76R	"	"	"	"	"	"	"	"	4140	1.050	- -	- -	- -	- -	"	"	"
77	"	"	"	"	1.5	0.00200	"	"	6335	1.150	- -	- -	- -	- -	"	1.562	0.562
101	"	1.00	"	"	0.8	0	"	0.25	- -	- -	- -	1.10	- -	- -	"	0.750	0.264
102	"	"	"	"	0.9	"	"	0.33	- -	- -	- -	"	- -	- -	"	0.644	0.198
103	"	"	"	"	0.7	"	"	0.20	- -	- -	- -	"	- -	- -	"	0.850	0.332
104	"	"	"	"	1.1	"	"	0.30	- -	- -	- -	1.43	- -	- -	"	0.875	0.282
105	"	"	"	"	1.0	"	"	"	- -	- -	- -	"	- -	- -	"	0.842	0.271
106	"	"	"	"	0.9	"	"	0.20	- -	- -	- -	"	- -	- -	"	1.150	0.454
107	"	"	"	"	0.9	"	"	"	- -	- -	- -	"	- -	- -	"	1.125	0.443
108	"	"	"	"	"	"	"	0.23	- -	- -	- -	"	- -	- -	"	0.968	0.356
109	"	1.50	"	"	0.7	"	"	0.30	- -	- -	- -	0.99	- -	- -	0.625	0.583	0.188
110	"	"	"	"	0.5	"	"	0.20	- -	- -	- -	"	- -	- -	"	0.625	0.247
111	"	"	"	"	0.7	"	"	0.30	- -	- -	- -	"	- -	- -	"	0.541	0.174
112	"	"	"	"	0.5	"	"	0.15	- -	- -	- -	"	- -	- -	"	0.750	0.342
113	"	"	"	"	0.8	"	"	0.25	- -	- -	- -	1.38	- -	- -	"	0.770	0.272
114	"	"	"	"	0.6	"	"	0.15	- -	- -	- -	"	- -	- -	"	0.957	0.430
115	"	0.50	"	"	1.0	"	"	0.20	- -	- -	- -	1.35	- -	- -	0.875	1.250	0.493
116	"	"	"	"	1.2	"	"	0.30	- -	- -	- -	"	- -	- -	"	0.966	0.312
117	"	"	"	"	0.9	"	"	0.15	- -	- -	- -	"	- -	- -	"	1.418	0.644
118	"	"	"	"	1.0	"	"	0.20	- -	- -	- -	"	- -	- -	"	1.188	0.469
119	WW	1.00	"	"	1.2	"	"	0.30	- -	- -	- -	1.02	- -	- -	0.750	0.958	0.309
120	"	"	"	"	0.7	"	"	0.20	- -	- -	- -	"	- -	- -	"	0.875	0.345
121	"	"	"	"	0.6	"	"	0.16	- -	- -	- -	"	- -	- -	"	0.859	0.379
122	"	"	"	"	1.0	"	"	0.25	- -	- -	- -	"	- -	- -	"	0.950	0.335
123	"	"	"	"	0.7	"	"	0.20	- -	- -	- -	"	- -	- -	"	0.875	0.345
124	"	"	"	"	1.2	"	"	0.30	- -	- -	- -	"	- -	- -	"	1.000	0.322
125	"	"	"	"	1.2	"	"	0.33	- -	- -	- -	"	- -	- -	"	0.924	0.284
126	"	"	"	"	1.0	"	"	0.30	- -	- -	- -	0.46	- -	- -	"	0.825	0.266
127	"	1.50	"	"	1.2	"	"	"	- -	- -	- -	0.91	- -	- -	0.625	0.967	0.312
128	"	"	"	"	0.9	"	"	"	- -	- -	- -	"	- -	- -	"	0.784	0.253
129	"	"	"	"	0.8	"	"	0.22	- -	- -	- -	"	- -	- -	"	0.898	0.339
130	"	"	"	"	0.5	"	"	0.14	- -	- -	- -	"	- -	- -	"	0.965	0.455
131	"	2.00	"	"	0.7	"	"	0.30	- -	- -	- -	0.65	- -	- -	0.500	0.558	0.180
132	"	"	"	"	0.4	"	"	0.15	- -	- -	- -	"	- -	- -	"	0.700	0.318
133	"	"	"	"	"	"	"	0.13	- -	- -	- -	"	- -	- -	"	0.673	0.329
134	"	"	"	"	1.1	"	"	0.28	- -	- -	- -	0.97	- -	- -	"	0.937	0.311
135	"	"	"	"	0.8	"	"	0.17	- -	- -	- -	"	- -	- -	"	1.118	0.478
136	"	"	"	"	0.6	"	"	0.15	- -	- -	- -	"	- -	- -	"	1.017	0.464
137	ST	1.38	"	"	0.9	"	"	0.29	- -	- -	- -	0.42	- -	- -	0.656	0.733	0.240
138	"	"	"	"	0.5	"	"	0.12	- -	- -	- -	"	- -	- -	"	0.959	0.490
139	"	"	"	"	0.6	"	"	0.17	- -	- -	- -	"	- -	- -	"	0.867	0.372
140	"	"	"	"	1.0	"	"	0.21	- -	- -	- -	0.74	- -	- -	"	1.142	0.441
141	"	"	"	"	1.1	"	"	0.22	- -	- -	- -	"	- -	- -	"	1.193	0.449
142	"	"	"	"	1.2	"	"	0.23	- -	- -	- -	"	- -	- -	"	1.304	0.481
143	"	"	"	"	0.9	"	"	0.17	- -	- -	- -	"	- -	- -	"	1.368	0.585
144	"	1.88	"	"	0.7	"	"	0.15	- -	- -	- -	0.45	- -	- -	0.531	1.166	0.532
145	"	"	"	"	0.6	"	"	0.13	- -	- -	- -	"	- -	- -	"	1.058	0.517
146	"	"	"	"	0.9	"	"	0.30	- -	- -	- -	"	- -	- -	"	0.750	0.242
147	"	"	"	"	0.7	"	"	0.20	- -	- -	- -	"	- -	- -	"	0.875	0.345
148	"	"	"	"	1.2	"	"	0.30	- -	- -	- -	0.61	- -	- -	"	1.000	0.323
149	"	"	"	"	0.8	"	"	0.16	- -	- -	- -	"	- -	- -	"	1.188	0.523
150	"	"	"	"	0.7	"	"	0.15	- -	- -	- -	"	- -	- -	"	1.218	0.553

TABLE I. BASIC EXPERIMENTAL DATA (cont'd)

Run No.	Model Type	Model Length a (ft)	Number of Models p	Width of Flume B (ft)	Total Discharge Q (cfs)	Slope of Bed S	Median Size of Bed Mat'l d_{50}	Normal Depth of Flow h_n (ft)	Time of Test t (min)	Maximum Scour Depth d_{SM} (ft)	Equilibrium Scour Depth d_{SE} (ft)	Limiting Scour Depth d_{SL} (ft)	Water Surface Drop Across Embankment: Initial Δh_{si} (ft)	Water Surface Drop Across Embankment: Final Δh_{sf} (ft)	Opening Ratio $M = \frac{B-pa}{B}$	Mean Velocity of flow V (ft/sec)	Froude Number F_n
151	ST	1.38	1	4	0.8	0	0.56	0.16	--	--	--	0.97	--	--	0.656	1.281	0.565
152	"	"	"	"	1.0	"	"	0.20	--	--	--	"	--	--	"	1.188	0.467
153	"	"	"	"	1.1	"	"	0.25	--	--	--	"	--	--	"	1.060	0.374
154	"	"	"	"	1.2	"	"	0.31	--	--	--	"	--	--	"	1.000	0.317
155	"	"	"	"	1.3	"	"	0.33	--	--	--	"	--	--	"	0.993	0.304
156	"	1.88	"	"	0.5	"	"	0.11	--	--	--	0.79	--	--	0.531	1.022	0.544
157	"	"	"	"	0.7	"	"	0.18	--	--	--	"	--	--	"	1.000	0.417
158	"	"	"	"	1.1	"	"	0.31	--	--	--	"	--	--	"	0.847	0.269
159	"	"	"	"	1.1	"	"	0.33	--	--	--	"	--	--	"	0.864	0.266
160	"	"	"	"	0.5	"	"	0.11	--	--	--	"	--	--	"	1.045	0.555
161	"	"	"	"	0.6	"	"	0.15	--	--	--	"	--	--	"	1.018	0.463
162	"	"	"	"	0.6	"	"	0.12	--	--	--	0.95	--	--	"	1.188	0.606
163	"	"	"	"	0.7	"	"	0.15	--	--	--	"	--	--	"	1.168	0.533
164	"	"	"	"	0.8	"	"	0.19	--	--	--	"	--	--	"	1.052	0.425
165	"	"	"	"	1.0	"	"	0.26	--	--	--	"	--	--	"	0.991	0.344
166	WW	1.50	"	8	2.0	--	"	0.41	--	--	--	0.70	--	--	0.812	0.595	0.164
167	"	"	"	"	3.0	--	"	0.50	--	--	--	0.69	--	0.006	"	0.750	0.187
168	"	"	"	"	5.5	--	"	0.87	--	--	--	0.68	--	0.014	"	0.790	0.149
169	"	"	"	"	6.0	--	"	0.77	--	--	--	1.27	--	0.009	"	0.975	0.196
170	"	"	"	"	7.2	--	"	0.96	--	--	--	1.26	--	0.019	"	0.938	0.169
171	"	"	"	"	3.4	--	"	0.41	--	--	--	"	--	0.005	"	1.038	0.286
172	"	"	"	"	2.1	--	"	0.26	--	--	--	"	--	0	"	1.010	0.349
173	"	4.00	"	"	3.6	--	"	0.84	--	--	--	0.79	--	0.018	0.500	0.536	0.103
174	"	"	"	"	4.6	--	"	1.10	--	--	--	0.84	--	0.016	"	0.523	0.088
175	"	"	"	"	3.0	--	"	0.44	--	--	--	1.10	--	0.021	"	0.853	0.227
176	"	"	"	"	3.5	--	"	0.40	--	--	--	1.44	--	0.025	"	1.093	0.304
177	"	"	"	"	3.0	--	"	0.33	--	--	--	"	--	0.040	"	1.135	0.349
178	"	"	"	"	5.2	--	"	0.78	--	--	--	"	--	0.024	"	0.833	0.166
179	ST	1.50	"	"	2.4	--	"	0.30	--	--	--	0.44	--	0.011	0.812	1.000	0.323
180	"	"	"	"	5.9	--	"	0.85	--	--	--	"	--	0.009	"	0.868	0.166
181	"	"	"	"	4.4	--	"	0.61	--	--	--	"	--	0.012	"	0.903	0.209
182	"	"	"	"	1.9	--	"	0.27	--	--	--	"	--	0.009	"	0.880	0.299
183	"	"	"	"	1.6	--	"	0.24	--	--	--	"	--	0.006	"	0.834	0.300
184	"	"	"	"	2.1	--	"	0.21	--	--	--	0.93	--	"	"	1.250	0.481
185	"	"	"	"	2.6	--	"	0.29	--	--	--	"	--	0.008	"	1.120	0.367
186	"	"	"	"	3.7	--	"	0.48	--	--	--	"	--	0.013	"	0.964	0.245
187	"	"	"	"	4.5	--	"	0.55	--	--	--	"	--	0.004	"	1.020	0.243
188	"	"	"	"	6.6	--	"	0.78	--	--	--	"	--	0.009	"	1.058	0.211
189	"	"	"	"	3.5	--	"	0.29	--	--	--	1.36	--	0.012	"	1.510	0.495
190	"	"	"	"	3.2	--	"	0.25	--	--	--	"	--	"	"	1.600	0.565
191	"	"	"	"	4.6	--	"	0.42	--	--	--	"	--	0.009	"	1.370	0.373
192	"	4.00	"	"	3.2	--	"	0.45	--	--	--	0.81	--	0.026	0.500	0.889	0.234
193	"	"	"	"	4.6	--	"	0.78	--	--	--	"	--	0.027	"	0.738	0.147
194	"	"	"	"	1.7	--	"	0.20	--	--	--	0.88	--	0.010	"	1.062	0.419
195	"	"	"	"	3.7	--	"	0.36	--	--	--	1.36	--	0.017	"	1.285	0.378
196	"	"	"	"	2.7	--	"	0.25	--	--	--	"	--	0.020	"	1.350	0.477
197	"	"	"	"	2.0	--	"	0.20	--	--	--	"	--	"	"	1.250	0.493
198	"	"	"	"	2.3	--	"	0.21	--	--	--	"	--	0.012	"	1.370	0.528
199	"	"	"	"	2.7	--	"	0.26	--	--	--	1.56	--	0.009	"	1.298	0.450
200	"	"	"	"	2.0	--	"	0.23	--	--	--	0.65	--	0.019	"	1.088	0.401
201	"	"	"	"	2.8	--	"	0.43	--	--	--	0.69	--	0.020	"	0.814	0.219
202	"	"	"	"	3.8	--	"	0.56	--	--	--	0.72	--	"	"	0.849	0.201
203	"	"	"	"	5.0	--	"	0.78	--	--	--	0.74	--	0.024	"	0.803	0.160
204	"	"	"	"	6.2	--	"	0.97	--	--	--	0.76	--	0.034	"	0.800	0.143
205	"	"	"	"	3.1	--	"	0.45	--	--	--	0.79	--	0.010	"	0.861	0.226
206	"	"	"	"	2.5	--	"	0.27	--	--	--	0.76	--	0.014	"	1.158	0.394
207	"	"	"	"	2.9	--	"	0.40	--	--	--	0.75	--	0.020	"	0.907	0.253
208	"	"	"	"	2.6	--	"	0.25	--	--	--	0.76	--	"	"	1.300	0.459
209	"	"	"	"	2.7	--	"	0.31	--	--	--	0.80	--	0.021	"	1.088	0.345
210	"	"	"	"	2.1	--	"	0.17	--	--	--	0.75	--	0.011	"	1.543	0.660
211	"	"	"	"	4.9	--	"	0.70	--	--	--	0.90	--	0.028	"	0.875	0.182
212	"	"	"	"	3.8	--	"	0.57	--	--	--	0.91	--	0.029	"	0.834	0.195
213	"	"	"	"	3.4	--	"	0.45	--	--	--	0.93	--	0.007	"	0.944	0.248
214	"	"	"	"	2.9	--	"	0.27	--	--	--	0.90	--	0.015	"	1.343	0.456

TABLE I. BASIC EXPERIMENTAL DATA (cont'd)

Run No.	Model Type	Model Length a (ft)	Number of Models p	Width of Flume B (ft)	Total Discharge Q (cfs)	Slope of Bed S	Median Size of Bed Mat'l d_{50}	Normal Depth of Flow h_n (ft)	Time of Test t (min)	Maximum Scour Depth d_{SM} (ft)	Equilibrium Scour Depth d_{SE} (ft)	Limiting Scour Depth d_{SL} (ft)	Water Surface Drop Across Embankment: Initial Δh_{si} (ft)	Water Surface Drop Across Embankment: Final Δh_{sf} (ft)	Opening Ratio $M = \frac{B-pa}{B}$	Mean Velocity of flow V (ft/sec)	Froude Number F_n
279	VW	3.00	1	8	4.5	0.00056	0.56	0.43	- -	- -	- -	1.03	- -	0.028	0.625	1.310	0.353
280	"	"	"	"	5.2	"	"	0.53	- -	- -	- -	1.10	- -	0.046	"	1.225	0.297
281	"	"	"	"	5.6	"	"	0.50	- -	- -	- -	1.11	- -	0.040	"	1.400	0.349
282	"	"	"	"	4.7	"	"	0.45	- -	- -	- -	1.14	- -	0.036	"	1.305	0.343
283	"	"	"	"	4.8	"	"	0.40	- -	- -	- -	1.12	- -	0.031	"	1.500	0.418
284	"	"	"	"	4.5	"	"	0.19	- -	- -	- -	1.06	- -	0.033	"	2.960	1.198
285	"	"	"	"	5.0	"	"	0.49	- -	- -	- -	"	- -	- -	"	1.275	0.322
286	"	"	"	"	4.3	"	"	0.31	- -	- -	- -	"	- -	- -	"	1.733	0.549
287	"	"	"	"	"	"	"	0.25	- -	- -	- -	"	- -	- -	"	2.150	0.757
288	"	1.00	"	"	10.8	0.00450	"	0.34	90	1.29	1.24	- -	- -	- -	0.875	3.970	1.202
289	"	"	"	"	7.8	- -	"	0.27	120	1.23	1.06	- -	- -	- -	"	3.610	1.227
290	"	"	"	"	6.0	0.00200	"	0.28	5	- -	1.10	- -	- -	- -	"	2.680	0.894
291	"	"	"	"	6.7	0.00100	"	0.31	60	1.18	1.16	- -	- -	- -	"	2.700	0.857
292	"	"	"	"	8.1	0.00750	"	0.28	60	1.19	1.15	- -	- -	- -	"	3.620	1.205
293	"	"	"	"	9.0	0.01000	"	0.33	50	1.21	1.14	- -	- -	- -	"	3.410	1.040
294	"	"	"	"	10.0	"	"	0.31	315	1.23	"	- -	- -	- -	"	4.030	1.279
295	"	2.00	"	"	6.0	0.00400	"	0.29	135	1.36	1.31	- -	- -	- -	0.750	2.585	0.847
296	"	"	"	"	7.1	0.00700	"	0.27	40	"	1.32	- -	- -	- -	"	3.285	1.115
297	"	"	"	"	8.0	0.00800	"	0.30	125	1.41	1.38	- -	- -	- -	"	3.335	1.070
298	"	"	"	"	9.2	0.00900	"	0.32	100	1.45	1.41	- -	- -	- -	"	3.600	1.120
299	"	"	"	"	10.2	0.01000	"	0.33	55	1.53	1.45	- -	- -	- -	"	3.870	1.190
300	"	"	"	"	11.0	0.01250	"	0.37	240	1.71	1.58	- -	- -	- -	"	3.715	1.080
301	VB	1.00	"	"	6.8	0.00900	"	0.28	65	1.05	0.98	- -	0.162	0.189	0.875	3.055	1.011
302	"	2.00	"	"	"	"	"	"	60	1.39	1.35	- -	0.177	0.178	0.750	"	"
303	"	1.00	"	"	5.8	0.00700	"	0.26	"	1.14	1.11	- -	0.167	0.142	0.875	2.790	0.965
304	"	2.00	"	"	"	"	"	"	"	1.33	1.24	- -	0.155	0.191	0.750	"	"
305	"	3.00	"	"	"	"	"	"	"	1.50	1.46	- -	0.163	0.222	0.625	"	"
306	"	1.00	"	"	8.0	0.00600	"	0.33	55	1.23	1.12	- -	0.151	0.181	0.875	3.030	0.928
307	"	2.00	"	"	"	"	"	"	60	1.35	1.33	- -	0.174	0.187	0.750	"	"
308	"	3.00	"	"	"	"	"	"	"	1.65	1.62	- -	0.180	0.182	0.625	"	"
309	"	1.00	"	"	10.2	0.00800	"	0.36	"	1.21	1.16	- -	0.189	0.187	0.875	3.540	1.039
310	"	2.00	"	"	"	"	"	"	"	1.62	1.60	- -	0.201	0.223	0.750	"	"
311	"	3.00	"	"	10.0	0.00800	"	0.34	90	1.88	1.82	- -	0.314	0.290	0.625	3.680	1.114
312	"	1.00	"	"	"	0.00480	"	0.48	60	1.09	1.03	- -	0.130	0.089	0.875	2.610	0.666
313	"	2.00	"	"	"	"	"	"	75	1.50	- -	- -	0.200	0.204	0.750	"	"
314	"	3.00	"	"	"	"	"	"	60	1.70	- -	- -	0.166	0.207	0.625	"	"
315	"	1.00	"	"	9.1	0.00300	"	0.42	"	1.03	1.01	- -	0.159	0.112	0.875	2.710	0.738
316	"	2.00	"	"	"	0.00530	"	0.53	"	1.49	- -	- -	0.170	0.213	0.750	2.145	0.520
317	"	3.00	"	"	"	0.00700	"	0.46	80	1.64	- -	- -	0.175	0.181	0.625	2.470	0.644
318	"	1.00	"	"	9.2	0.00650	"	0.49	60	1.30	- -	- -	0.107	0.080	0.875	2.350	0.592
319	WW	1.50	"	"	10.0	0.00580	"	0.52	90	0.93	0.86	- -	0.063	0.052	0.812	2.430	0.595
320	"	3.00	"	"	"	"	"	"	1190	1.28	1.22	- -	0.152	0.147	0.625	"	"
321	ST	1.50	"	"	"	"	"	"	1130	1.04	0.76	- -	0.082	0.050	0.812	"	"
322	"	3.00	"	"	"	"	"	"	135	1.49	1.33	- -	0.143	0.161	0.625	"	"
323	"	1.50	"	"	"	"	"	"	180	0.79	0.70	- -	0.153	0.117	0.812	"	"
324	"	3.00	"	"	"	"	"	"	"	0.95	0.75	- -	0.162	0.127	0.625	"	"
325	WW	1.50	"	"	9.5	0.00500	"	0.38	165	1.31	1.26	- -	0.059	0.037	0.812	3.120	0.900
325R	"	"	"	"	"	"	"	"	125	1.37	1.29	- -	0.024	0.033	"	"	"
325RR	"	"	"	"	10.0	"	"	"	150	1.38	1.25	- -	- -	- -	"	3.290	0.939
326	ST	"	"	"	9.5	"	"	"	220	1.24	0.87	- -	0.062	0.120	"	3.120	0.900
327	"	"	"	"	"	"	"	"	140	0.85	0.72	- -	0.171	0.124	"	"	"
328	WW	3.00	"	"	"	"	"	"	115	1.48	1.40	- -	0.168	- -	0.625	"	"
329	ST	"	"	"	"	"	"	"	125	1.65	1.52	- -	0.187	0.263	"	"	"
330	"	"	"	"	"	"	"	"	110	1.00	0.96	- -	0.183	0.247	"	"	"
331	WW	1.50	"	"	8.0	0.00300	"	0.57	"	0.87	0.80	- -	0.063	0.058	0.813	1.753	0.408
332	ST	"	"	"	"	"	"	"	155	1.05	0.90	- -	0.082	0.076	"	"	"
332R	"	"	"	"	"	"	"	"	160	1.28	- -	- -	0.046	0.067	"	"	"
333	"	"	"	"	"	"	"	"	175	0.72	0.66	- -	0.096	0.125	"	"	"

TABLE II COMPUTATION OF DATA PERTAINING TO NORMAL FLOW

Run No.	S	h_n	V	F_n	T_o	V*	$\frac{V*}{\omega}$	$\frac{V}{V*}$	$\frac{T_o}{(\gamma_s-\gamma)d_{50}}$	$\frac{V}{V*}\frac{T_o}{(\gamma_s-\gamma)d_{50}}$	$\frac{h_n}{d}$	$\left(\frac{h_n}{d}\right)^{0.132}$	$S^{0.286}$	$F_n^{0.7}$	K	$\frac{V*d_{50}}{\gamma}$	C_a	$h_n^{.54}$	$S^{.33}$	V
2-9	0.00253	0.46	1.80	0.467	0.073	0.193	0.737	9.30	0.383	3.56	250	2.07	0.177	0.590	0.516	29.2	20	0.657	0.138	1.81
10-16	0.00230	0.77	2.11	0.424	0.111	0.239	0.912	8.83	0.583	5.15	419	2.22	0.173	0.553	0.724	36.1	"	0.868	0.135	2.35
17-19	0.00270	0.62	2.02	0.452	0.105	0.232	0.886	8.69	0.551	4.79	337	2.15	0.181	0.579	0.697	35.1	"	0.773	0.142	2.20
33	0.00370	0.50	2.13	0.531	0.115	0.244	0.931	8.73	0.609	5.32	272	2.10	0.198	0.648	0.774	36.9	"	0.688	0.157	2.16
33R	0.00340	"	2.10	0.524	0.107	0.234	0.893	8.97	0.560	5.02	"	"	0.194	0.640	0.723	35.4	"	"	0.153	2.11
34	0.00350	"	"	"	0.109	0.237	0.905	8.86	0.576	5.10	"	"	0.195	"	0.740	35.8	"	"	0.155	2.13
35	0.00050	0.51	1.19	0.294	0.016	0.091	0.347	13.08	0.084	1.10	277	"	0.111	0.428	0.136	13.8	"	0.695	0.082	1.14
36	0.00044	0.51	1.20	0.297	0.014	0.085	0.324	14.12	0.073	1.03	275	"	0.107	0.430	0.122	12.9	"	0.692	0.078	1.08
37	0.00045	0.50	1.21	0.302	"	"	"	14.24	0.074	1.05	272	"	0.108	0.436	0.123	"	"	0.688	0.079	1.09
38	0.00068	"	"	"	0.021	0.104	0.397	11.64	0.112	1.30	"	"	0.122	"	0.173	15.7	"	"	0.090	1.24
39	0.00046	"	1.00	0.250	0.014	0.086	0.328	11.63	0.076	0.88	"	"	0.108	0.382	0.118	12.9	"	"	0.079	1.09
40	0.00046	0.54	0.93	0.222	0.016	0.089	0.341	10.35	0.082	0.86	293	2.12	"	0.352	0.123	13.5	"	0.716	"	1.13
41-54	0.00069	0.52	1.20	0.294	0.022	0.110	0.420	10.92	0.118	1.29	283	2.11	0.122	0.428	0.174	16.6	"	0.702	0.091	1.28

d_{50} = 0.56 m = 0.132 N = 0.70 λ = 0.286

Run No.	S	h_n	V	F_n	T_o	V*	$\frac{V*}{\omega}$	$\frac{V}{V*}$	$\frac{T_o}{(\gamma_s-\gamma)d_{50}}$	$\frac{V}{V*}\frac{T_o}{(\gamma_s-\gamma)d_{50}}$	$\frac{h_n}{d}$	$\left(\frac{h_n}{d}\right)^{0.136}$	$S^{0.284}$	$F_n^{0.7}$	K	$\frac{V*d_{50}}{\gamma}$	C_a	$h_n^{.57}$	$S^{.34}$	V
288	0.00450	0.34	3.97	1.202	0.095	0.222	0.787	17.88	0.470	8.40	173	2.02	0.209	1.130	0.769	35.9	33	0.540	0.159	10.50
289	- -	0.27	3.61	1.227	- -	- -	- -	- -	- -	- -	- -	- -	- -	- -	- -	- -	"	- -	- -	- -
290	0.00200	0.28	2.68	0.894	0.035	0.134	0.475	20.00	0.172	3.44	142	1.96	0.166	0.925	0.315	21.7	"	0.484	0.121	1.93
291	0.00100	0.31	2.70	0.857	0.019	0.100	0.355	27.00	0.095	2.57	157	1.99	0.135	0.898	0.194	16.2	"	0.513	0.096	1.63
292	0.00750	0.28	3.62	1.205	0.131	0.260	0.922	13.92	0.646	8.99	142	1.96	0.243	1.140	0.978	42.1	"	0.484	0.190	3.03
293	0.01000	0.33	3.41	1.040	0.206	0.326	1.156	10.46	1.015	10.62	168	2.01	0.264	1.030	1.354	52.8	"	0.532	0.209	3.67
294	"	0.31	4.03	1.279	0.193	0.316	1.121	12.75	0.953	12.15	157	1.99	"	1.180	1.366	51.2	"	0.513	"	3.54
295	0.00400	0.29	2.59	0.847	0.072	0.193	0.684	13.32	0.357	4.76	147	1.97	0.202	0.892	0.547	31.2	"	0.494	0.152	2.48
296	0.00700	0.27	3.29	1.115	0.118	0.246	0.872	13.39	0.580	7.77	137	1.95	0.238	1.070	0.886	39.8	"	0.474	0.185	2.89
297	0.00800	0.30	3.34	1.070	0.150	0.278	0.986	12.00	0.738	8.86	152	1.98	0.247	1.050	1.053	45.0	"	0.504	0.194	3.23
298	0.00900	0.32	3.60	1.120	0.180	0.304	1.078	11.84	0.886	10.49	162	2.00	0.255	1.045	1.280	49.2	"	0.522	0.202	3.48
299	0.01000	0.33	3.87	1.190	0.206	0.326	1.156	11.87	1.015	12.05	168	2.01	0.264	1.125	1.407	52.8	"	0.532	0.209	3.67
300	0.01250	0.37	3.72	1.080	0.289	0.385	1.365	9.65	1.420	13.70	188	2.04	0.278	1.055	1.766	62.3	"	0.568	0.226	4.23
301	0.00900	0.28	3.04	1.011	0.157	0.285	1.011	10.65	0.775	8.25	142	1.96	0.255	1.000	1.073	46.5	"	0.484	0.202	3.22
302	"	"	"	"	"	"	"	"	"	"	"	"	"	"	"	"	"	"	"	"
303	0.00700	0.26	2.79	0.965	0.114	0.242	0.858	11.53	0.560	6.46	132	1.94	0.238	0.976	0.812	39.2	"	0.464	0.185	2.83
305	"	"	"	"	"	"	"	"	"	"	"	"	"	"	"	"	"	"	"	"
306	0.00600	0.33	3.03	0.928	0.123	0.252	0.894	12.02	0.609	7.32	168	2.01	0.228	0.950	0.874	40.8	"	0.532	0.176	3.09
308	"	"	"	"	"	"	"	"	"	"	"	"	"	"	"	"	"	"	"	"
309	0.00800	0.36	3.54	1.039	0.180	0.304	1.078	11.65	0.886	10.32	183	2.03	0.247	1.025	1.225	49.2	"	0.559	0.194	3.58
310	"	"	"	"	"	"	"	"	"	"	"	"	"	"	"	"	"	"	"	"
311	"	0.34	3.68	1.114	0.169	0.296	1.050	12.43	0.856	10.39	173	2.02	"	1.070	1.187	47.9	"	0.541	"	3.46
312	0.00480	0.48	2.61	0.666	0.144	0.273	0.968	9.56	0.700	6.78	244	2.12	0.213	0.753	0.905	44.2	22.5	0.658	0.163	2.42
314	"	"	"	"	"	"	"	"	"	"	"	"	"	"	"	"	"	"	"	"
315	0.00300	0.42	2.71	0.738	0.079	0.201	0.713	13.48	0.387	5.22	213	2.08	0.187	0.810	0.578	32.5	33	0.610	0.139	2.79
316	0.00530	0.53	2.15	0.520	0.175	0.301	1.067	7.13	0.864	6.16	269	2.15	0.219	0.637	0.996	48.7	22.5	0.696	0.168	2.63
317	0.00700	0.46	2.47	0.644	0.210	0.322	1.142	7.67	0.990	7.59	234	2.10	0.238	0.736	1.169	52.1	"	0.642	0.185	2.67
318	0.00650	0.49	2.35	0.592	0.199	0.320	1.135	7.34	0.979	7.19	249	2.12	0.234	0.696	1.140	51.8	"	0.666	0.181	2.72
319	0.00380	0.52	2.43	0.595	0.122	0.251	0.890	9.68	0.602	5.83	261	2.14	0.200	0.705	0.773	40.6	"	0.685	0.150	2.31
324	"	"	"	"	"	"	"	"	"	"	"	"	"	"	"	"	"	"	"	"
325	0.00500	0.38	3.12	0.900	0.119	0.248	0.876	12.63	0.585	7.39	193	2.05	0.216	0.934	0.834	40.0	33	0.576	0.165	3.14
330	"	"	"	"	"	"	"	"	"	"	"	"	"	"	"	"	"	"	"	"
331	0.00300	0.57	1.75	0.408	0.107	0.235	0.833	7.46	0.526	3.92	289	2.16	0.187	0.531	0.639	38.0	22.5	0.726	0.139	2.27
333	"	"	"	"	"	"	"	"	"	"	"	"	"	"	"	"	"	"	"	"
325RR	0.00500	0.38	3.29	0.939	0.119	0.247	0.876	13.32	0.585	7.79	193	2.05	0.216	0.961	0.854	40.0	33	0.576	0.165	3.17

d_{50} = 0.60 mm m = 0.136 N = 0.70 λ = 0.284

TABLE III. COMPUTATION OF DATA PERTAINING TO DEPTH OF SCOUR

Run No.	Model Type	a	h_n	F_n	d_{SE}	d_{SM}	$\frac{d_{SE}}{h_n}$	$\frac{d_{SM}}{h_n}$	$F_n^{1/3}$	$\frac{a}{h_n}$	$\left(\frac{a}{h_n}\right)^{0.4}$	$\left(\frac{a}{h_n}\right)^{0.4} F_n^{1/3}$
2	VW	0.75	0.46	0.467	0.898	1.058	1.952	2.300	0.776	1.630	1.216	0.944
3	"	1.00	"	"	1.013	1.113	2.205	2.420	"	2.175	1.389	1.076
4	"	1.25	"	"	1.173	1.218	2.550	2.650	"	2.720	1.492	1.158
5	"	1.50	"	"	1.213	1.403	2.635	3.050	"	3.260	1.604	1.244
5A	"	1.50	"	"	1.273	1.428	2.770	3.102	"	"	"	"
6	"	1.75	"	"	1.243	1.413	2.700	3.070	"	3.805	1.707	1.324
6A	"	1.75	"	"	1.363	1.513	2.965	3.290	"	"	"	"
7	"	2.00	"	"	1.413	1.613	3.075	3.505	"	4.345	1.810	1.403
8	"	2.25	"	"	1.523	1.783	3.315	3.870	"	4.890	1.888	1.464
9	"	2.50	"	"	1.693	1.893	3.685	4.110	"	5.440	1.969	1.526
10	"	0.50	0.77	0.424	1.050	1.405	1.363	1.825	0.751	0.650	0.850	0.638
11	"	0.75	"	"	1.260	1.425	1.637	1.852	"	0.975	0.990	0.743
12	"	1.00	"	"	1.340	1.593	1.740	2.072	"	1.300	1.111	0.834
13	"	1.50	"	"	1.610	1.743	2.090	2.265	"	1.950	1.306	0.981
14	"	2.00	"	"	- -	- -	- -	- -	"	- -	- -	- -
15	"	3.00	"	"	1.920	2.046	2.493	2.655	"	3.890	1.721	1.294
16	"	1.50	"	"	1.460	1.716	1.896	2.230	"	1.950	1.306	0.981
17	"	1.00	0.62	0.452	1.150	1.343	1.855	2.168	0.767	1.615	1.211	0.930
18	"	1.50	"	"	1.380	1.683	2.225	2.715	"	2.425	1.425	1.093
19	"	0.25	"	"	0.650	1.003	1.049	1.619	"	0.405	0.698	0.535
33	"	1.00	0.50	0.531	1.150	1.338	2.300	2.680	0.810	2.000	1.320	1.070
33R	"	1.00	"	0.524	1.100	1.365	2.200	2.730	0.806	"	"	1.065
34	"	2.00	"	"	1.520	1.631	3.040	3.260	"	4.000	1.740	1.404
289	"	1.00	0.27	1.227	1.060	1.230	3.921	4.555	1.070	3.700	1.687	1.805
292	"	"	0.28	1.205	1.150	1.190	4.109	4.251	1.063	3.570	1.664	1.770
293	"	"	0.33	1.040	1.140	1.210	3.455	3.665	1.013	3.030	1.558	1.578
294	"	"	0.31	1.279	"	1.230	3.680	3.965	1.086	3.230	1.598	1.733
295	"	2.00	0.29	0.847	1.310	1.360	4.516	4.690	0.946	6.900	2.165	2.050
296	"	"	0.27	1.115	1.320	"	4.890	5.036	1.036	7.420	2.229	2.308
297	"	"	0.30	1.070	1.380	1.410	4.600	4.700	1.023	6.670	2.136	2.182
298	"	"	0.32	1.120	1.410	1.450	4.405	4.532	1.038	6.250	2.082	2.161

TABLE III. COMPUTATION OF DATA PERTAINING TO DEPTH OF SCOUR (cont'd.)

Run No.	Model Type	a	h_n	F_n	d_{SE}	d_{SM}	$\frac{d_{SE}}{h_n}$	$\frac{d_{SM}}{h_n}$	$F_n^{1/3}$	$\frac{a}{h_n}$	$\left(\frac{a}{h_n}\right)^{0.4}$		$\left(\frac{a}{h_n}\right)^{0.4} F_n^{1/3}$
299	VW	2.00	0.33	1.190	1.450	1.530	4.392	4.638	1.060	6.060	2.056		2.177
300	"	"	0.37	1.080	1.580	1.710	4.270	4.620	1.026	5.410	1.964		2.015
301	VB	1.00	0.28	1.011	0.980	1.050	3.500	3.750	1.003	3.570	1.664		1.668
302	"	2.00	"	"	1.350	1.390	4.821	4.966	"	7.140	2.195		2.200
303	"	1.00	0.26	0.965	1.110	1.140	4.270	4.385	0.988	3.850	1.715		1.696
304	"	2.00	"	"	1.240	1.330	4.770	5.120	"	7.700	2.262		2.239
305	"	3.00	"	"	1.460	1.500	5.618	5.773	"	11.530	2.659		2.626
306	"	1.00	0.33	0.928	1.120	1.230	3.395	3.726	0.975	3.030	1.558		1.519
307	"	2.00	"	"	1.330	1.350	4.030	4.095	"	6.060	2.056		2.002
308	"	3.00	"	0.927	1.620	1.650	4.910	5.000	"	9.090	2.418		2.358
309	"	1.00	0.36	1.039	1.160	1.210	3.221	3.360	1.013	2.780	1.505		1.522
310	"	2.00	"	"	1.600	1.620	4.445	4.500	"	5.560	1.985		2.010
311	"	3.00	0.34	1.114	1.820	1.880	5.350	5.540	1.036	8.830	2.390		2.478
312	"	1.00	0.48	0.666	1.030	1.090	2.144	2.270	0.873	2.085	1.342		1.173
315	"	"	0.42	0.738	1.010	1.030	2.403	2.452	0.899	2.380	1.410		1.270
44	WW	1.50	0.52	0.294	0.775	0.885	1.490	1.700	0.665	2.885	1.528	Clear	1.016
45	"	3.00	"	"	1.060	1.200	2.040	2.308	"	5.770	2.016	Water	1.340
319	"	1.50	"	0.595	0.860	0.930	1.670	1.807	0.841	2.910	1.533		1.290
320	"	3.00	"	"	1.220	1.280	2.369	2.483	"	5.820	2.023		1.702
325	"	1.50	0.38	0.900	1.260	1.310	3.316	3.450	0.965	3.950	1.732		1.673
325R	"	"	"	0.892	1.290	1.370	3.395	3.603	0.963	"	"		"
325RR	"	"	"	0.939	1.250	1.380	3.290	3.635	0.979	"	"		1.697
328	"	3.00	"	0.900	1.400	1.480	3.682	3.896	0.965	7.900	2.286		2.205
331	"	1.50	0.57	0.408	0.800	0.870	1.403	1.527	0.742	2.630	1.472		1.092
48	ST(VCO)	"	0.52	0.294	0.780	0.920	1.500	1.770	0.665	2.885	1.528	Clear	1.016
50	"	3.00	"	"	0.940	1.305	1.810	2.510	"	5.770	2.016	Water	1.340
52	"	4.00	"	"	1.020	1.200	1.960	2.310	"	7.690	2.239		1.505
321	"	1.50	"	0.595	0.760	1.040	1.475	2.020	0.841	2.910	1.533		1.290
322	"	3.00	"	"	1.330	1.490	2.581	2.892	"	5.820	2.023		1.702
326	"	1.50	0.38	0.900	0.870	1.240	2.290	3.260	0.965	3.950	1.732		1.673
329	"	3.00	"	"	1.520	1.650	4.000	4.340	"	7.900	2.286		2.205
332	"	1.50	0.57	0.408	0.900	1.050	1.580	1.840	0.742	2.630	1.472		1.092
332R	"	"	"	"	- -	1.280	- -	2.242	"	"	"		"

TABLE III. COMPUTATION OF DATA PERTAINING TO DEPTH OF SCOUR (cont'd.)

Run No.	Model Type	a	h_n	F_n	d_{SE}	d_{SM}	$\frac{d_{SE}}{h_n}$	$\frac{d_{SM}}{h_n}$	$F_n^{1/3}$	$\frac{a}{h_n}$	$\left(\frac{a}{h_n}\right)^{0.4}$		$\left(\frac{a}{h_n}\right)^{0.4}(F_n)^{1/3}$
49	ST(Full)	1:50	0.52	0.294	0.400	0.500	0.769	0.962	0.665	2.885	1:528	Clear Water	1:016
51	"	3.00	"	"	0.700	0.900	1.350	1.730	"	5.770	2:016		1:340
53	"	4:00	"	"	0.820	1.050	1.580	2.020	"	7.690	2:239		1:505
323	"	1:50	"	0.595	0.700	0.790	1.360	1.535	0.841	2.910	1:533		1:290
324	"	3:00	"	"	0.750	0.950	1.457	1.845	"	5.820	2:023		1:702
327	"	1:50	0.38	0.900	0.720	0.850	1.892	2.236	0.965	3.950	1:732		1:673
330	"	3:00	"	"	0.960	1.000	2.525	2.630	"	7.900	2:286		2:205
333	"	1.50	0.57	0.408	0.660	0.720	1.158	1.263	0.742	3.950	1.732		1.092

TABLE III. COMPUTATION OF DATA PERTAINING TO DEPTH OF SCOUR (limiting scour)

Run No.	Model Type	h_n	d_{SL}	q	$h_n^{3/2}$	$\frac{q}{h_n^{3/2}}$	$\frac{d_{SL}}{h_n}$	$\frac{F}{M}$
101	VW	0.25	1.10	0.187	0.125	1.51	4.40	0.352
102	"	0.33	"	0.212	0.185	1.15	3.33	0.264
103	"	0.20	"	0.170	0.089	1.91	5.50	0.443
104	"	0.30	1.43	0.263	0.164	1.60	4.77	0.376
105	"	"	"	0.252	"	1.53	"	0.361
106	"	0.20	"	0.230	0.089	2.59	7.15	0.605
107	"	"	"	0.222	"	2.50	"	0.591
108	"	0.23	"	"	0.111	2.00	6.22	0.475
109	"	0.30	0.99	0.175	0.164	1.07	3.30	0.299
110	"	0.20	"	0.125	0.089	1.40	4.95	0.395
111	"	0.30	"	0.162	0.164	0.99	3.30	0.278
112	"	0.15	"	0.112	0.058	1.93	6.60	0.548
113	"	0.25	1.38	0.192	0.123	1.56	5.52	0.435
114	"	0.15	"	0.147	0.060	2.45	8.98	0.688
115	"	0.20	1.35	0.250	0.089	2.81	6.75	0.563
116	"	0.30	"	0.290	0.164	1.77	4.50	0.356
117	"	0.15	"	0.212	0.058	3.66	9.00	0.736
118	"	0.20	"	0.237	0.089	2.66	6.75	0.536

TABLE IV. ANALYSIS OF DATA ON Δh_s FOR RIGID CHANNEL

Run No.	Model Type	Opening b (ft)	Width of Flume B (ft)	Total Discharge Q (cfs)	Slope of Bed S	Normal Depth of Flow h_n (ft)	h_U	h_D	F_n	M	$F_n^{1.65}$	$M^{1.75}$	$\frac{F_n^{1.65}}{M^{1.75}}$	$\Delta h_s = h_U - h_D$	$\frac{h_U - h_D}{h_n}$	Roughness
357	VB	2.00	1.9	2.5	0.00120	0.33	0.621	0.282	0.289	0.253	0.129	0.090	1.433	0.339	1.018	Bar
358	"	3.00	"	"	"	"	0.497	0.289	"	0.380	"	0.185	0.697	0.208	0.625	"
359	"	4.00	"	"	"	"	0.426	0.296	"	0.505	"	0.303	0.426	0.130	0.390	"
360	"	5.00	"	"	"	"	0.390	0.305	"	0.633	"	0.451	0.286	0.085	0.255	"
361	"	6.00	"	"	"	"	0.366	0.311	"	0.760	"	0.620	0.208	0.055	0.165	"
598	"	"	"	5.0	0.00200	0.42	0.487	0.361	0.415	0.760	0.235	0.620	0.379	0.126	0.303	"
599	"	5.00	"	"	"	"	0.544	0.345	"	0.633	"	0.451	0.521	0.199	0.478	"
600	"	4.00	"	"	"	"	0.627	0.330	"	0.505	"	0.303	0.776	0.297	0.713	"
601	"	3.00	"	"	"	"	0.750	0.319	"	0.380	"	0.185	1.270	0.431	1.036	"
602	"	2.00	"	"	"	"	0.955	0.280	"	0.253	"	0.090	2.610	0.675	1.622	"
754	"	4.00	"	"	0.00120	0.48	0.650	0.423	0.332	0.505	0.162	0.303	0.535	0.227	0.469	"
755	"	3.00	"	"	"	"	0.766	0.404	"	0.380	"	0.185	0.876	0.362	0.748	"
757	"	5.00	"	"	"	"	0.586	0.434	"	0.633	"	0.451	0.360	0.152	0.314	"
872	"	3.00	"	"	"	"	0.767	0.414	"	0.380	"	0.185	0.876	0.353	0.730	"
873	"	4.00	"	"	"	"	0.659	0.436	"	0.505	"	0.303	0.535	0.223	0.461	"
874R	"	4.97	"	"	"	"	0.590	0.445	"	0.630	"	0.448	0.362	0.145	0.300	"
301	"	5.97	"	"	"	"	0.536	"	"	0.756	"	0.615	0.263	0.091	0.188	"
302	"	5.00	"	"	"	"	0.581	0.433	"	0.633	"	0.451	0.359	0.148	0.306	"
303	"	4.00	"	"	"	"	0.646	0.416	"	0.505	"	0.303	0.535	0.230	0.475	"
304	"	3.00	"	"	"	"	0.765	0.402	"	0.380	"	0.185	0.876	0.363	0.750	"
305	"	2.00	"	"	"	"	0.968	0.377	"	0.253	"	0.090	1.800	0.591	1.222	"
225	"	6.00	"	"	"	"	0.536	0.447	"	0.760	"	0.620	0.261	0.089	0.184	"
226	"	5.00	"	"	"	"	0.578	0.433	"	0.633	"	0.451	0.359	0.145	0.300	"
227	"	4.00	"	"	"	"	0.650	0.419	"	0.505	"	0.303	0.535	0.231	0.477	"
228	"	3.00	"	"	"	"	0.770	0.407	"	0.380	"	0.185	0.876	0.363	0.750	"
229	"	2.00	"	"	"	"	0.967	0.386	"	0.253	"	0.090	1.800	0.581	1.201	"
261	"	"	"	"	"	"	0.973	0.391	"	"	"	"	"	0.582	1.203	"
603	"	6.00	"	2.72	0.00200	"	0.496	0.461	0.184	0.760	0.061	0.620	0.099	0.035	0.073	Baffle
604	"	5.00	"	"	"	"	0.514	0.457	"	0.633	"	0.451	0.136	0.057	0.119	"
605	"	4.00	"	"	"	"	0.542	0.452	"	0.505	"	0.303	0.202	0.090	0.188	"
606	"	3.00	"	"	"	"	0.593	0.449	"	0.380	"	0.185	0.331	0.144	0.301	"
607	"	2.00	"	"	"	"	0.710	0.440	"	0.253	"	0.090	0.681	0.270	0.564	"
450	VB	6.00	"	2.50	0.00120	0.52	0.535	0.510	0.148	0.760	0.043	0.620	0.069	0.025	0.048	"
451	"	5.00	"	"	"	"	0.549	0.507	"	0.633	"	0.451	0.095	0.042	0.080	"
452	"	4.00	"	"	"	"	0.571	0.506	"	0.505	"	0.303	0.142	0.065	0.124	"
453	"	3.00	"	"	"	"	0.615	0.500	"	0.380	"	0.185	0.233	0.115	0.220	"
454	"	2.00	"	"	"	"	0.715	0.496	"	0.253	"	0.090	0.478	0.219	0.418	"
459	"	6.00	"	5.00	"	0.72	0.744	0.700	0.184	0.760	0.061	0.620	0.099	0.044	0.061	"
460	"	5.00	"	"	"	"	0.768	0.691	"	0.633	"	0.451	0.136	0.077	0.107	"
461	"	4.00	"	"	"	"	0.810	0.688	"	0.505	"	0.303	0.202	0.122	0.170	"
462	"	3.00	"	"	"	"	0.891	0.680	"	0.380	"	0.185	0.331	0.211	0.294	"
463	"	2.00	"	"	"	"	1.064	0.672	"	0.253	"	0.090	0.681	0.392	0.545	"
1288	VW	2.81	"	3.00	"	0.36	0.543	0.304	0.309	0.356	0.144	0.164	0.879	0.239	0.664	Bar
1289	"	3.82	"	"	"	"	0.463	0.323	"	0.484	"	0.281	0.511	0.140	0.389	"
1290	"	4.84	"	"	"	"	0.423	0.331	"	0.612	"	0.424	0.340	0.092	0.256	"
1291	"	5.87	"	"	"	"	0.398	0.339	"	0.744	"	0.600	0.240	0.059	0.164	"
1292	"	6.85	"	"	"	"	0.379	0.349	"	0.866	"	0.778	0.185	0.030	0.083	"
1302	"	2.83	"	5.00	"	0.48	0.754	0.390	0.332	0.358	0.162	0.165	0.983	0.364	0.752	"
1303	"	3.83	"	"	"	"	0.633	0.420	"	0.484	"	0.282	0.575	0.213	0.440	"
1304	"	4.85	"	"	"	"	0.570	0.433	"	0.614	"	0.426	0.381	0.137	0.283	"
1305R	"	5.85	"	"	"	"	0.527	0.453	"	0.741	"	0.592	0.274	0.074	0.153	"
1306R	"	6.87	"	"	"	"	0.505	0.467	"	0.870	"	0.788	0.206	0.038	0.077	"

TABLE V. COMPUTATION OF DATA ON Δh_{sf} (FINAL) FOR ALLUVIAL CHANNEL FOR COMPARISON WITH Δh_s FOR RIGID CHANNEL

Run No.	Model Type	Δh_{sf}	M	F	h_n	$\frac{\Delta h_{sf}}{h_n}$	$F^{1.65}$	$M^{1.75}$	$\frac{F^{1.65}}{M^{1.75}}$	$\frac{\Delta h_s}{h_n}$
						Alluvial Bed				Rigid Bed
2	VW	0.113	0.812	0.467	0.46	0.246	0.285	0.700	0.407	0.31
3	"	0.130	0.750	"	"	0.283	"	0.602	0.474	0.36
4	"	0.127	0.687	"	"	0.276	"	0.520	0.548	0.43
7	"	0.146	0.500	"	"	0.318	"	0.295	0.966	0.73
36	"	0.061	0.750	0.297	0.51	0.119	0.133	0.602	0.221	0.12
37	"	0.035	0.937	0.302	0.50	0.070	0.135	0.880	0.154	0.06
38	"	0.047	0.812	"	"	0.094	"	0.700	0.193	0.09
41	"	0.043	0.750	0.294	0.52	0.083	0.132	0.602	0.219	0.11
42	"	0.025	0.875	"	"	0.048	"	0.780	0.169	0.08
43	VB	0.062	0.625	"	"	0.119	"	0.440	0.300	0.20
301	"	0.162	0.875	1.011	0.28	0.579	1.020	0.780	1.310	1.00
302	"	0.177	0.750	"	"	0.633	"	0.602	1.696	1.18
310	"	0.201	"	1.039	0.36	0.558	1.050	"	1.745	1.20
311	"	0.314	0.625	1.114	0.34	0.925	1.180	0.440	2.670	1.62
312	"	0.130	0.875	0.666	0.48	0.271	0.510	0.780	0.656	0.56
313	"	0.200	0.750	"	"	0.417	"	0.602	0.848	0.73
315	"	0.159	0.875	0.738	0.42	0.379	0.590	0.780	0.757	0.66